



ION CHANNELS
WITH AND WITHOUT THE PRESENCE OF
PROTEINS

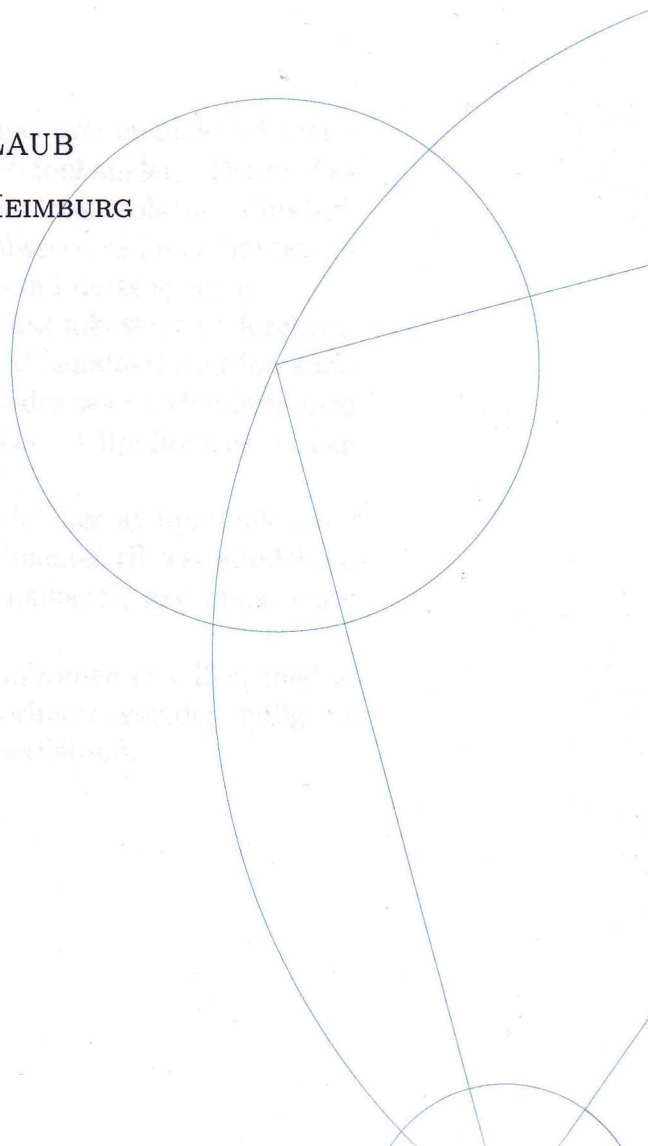
KATRINE RUDE LAUB

SUPERVISOR: THOMAS HEIMBURG

A Thesis Presented for the Degree of
Cand. Scient. in Biophysics

Niels Bohr Institute
University of Copenhagen
Denmark

December 14, 2010



Acknowledgments

I would like to thank:

- Thomas Heimbürg for inspirations and for providing the project.
- Andreas Blicher for always being ready to help, discuss and answer questions.
- Erik Hviid Larsen (August Krogh Institute, University of Copenhagen) for introducing me to protein channel experiments, and providing data and computer power.
- Katja Witschas (Institute of Physiology, University Hospital Aachen) for protein channel data, discussions, and answering a lot of questions.
- Alfredo González-Pérez for providing the polymers.
- C floor hangarounds for proofreading, distraction, and moral support.

The thesis is submitted to fulfill the requirements for the M.Sc. in Biophysics at the Niels Bohr Institute, Faculty of Science, University of Copenhagen, Denmark. The experimental work was conducted at the Niels Bohr Institute, University of Copenhagen.

Figures are unless otherwise specified made by myself in Inkscape or Igor Pro.

Contents

1	Introduction	1
2	Biological membranes	3
2.1	Lipids	4
2.2	Membrane proteins	5
3	Transitions and structure of membranes	8
3.1	Structure and phase transitions in membranes	8
3.2	The laws of thermodynamics and fluctuations	11
3.2.1	Susceptibilities	13
3.3	Effect of voltage	16
3.4	Transitions in biological membranes	17
4	Permeability	21
4.1	Protein ion channels	21
4.2	Selection of previous permeability studies	24
4.3	Models for lipid ion channels	28
4.3.1	Domain interface model	28
4.3.2	Fluctuation model	29
4.3.3	Pore structure models	30
4.4	Copolymer membranes as an alternative?	31
4.5	Methods for electrophysiological measurements	32
4.5.1	Montal-Mueller	32
4.5.2	Patch clamp	33
4.5.3	Tip of pipette	34
5	Lipid-protein interactions	36
6	Materials and methods	40
6.1	Preceding considerations about experiments with cytochrome c and DMPG	40
6.2	Sample preparation	41
6.2.1	Materials	41
6.2.2	Samples for calorimetry	42
6.2.3	Samples for permeability experiments	43
6.3	Calorimetry	43
6.4	Permeability experiments	44
6.4.1	Setup	44
6.4.2	Pipette preparation	46
6.4.3	Silanization	46

6.4.4	Bilayer formation and capacitance test	47
6.4.5	Addition of cytochrome c	49
7	Results and discussions	50
7.1	Membrane formation techniques	50
7.2	Calorimetry	53
7.2.1	Discussion	56
7.3	Different membrane behaviors	58
7.3.1	Discussion	65
7.3.2	Comparison with protein channels	67
7.4	Charged membranes	72
7.4.1	Discussion	73
7.5	Cytochrome c	74
7.5.1	Discussion	74
7.6	Temperature dependence	74
7.6.1	Discussion	77
7.7	Voltage dependence	79
7.7.1	Discussion	81
7.8	Copolymer membranes	82
7.8.1	Discussion	84
8	Conclusions	87
9	Future research	88
10	Bibliography	89
A	Various behaviors of a single membrane	100
B	Supplementary figures of various membrane behaviors	103
B.1	Stable quantized events	103
B.2	Overload events	104
B.3	Non-quantized events	104
B.4	Burst	105
B.5	Sawteeth	105
B.6	Baseline drift	107
B.7	Baseline jumps and stairs	108
B.8	Spikes	109
B.9	Breakage	110
C	Protein channel data	112

D Voltage dependence

114

1 Introduction

The fundamental building blocks of living organisms are cells. From single-celled bacteria to humans consisting of 10^{14} of these functional units are the basis of life. What defines the cell is the cell membrane. It isolates the inside of the cell from its environment. But without interactions with the outside the cell would die. Without nutrients, waste, essential molecules, and ions crossing the membrane it would not be able to fulfill its function of for example nerve signal conduction, energy conversion, growth, or protein creation.

The subject of this thesis is transport, or more precisely the passive permeation, of ions across membranes. The standard explanation is that the ions diffuse through protein channels embedded in the membrane. A standard method for investigation of protein ion channels is to confine a patch of membrane and measure the current running through it in response to an applied voltage. If quantized current steps are observed these are attributed to opening and closing of a protein channel. They are even referred to as the "characteristic electrical signature"[1] of protein channels. The problem is just that the same kind of current steps are observed in membranes that do not contain any proteins. This experimental fact is often neglected by biologists even though it has been known for at least 30 years. Unfortunately there is currently no way to measure the conductance of protein channels without incorporating them into lipid membranes. This means that one has a severe interpretation problem in the case of protein channel data.

The aim of this thesis is to make a further investigation of lipid ion channels and to examine if they actually are so similar to protein ion channels as claimed. More resemblances than previously reported are found in this thesis. The similarities are found through experiments with a patch clamp-like setup on artificial membranes. But before getting to the experimental part some background information is provided.

Section 2 presents the basic knowledge about biological membranes and some of its constituent. The next section describes the membrane structure in more details including that membranes can exist in several phases with different characteristics. Especially the transitions between the phases has some interesting features. Presumably some of these has a direct influence on the permeability of membranes. It is further described what influences the transitions and transitions are put into perspective by their relevance in relation to biological membranes.

In section 4 I go deeper into the permeability of membranes. The traditional view is represented by a section about protein channels, while evidence

for the existence of lipid ion channels is given in a presentation of previous experimental and theoretical publications about the subject. Also a novel type of membrane created of polymers is introduced as a possible solution to the problem of investigating protein channels in lipid membranes. In the end is given an overview of the methods that can be used to measure the permeability of membranes on a single channel level.

Despite being the two major constituents that together make up a biological membrane, proteins and lipids are often treated independently. In section 5 it is argued that interactions should also be taken into account for the function of cell membranes. In some cases the presence of proteins may even induce lipid ion channels.

After the section providing the details about materials and methods the experimental results are presented and discussed. Through the experiments the aim of this thesis will be pursued by the following objectives:

- Reproduce the existence of channel events in pure lipid membranes and compare them with protein ion channel events
- Make calorimetric scans to test if they can be related to the permeability of membranes
- Add a non-channel protein to test if it affects the channel events
- Test if copolymer membranes could be an alternative to lipid membranes for the purpose of protein channel experiments

Enjoy the reading!

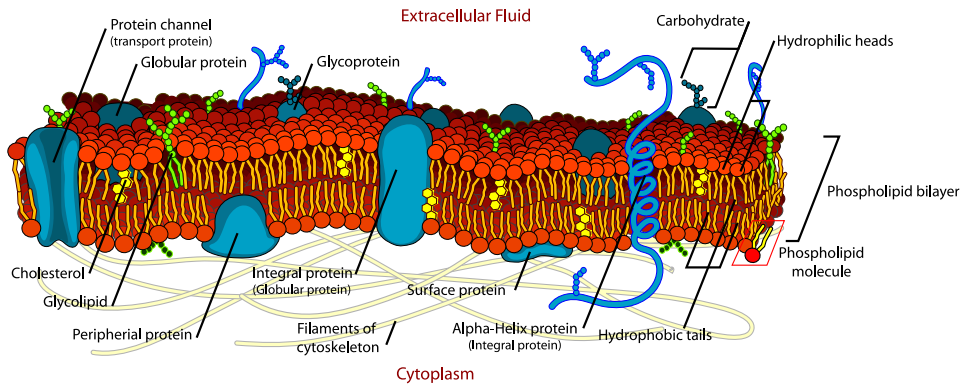


Figure 1: The cell membrane consists of a phospholipid bilayer, which contains a number of biological molecules such as proteins, sugars and other lipids. Figure taken from wikipedia.org

2 Biological membranes

Living organisms are all made of the same fundamental unit, the cell. All cells, whether they are bacterial, plant or animal, are enclosed by a membrane. The membrane defines the boundary between what is cell and what is the outside world. It acts as a barrier that controls what gets in and what gets out. Examples are entry of nutrients and exit of waste products, and maintenance or generation of differences in ion concentration and thereby potential.

By studying red blood cells from different animals Gorter and Grendel in 1925 found out that the area of extracted lipids corresponded to two times the area of the cell.[2] By this the concept of a lipid bilayer as the fundamental structure of biological membranes was born and have been found common to all biological cells and their organelles. Into this bilayer a variety of proteins are embedded (figure 1). The mass and volume ratios between proteins and lipids in the membrane range from 0.25 to 4 depending on cell type.[3] A typical ratio is 1 including proteins only residing on the surface and extra-membraneous parts of other proteins. This means that the major area in the plane of the membrane consists of lipids.

Although only 5nm thick the lipid bilayer is considered impermeable to polar substances because of its hydrophobic inner. The free energy of a charge q in a dielectric medium is proportional to the electrostatic potential $\Psi = \frac{q}{\epsilon_0 \epsilon_r r}$ where ϵ_0 is the vacuum permittivity, ϵ_r is the dielectric constant, and r is the distance from the charge.[3] The dielectric constant is about 80 for water and about 2 for the interior of a lipid bilayer.[4] This means

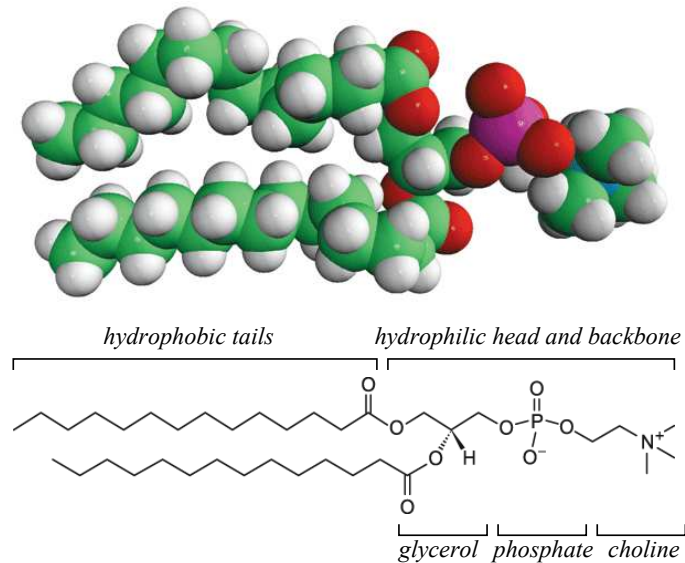


Figure 2: Structure of the phospholipid DMPC. Modified figure from www.avantilipids.com

that electrostatic free energy is 40 times higher for the bilayer compared to water. So finding an ion inside the lipid bilayer is unlikely. It is therefore common to assume that the proteins are responsible for all transport across the membrane.

2.1 Lipids

The major part of lipids in the cell membrane are glycerophospholipids such as the one shown in figure 2. They can be divided into three parts: head-group, backbone, and tail. The backbone is in this case a glycerol, which can be esterified in three positions whereby headgroup and chains can be attached. These characterize the different lipids. The composition of lipids species is very diverse in different cell types within the same organism. It even differs in the various organelles within the same cell.

Headgroups vary in size and charge. They can be either uncharged, negatively charged or zwitterionic. Positively charged lipids are not found in nature.[5] Examples of common headgroups are phosphatidylcholine (PC), phosphatidylethanolamine (PE), phosphatidylserine (PS) and phosphatidylglycerol (PG). PC and PE are zwitterionic with no net charge while PG and PS are negatively charged. In many biological membranes the amount of charged lipids is around 10-20% but can be as high as 40% in mitochondria.[6]

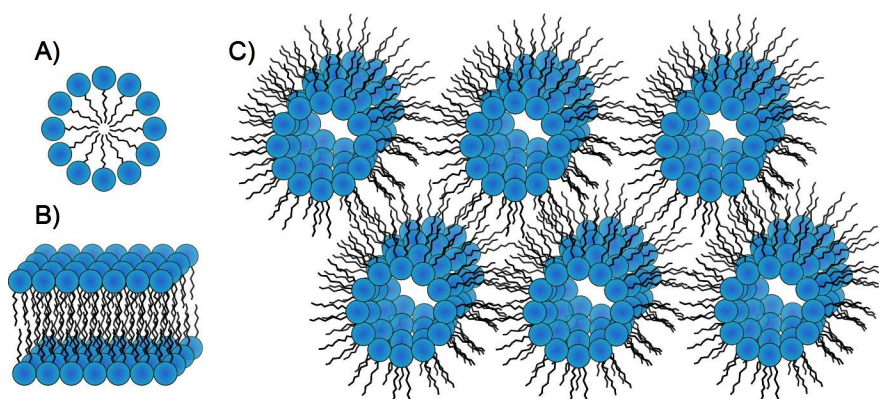


Figure 3: Lipids form aggregates in polar solvents to avoid exposure of their hydrophobic tails. Some examples are: A) cross-section of a micelle, B) a bilayer, and C) an inverted hexagonal phase.

The different headgroups are important for phase behavior and the affinity of the membrane to bind various proteins and drugs as will be made use of in this thesis.

The tail consists of hydrophobic hydrocarbon chains. Chains can vary in number, length and saturation. The number of chains can be from 1-3 with 2 being most common. In biological membranes chain lengths from 14-24 carbon atoms are found with 16-18 being typical.[6]

The amphiphilic nature of lipids make them aggregate when added to a polar solvent. It is energetically favorable for them to face the hydrophobic tails toward each other, such that only the hydrophilic headgroups get in contact with water. There are a number of ways to do this depending on lipid species, some of which are shown in figure 3. Of these the bilayer is the one found in cell membranes and the one of interest in this thesis.

2.2 Membrane proteins

Proteins can be attached to the membrane in a number of ways depending on their properties as shown in figure 4. Peripheral proteins can be attached to the lipid bilayer by a combination of hydrophobic, electrostatic, and other non-covalent interactions. These can among others act as catalysts or cell adhesion molecules that allow cells to identify each other and interact.

Transmembrane proteins have a hydrophobic domain in the middle and hydrophilic ends, which makes it favorable to span the membrane. Examples of transmembrane proteins are protein ion channels and pumps, which are

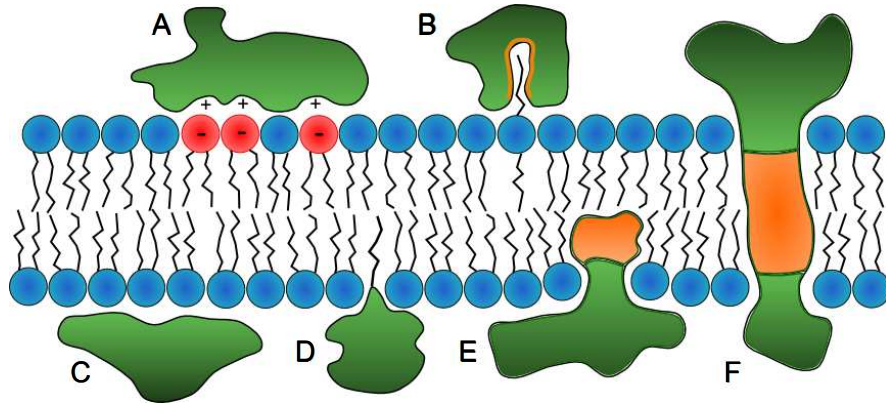


Figure 4: Schematic illustration of protein binding strategies: A) electrostatic binding, B) anchoring via a lipid extended conformation, C) non-specific binding by weak physical forces, D) anchoring by a hydrocarbon chain attached to the protein, E) partly penetrating amphiphilic protein, F) transmembrane spanning by amphiphilic protein. Orange color indicate hydrophobic part of protein. After inspiration from [5]

responsible for moving molecules in and out of the cell by passive and active transport respectively.

In these experiments cytochrome c (cyt c) and gramicidin A (gA) will be used. Cyt c is used to investigate the effect of a non-channel protein and gA to see if a channel protein behaves different from the lipid ion channels. Cyt c is a peripheral protein. It is nearly globular (see figure 5) with a positive net charge of 8 at neutral pH and therefore binds electrostatically to negatively charged membranes.[7] The protein is primarily found in mitochondria where it is involved in electron transport and apoptosis (i.e. programmed cell death).

gA is strictly speaking not a protein but a peptide due to its short chain of only 15 amino acids.¹ It is helical (see figure 6) with only approximately half the length of the membrane thickness. Most of it is extremely hydrophobic and it therefore penetrates the membrane. It is nevertheless relatively impermeant in membranes.[8] By forming a dimer it can create a pore with a hydrophilic lumen through the membrane. In its natural form it is secreted by *Bacillus brevis* but its function there is unknown.[8] It was however the first clinically used antibiotic (e.g. [8, 9]).

¹Peptides and proteins have the same chemical structure. They are both polymers of amino acids. The convention for discrimination is not clear but is often set around 50 amino acids.

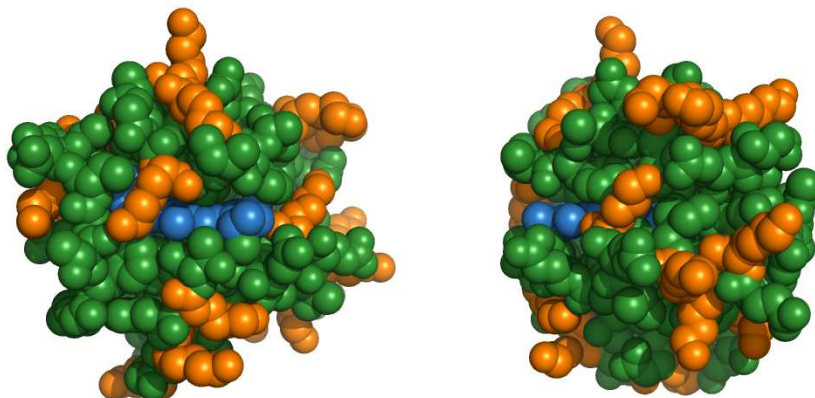


Figure 5: Space filling model of all non-hydrogen atoms in cytochrome c from one side and rotated 90° . The net positive charge arises primarily from the orange lysine groups. Marked with blue is a heme group which is involved in electron transfer. Visualized with PyMol from the crystalline structure 1HRC.pdb from the RCSB protein data bank.

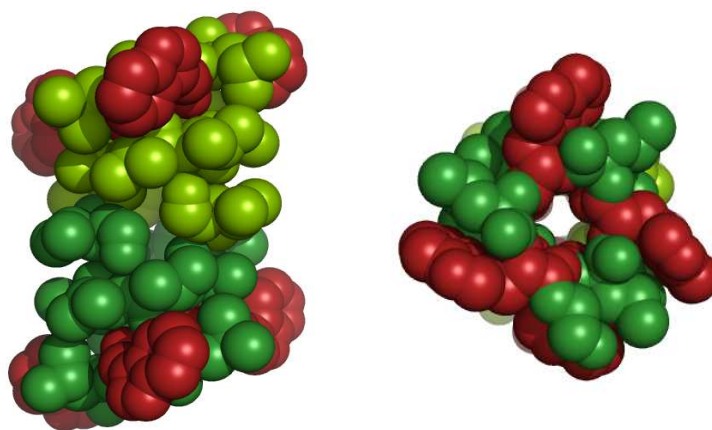


Figure 6: Space filling model of all non-hydrogen atoms in a gramicidin A dimer. The monomers are colored in different shades of green. The dimer is seen in the plane of the membrane (left) and tilted 90° for a look through the channel (right). Red units are tryptophan. Made from the crystalline structure 1JNO.pdb.

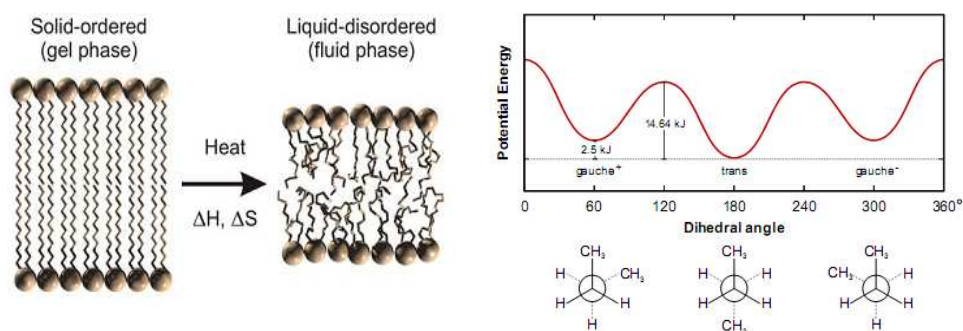


Figure 7: *Left* As the membrane changes from gel to fluid phase enthalpy and entropy increase. Kinks in the chains result in change in area and volume of the membrane. *Right* The kinks arise from the different possible conformations arising from rotations around the C-C bonds. The lowest energy state is the all-trans conformation, which is illustrated by the sawtooth pattern seen in the gel state. Addition of heat allows for gauche isomers with higher energy and degeneracy. Figures are taken from [10].

3 Transitions and structure of membranes

Just as water can be solid, fluid, or vaporized, lipid membranes can exist in different phases. During transitions between the phases a lot of interesting features are affected. A few examples are permeability, compressibility and relaxation times. Some of these will be described in more detail later, but first is given a description of the phases and what influences them.

3.1 Structure and phase transitions in membranes

Of the phospholipid membrane phases the gel and fluid are the ones most relevant to biological membranes. The gel (also known as solid ordered) phase is characterized by the headgroups being ordered in a hexagonal lattice and the chains being straightened out in a so called all-trans conformation. This is the state with the lowest internal energy. Other conformations are obtained by rotation around the C-C bonds. Due to steric repulsion 3 conformations are stable as pictured in figure 7. The stable states are rotations of $\pm 120^\circ$ from the trans conformation, which is called a gauche conformations. As the temperature rises the gauche conformations with higher internal energy become accessible. These gauche conformations make the chains kink with the result that they take up more space. The lattice structure gets disrupted and the lipids are able to move around freely as in a 2-dimensional fluid.

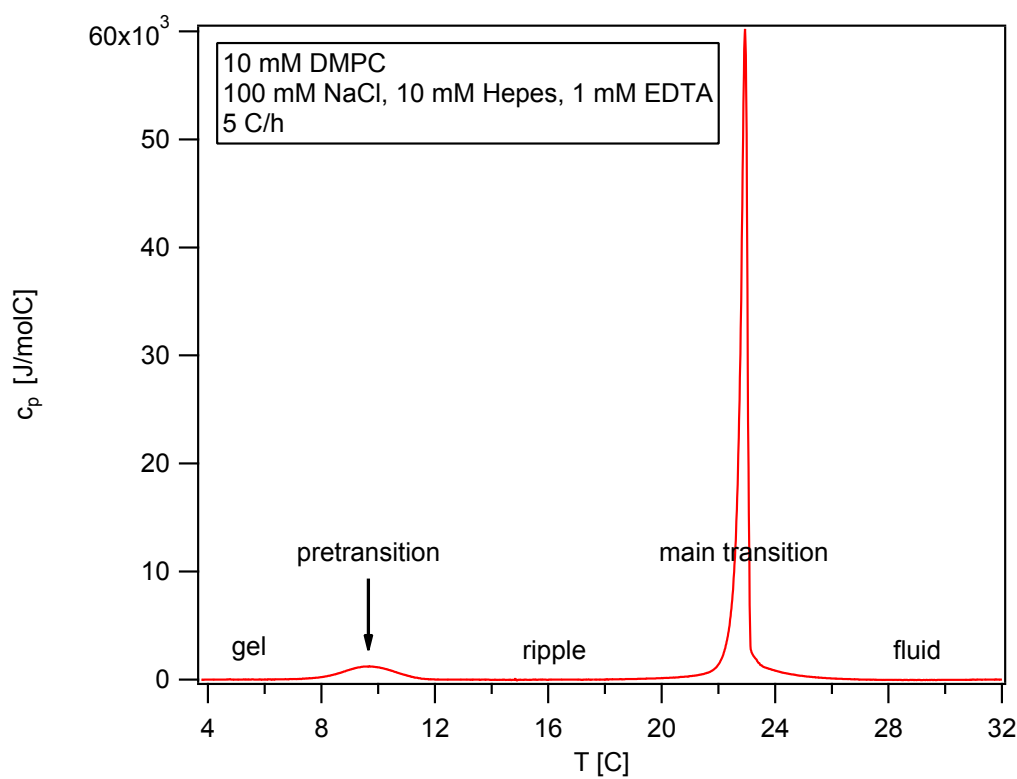


Figure 8: A calorimetric scan gives the heat capacity profile of dimyristoyl phosphatidylcholine (DMPC). The pretransition and main transition are seen as peaks in the curve.

Therefore the fluid phase is also known as liquid disordered. The changed conformation results in the area increasing 25% and the volume 4% from gel to fluid state. [11]

Phase transitions may be characterized by the fact that the addition of heat does not change the temperature as the energy is stored in conformational changes. Transitions therefore show up as peaks in a heat capacity profile as shown in figure 8. Some lipids show additional transitions. For example, saturated phosphatidylcholines have an intermediate phase between gel and fluid known as the ripple phase because of periodic ripples on the surface. The ripples have been suggested to arise from line defects of melted lipids which induce local curvature.[12] The transition from gel to ripple phase is called the pretransition, while the transition to fluid phase is the main transition. Phosphatidylglycerols also show additional transitions depending on the ionic strength and pH of the buffer.[13, 14, 15] The nature of

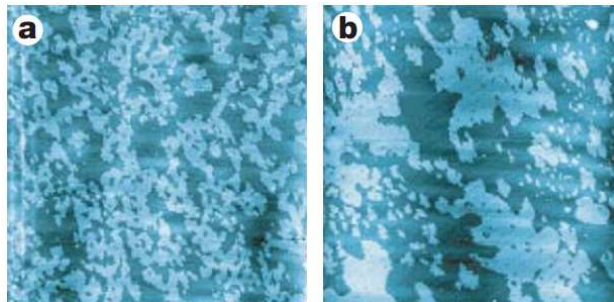


Figure 9: Domain formation in the transition. Here revealed by atomic force microscopy. **a** dimyristoyl phosphatidylcholine (25x25 μm^2) **b** dipalmitoyl phosphatidylcholine (20x20 μm^2). From [16].

these transitions are not well established.

Lipids exhibit cooperative melting. This means that neighboring lipids influence each other as it is energetically most favorable for example to have the same length. High cooperativity typically results in narrow phase transitions. The cooperativity can be lowered if other molecules e.g. other lipids or proteins are added to the membrane.[17] The cooperative units show up as domains i.e. segregation of areas with the same properties (see figure 9).

The most accurate definition of the transition temperature T_m is where half of the lipids are fluid and the other half gel. Here the free energy difference ΔG between the two states is zero.

$$\Delta G = G_f - G_s = 0 \quad (1)$$

Knowing that the free energy difference is also given by

$$\Delta G = \Delta H - T_m \Delta S \quad (2)$$

where ΔH denotes the melting enthalpy and ΔS the melting entropy it follows that

$$T_m = \frac{\Delta H}{\Delta S} \quad (3)$$

However, in this thesis I will instead use the peak temperature in heat capacity profiles for reasons that will become clear later. In practice the difference is often very small.

The various lipids have different transition temperatures ranging from -20 to 60°C.[6] It depends on intrinsic properties of the lipid such as head-group, chain length and saturation. For example, longer chains have higher

transition temperature. But also intensive thermodynamic variables such as pressure and electrical potential, which determine the overall entropy of the membrane, influence the state of the membrane.

3.2 The laws of thermodynamics and fluctuations

In the following will be given an introduction to how thermodynamics can provide information about transitions in membranes and fluctuations that may play a central role in the formation of lipid ion channels.²

Not only temperature affect the state of a membrane. Like any other thermodynamic system its state can be completely characterized by its internal energy E or the entropy S . All changes that can occur in a system is likewise completely specified by the fundamental equations for dE and dS . The total change of energy dE of a system with time dt is given by

$$dE = dQ + dW, \quad (4)$$

where dQ is the heat added and dW is the work done on the system. Equation 4 is the first law of thermodynamics and reflects the conservation of energy.

dW is the sum of all the possible forms of work that can be performed on the system where each term is a product of an intensive variable (i.e. variables independent of system size) and the differential of its associated extensive variable (i.e. variables that dependent on system size) such as pressure p and volume V , lateral pressure π and area A , electrostatic potential Ψ and charge q , chemical potential μ and particle number n (of the i th component) and many more

$$dW = -pdV - \pi dA + \Psi dq + \sum_i \mu_i dn_i + \dots \quad (5)$$

Changing any of the intensive variables therefore affect the state of the system and in particular change the phase transition of a membrane. How these variables influence the transition is among others described for pressure [20] and pH [21], but is only in some cases quantified in a theoretically based formula.

The change of heat can be related to temperature T by the state function entropy S

$$\oint dS_r \equiv \oint \frac{dQ}{T} = 0. \quad (6)$$

The index r indicates that this is only true for a reversible process such as membrane melting. In general

²This section among others is inspired by [3], [18], and [19]

$$dS = dS_r + dS_i \geq \frac{dQ}{T} \quad (7)$$

with the irreversible part $dS_i \geq 0$. This is the second law of thermodynamics.

The second law means that in equilibrium the entropy is in a maximum i.e. the state with the highest entropy is the most likely. But the entropy is a function of parameters that fluctuate and therefore changes in entropy occur. Equation 7 can be rewritten to entropy as a function of these fluctuating parameters with the use of 4 and 5.

$$dS \geq \frac{1}{T}dE + \frac{p}{T}dV + \frac{\pi}{T}dA - \frac{\Psi}{T}dq - \sum_i \frac{\mu_i}{T}dn_i + \dots \quad (8)$$

The local fluctuations in the extensive variables is generated by thermal motion within the system. In the transition the difference in free energy between the gel and the fluid state is zero. This means that the energy required to change the parameters is very small. Thermal fluctuations of the order $k_B T$ are therefore enough to make a considerable change of the state locally.

As the system in equilibrium has maximum entropy, any fluctuation can only reduce entropy. The response of the system to these perturbations is a tendency to spontaneous entropy producing irreversible processes that drive the system back to equilibrium. An intuitive understanding of this can be obtained if one considers the entropy as a potential where thermodynamic forces restore the effect of the perturbations. It can be quantified by expanding the entropy function as a power series in the fluctuating parameters.

$$S = S_0 + \sum_i \left(\frac{\partial S}{\partial \xi_i} \right)_0 \xi_i + \frac{1}{2} \sum_i \sum_j \left(\frac{\partial^2 S}{\partial \xi_i \partial \xi_j} \right)_0 \xi_i \xi_j + \dots \quad (9)$$

where $\xi_i = \alpha_i - \alpha_{i,0} = \alpha_i - \langle \alpha_i \rangle$ is the deviation of an extensive parameter α from its equilibrium value. As the entropy is at max in an equilibrated system the linear term has to be zero. For small fluctuations one then gets

$$S \approx S_0 + \frac{1}{2} \sum_i \sum_j \left(\frac{\partial^2 S}{\partial \xi_i \partial \xi_j} \right)_0 \xi_i \xi_j \quad (10)$$

Figure 10 shows the entropy as a potential function of the deviations of the extensive parameters. The above equation is of the same form as a classical harmonic potential. As in the classical case the thermodynamic forces can then be defined as $X_i \equiv \frac{\partial S}{\partial \xi_i}$.

For a thermodynamic system with extensive variables such as energy E , volume V , area A , charge q , and the number of particles n_i , the force will be respectively $\frac{1}{T}$, $\frac{p}{T}$, $\frac{\pi}{T}$, $-\frac{\Psi}{T}$, and $-\frac{\mu_i}{T}$ (see equation 8).

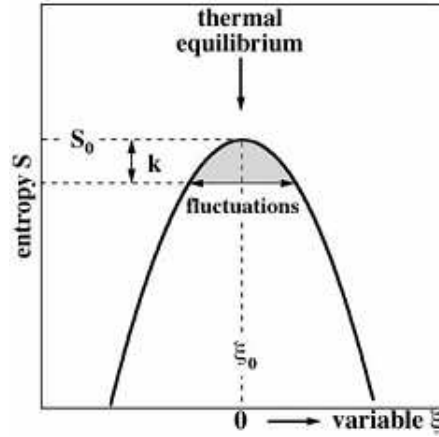


Figure 10: The entropy potential S as a function of extensive variables ξ . The maximum corresponds to thermal equilibrium. The exact shape of the entropy function is unknown as the quantitative contribution from each of the variables is unspecified. Figure adapted from [3]

3.2.1 Susceptibilities

The above introduction is supposed to give an intuitive understanding of the nature of fluctuations. These fluctuations give rise to a large number of interesting properties and the following could be derived directly from the the equations in section 3.2 (see for example [3]). Here is instead given a more general derivation in which one does not have to make assumptions of a harmonic entropy potential.

First it is necessary to define thermodynamic averages of a quantity Y .

$$\langle Y \rangle \equiv \sum_i \frac{Y_i \cdot e^{-H_i/RT}}{Z} \quad (11)$$

where i indicates all possible states and the partition function Z is given by $Z \equiv \sum_i e^{-H_i/RT}$ with $H = E + pV + \Pi A$ being enthalpy and R the gas constant.

Functions that are given by the derivative of an extensive variable with respect to an intensive variable are called susceptibilities or response functions. Heat capacity and compressibility are such functions. The heat capacity at constant pressure c_p is defined as

$$c_p \equiv \left(\frac{d\langle H \rangle}{dT} \right)_p \quad (12)$$

Calculating the differential one gets

$$\frac{d\langle H \rangle}{dT} = \left(\frac{d}{dT} \sum_i \frac{H_i e^{-H_i/RT}}{Z} \right)_p \quad (13)$$

$$= \frac{Z \cdot \sum_i \frac{d}{dT} (H_i e^{-H_i/RT}) - \sum_j H_j e^{-H_j/RT} \frac{d}{dT} Z}{Z^2} \quad (14)$$

$$= \frac{\sum_i \frac{H_i^2}{RT^2} e^{-H_i/RT}}{Z} - \frac{\sum_i H_i e^{-H_i/RT}}{Z} \frac{\sum_j \frac{H_j}{RT^2} e^{-H_j/RT}}{Z} \quad (15)$$

$$= \frac{\langle H^2 \rangle - \langle H \rangle^2}{RT^2} \quad (16)$$

whereby it is seen that the heat capacity is proportional to the fluctuations in enthalpy.

A similar derivation can be made for the isothermal area compressibility κ_T^A which turns out to be proportional to the fluctuations in area

$$\kappa_T^A \equiv - \left(\frac{1}{\langle A \rangle} \frac{d\langle A \rangle}{d\Pi} \right)_T \quad (17)$$

$$= \frac{\langle A^2 \rangle - \langle A \rangle^2}{\langle A \rangle RT} \quad (18)$$

and the isothermal volume compressibility κ_T^V which is proportional to fluctuations in volume

$$\kappa_T^V \equiv - \left(\frac{1}{\langle V \rangle} \frac{d\langle V \rangle}{dp} \right)_T \quad (19)$$

$$= \frac{\langle V^2 \rangle - \langle V \rangle^2}{\langle V \rangle RT}. \quad (20)$$

The enthalpy (and thereby the heat capacity) can be divided into two parts that are additive: The intrinsic enthalpy H_0 which is associated with intramolecular fluctuations and the excess enthalpy ΔH which is related to fluctuations in the membrane state and the one measured in experiments.

$$c_p = \frac{d}{dT} (H_0 + \Delta H)_p = c_{p,0} + \Delta c_p \quad (21)$$

$$= \frac{\langle H_0^2 \rangle - \langle H_0 \rangle^2}{RT^2} + \frac{\langle \Delta H^2 \rangle - \langle \Delta H \rangle^2}{RT^2} \quad (22)$$

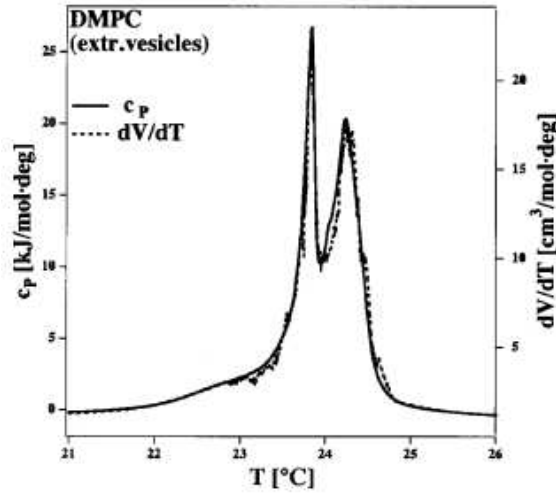


Figure 11: Curves of heat capacity c_p and volume expansion coefficient dV/dT are completely superimposable. This demonstrates the proportionality of enthalpy H and volume V as $H = \int c_p dT$ according to equation 12. Figure adapted from [20].

The same separation can be made for area $A = A_0 + \Delta A$ and volume $V = V_0 + \Delta V$.

It is an experimental finding that in the transition the excess volume is proportional to excess enthalpy as shown in figure 11. [20, 23]

$$\langle \Delta V \rangle = \gamma_V \langle \Delta H \rangle \quad (23)$$

This relation has remarkable consequences, which will be shown below. It is not a general feature and purely experimental but has shown to hold for lipids. Ebel et al [20] demonstrated that the proportionality even holds for complex biological membranes.

Assuming equation 23 is true for all temperatures it can be shown that also³

$$\langle \Delta V^2 \rangle = \gamma_V \langle \Delta H^2 \rangle. \quad (24)$$

Therefore

³For details see appendix in [11].

$$(\langle \Delta V^2 \rangle - \langle \Delta V \rangle^2) = \gamma_V^2 (\langle \Delta H^2 \rangle - \langle \Delta H \rangle^2). \quad (25)$$

This gives us the central proportionality between compressibility and heat capacity

$$\Delta \kappa_T^V = \frac{\gamma_V^2 T}{\langle V \rangle} \Delta c_p. \quad (26)$$

There is to my knowledge no direct evidence for a proportionality between excess enthalpy and excess area, but it is a plausible postulate and leads to correct predictions of the bending elasticity modulus.[6] Assuming it to be true one gets an analogous relation for the isothermal area compressibility

$$\Delta \kappa_T^A = \frac{\gamma_A^2 T}{\langle A \rangle} \Delta c_p. \quad (27)$$

Accordingly the membrane gets softer in the transition and less work is required to form a pore.

3.3 Effect of voltage

In all the permeability experiments performed in this thesis the membrane is subject to a transmembrane voltage. It is therefore appropriate to examine closer which effect it has on membranes and especially on their transitions. Both within theoretical and experimental studies of voltage effects on transition there is found to be a considerable the disagreement about the result.

Several kinds of effects on the membrane itself have been reported. According to Berestovsky et al [24] and Crowley [25] the membrane gets thinner in response to voltage. Stulen [26] finds a changed orientation of the lipid heads but not the chains, while Sugár [27] has developed theoretical expressions for the alterations of chain conformations in response to voltage.

Sugár uses statistical considerations to predict the effect of voltage on the transition. He finds that voltage decreases the transition temperature due to a loosening of the membrane structure. This is because an applied voltage cause a compressive electric force on the membrane that induces gauche conformations. For a DPPC membrane subject to 140mV Sugár finds the transition to shift about 20K downwards. Another attempt of theoretical predictions comes from Cotterill [28] who suggests the transition of a DPPC membrane to shift 2K upwards in an electric field of 10^7 V/m i.e. 50mV

assuming a 5nm membrane. His predictions are based on the effect of an electric field on the tilt of the zwitterionic headgroups.

Apparently very few experiments have been performed to reveal the effect of voltage on phase transitions. Antonov et al [29] have performed experiments both with zwitterionic PCs and with DPPA, which is a lipid with a negatively charged headgroup just as PG used in this thesis. He identifies the transition as an increase in electric membrane conduction. At a voltage of 150mV he finds the transition temperature to increase with a few degrees for the PCs and about 8K for DPPA.⁴

Another experimental study is performed by Thürk and Porschke [30]. Here transition temperatures are identified by a discontinuity of light scattering amplitudes. In contrast to the experiment by Antonov et al they here use a pulsed electric field. It is found that the transition of DMPG is independent of electric fields up to 35kV/cm, which corresponds to a voltage of around 200mV across a single membrane.⁵

The conclusion of this section must be that the effect of voltage is not well established. It is likely to be impossible to make a simple correlation between voltage and shift in transition temperature. The effect might not be a simple transition from gel to fluid but could also be some other kind of conformational change such as a tilt of heads or chains. The consequence of electric fields is further complicated by the symmetry of the membrane that might lead to opposing effects on the two sides of the bilayer.

3.4 Transitions in biological membranes

Biological membranes are typically found in the fluid phase just above the transition. Generally homeotherms⁶ and bacteria are found to have transitions 5-15°C below physiological temperature (see figure 12).[6, 32] Exper-

⁴The stated changes in transition temperature in [29] is based on the temperature changes in figures 2 and 3. Table 1 which compares transition temperatures determined by calorimetry and by conductance jumps (at allegedly minimal voltage) apparently disagrees with the figures. I have checked the reference for the transition of DPPA and the quoted transition temperature is cited right. This corresponds to the transition measured by Antonov et al at 150mV according to figure 2a. I here assume that the figures show the right temperature changes, which are the same as stated in the text, even though the scale might be shifted.

⁵The transmembrane voltage is calculated from the following equation which states that in an external electric field E the transmembrane voltage U of a sphere with radius r is given by $U = 1.5rE \cos\theta$. [31] θ is the angle between the site on the vesicle membrane and the direction of the electric field. A radius of 25-50nm is given in the article. Here is used $\theta = 0$

⁶Animals with a stable body temperature.

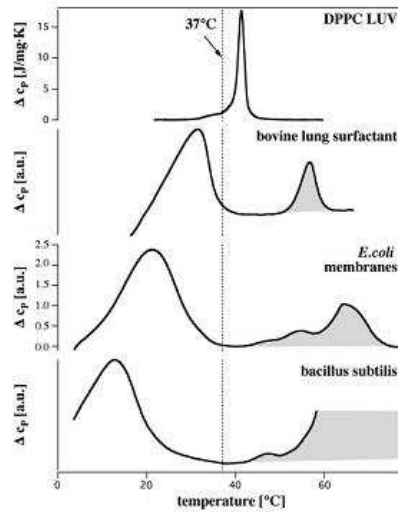


Figure 12: Heat capacity profiles of DPPC vesicles, bovine lung surfactant, and membranes of *E. coli* and *B. subtilis*. Gray areas indicate protein denaturation and white areas lipid melting. Growth temperature of the bacteria and body temperature is indicated by the line at 37°C. All the biological membranes have transitions just below physiological temperature. The large variety of lipids gives low cooperativity and thereby broad transitions. Figure taken from [6].

iments on *E. coli* have shown that if the bacteria are grown at different temperatures, they alter the lipid composition of their membranes in a way that maintains the transition to be just below growth temperature.[6, 33] This is done by increasing the fraction of unsaturated fatty acids as growth temperature is lowered.[34] Unsaturated lipids melt at considerably lower temperatures than corresponding saturated lipids.

The same effect has been demonstrated by altering another thermodynamic variable namely pressure. High pressure increase the melting point of membranes as the pressure stabilizes the ordered gel state. DeLong and Yayanos has investigated barophilic marine bacteria and shown that the ratio of unsaturated to saturated chains increase with pressure.[35] Similar adaptations are also found for changes in hydrostatic pressure and pH for deep-water fish and certain bacteria.[32]

The capability of altering the composition of the lipid bilayer in order to maintain a certain fluidity in response to environmental factors is known as *homeoviscous adaptation*.[33, 36]

Adaptation is also seen in eukaryotes. The temperature gradient of the

reindeer leg is accompanied by an increased amount of unsaturated lipids near the hooves compared to closer to the body.[37] Some animals are even able to change their lipid composition within hours. The fish, Sonoran desert teleost, decreases the percentage of diunsaturated species of PC in the membranes of muscle microsomes from the cold mornings to the warm afternoons.[32]

The effect of homeoviscous adaptation have even been shown for humans. It is known that the membranes of erythrocytes of chronic alcoholics have a higher amount of cholesterol than non-alcoholics.[38] Alcohol lowers the transition temperature, which is counteracted so that the fluidity is maintained under permanent intoxication.[39] Rats on an ethanol diet in addition to an increased ratio of saturated lipids also showed a lower quantity of polyunsaturated PE in microsomal membranes.[40]

All these examples indicate that having the membrane in the fluid phase is crucial to the cell. The question is whether being close to the transition also plays a role. This is not unlikely. As described in section 3.2 there is a number of ways to alter the state of the membrane. For example a local change in pH or other thermodynamic variables can without difficulty induce a transition. In addition several possibly important features are changed in the transition. Below are given a few examples.

As will be described later some proteins prefer one phase over the other. This means that these proteins will aggregate into domains of the favored phase that arise in the transition as shown by Monte Carlo simulations and atomic force microscopy.[17, 41] This could be a method for protein communication.

As shown in section 3.2.1 the transition is associated with large fluctuations. These can be used constructively. One example is that the elastic constants of the membrane as derived changes significantly which can promote structural changes such as cell division. Another is the activity of phospholipase A₂ (PLA). PLA is an enzyme that hydrolyzes phospholipids into a lysolecithin and a fatty acid. By use of fluorescence microscopy the hydrolysis is found to be done on lipids in the ordered state starting from domain boundaries (see figure 13).[42, 43] Biltonen relates the activation rate of PLA to fluctuations [44]: "It thus appears that the rate of activation of the enzyme requires that the substrate exists in a phase-transition region and that the rate of activation is proportional to the magnitude of the thermodynamic fluctuations characteristic of the system."

The complexity of biological membranes complicates an unambiguous assignment of a physiological process to a certain physical mechanism. There is nevertheless numerous indications that phases and phase transitions play a role in cell membranes.

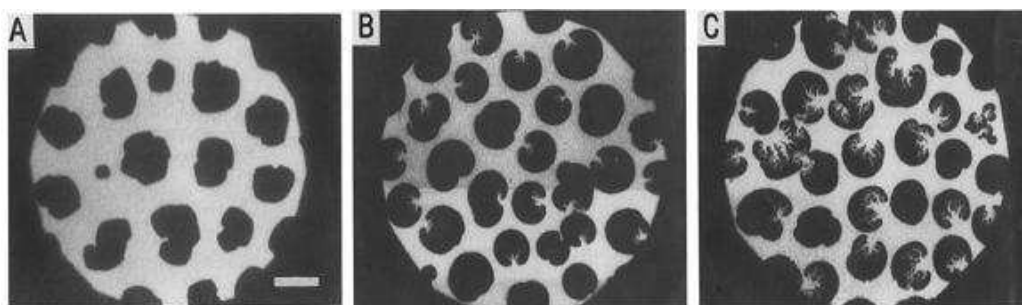


Figure 13: Pictures of fluorescent DPPC monolayer. Gel domain appear black while fluid lipids are bright. With time the gel domains are degraded by phospholipase A_2 . Pictures are taken 0 min (A), 10 min (B), and 15 min (C) after injection of the enzyme. Figure taken from [42].

4 Permeability

Membrane permeability can arise from several sources. It can be from incorporated protein ion channels or from lipid pores. This section is dedicated to the different kinds of ion channels and how they can be measured on a single-channel level.

4.1 Protein ion channels

When talking about ion channels people most often refer to transmembrane proteins. Proteins consist of long chains of amino acids. Forces among the units and from the external environment fold the chain into three dimensional structures known as conformational states. Protein channels are often made of several protein subunits. These subunits together form a channel with a hydrophilic environment through the membrane.

It is essential to all cells to be able to regulate the permeability and select which ions can pass. This is the function of the protein ion channels. For example, a lot of diseases, known as channelopathies, are associated to defects in protein channels and for the same reason there is a large industry of drugs designed to act on protein channels. The ion channels are also believed to be the key component in conductance of nerve signals. Hodgkin and Huxley who in 1952 measured and modeled the action potential in nerves suggested the existence of specific channels to conduct different kinds of ions. But it wasn't until twenty years later the conductance of single channels was measured. It was among others done by Hladky and Haydon who measured the conductance of an artificial membrane containing gramicidin A.[45]

The membrane is subject to a transmembrane potential generated by ionic transporters which are proteins that pump ions against their concentration gradient by means of chemical energy. In animal cells the potential is of the order of 100 mV. Differences in concentration and potential on each side of the membrane make ions diffuse from one side to the other when a channel opens.

Opening and closing of the protein channels are referred to by the term *gating* based on the idea of a gate that guards the opening. Different cellular changes can trigger gating such as voltage, binding of ligands, pH, or mechanical changes. Note that these are also thermodynamic variables that affect the state of the membrane. The molecular details of gating are still controversial.[1]

Until more detailed information of the channel structure was obtained, protein channels were only pictured as cartoons with hinges, balls, and chains. Atomic resolution of the proteins was first obtain in 1998, where MacKinnon

managed to crystallize a protein ion channel. For this he got the Nobel prize in chemistry in 2003. Crystallization has since evolved to be an important tool to determine the structure of ion channels. However so far most crystal structures are of bacterial analogs of the animal ion channels.[1] The problem of crystallography is that the obtained structure is necessarily static. Channels are expected to change conformation when they open and close so the crystal structure can only be one of these structures if any as the crystal environment is different from a natural environment.

Besides the above structural studies information about ion channels is obtained through electrophysiological measurements. Hladky and Haydon were the first to measure single channel conductance of protein channels but their method could only be used for proteins that could be separated from their natural environment and incorporated into artificial membranes. This problem was solved with the invention of the patch clamp technique by Neher and Sakmann in 1976.[46] For this they received the Nobel prize in 1991. The idea of the patch clamp technique is to separate a small patch of membrane containing only a few channels with a glass pipette. More details are given in section 4.5.2. The method is still widely used in modern electrophysiology to study the kinetics and blocking of channels. Channel blockers are agents that bind to specific ion channels and block conductance. Blocking of channels is taken as a proof of protein channel existence.

Today when one wants to make electrophysiological studies of a specific protein channel there is 3 different ways to localize it. Either it can be incorporated into an artificial lipid membrane, or one can chose a cell that is known to contain a lot of channels of the specific type (i.e. native cells), or it can be transfected into a cell which naturally have few channels in its membrane. Transfection means that one incorporate DNA that code for the channel into the cell and thereby gets the cell to express the channel. Typical cell-types used for transfection are human embryonic kidney (HEK-293) cells or chinese hamster ovary (CHO) cells.

Traditionally channels are considered to exist in a few stable conformations with almost instantaneous switches between them. One way to represent these states is by kinetic diagrams such as the one shown in figure 14. Opening and closing kinetics is fitted with a number of exponential functions to model the stochastic process of leaving a state. Each exponential term is then assumed to represent an individual conformational state. This way one might end up with more adjustable parameters than can be determined from experiment as one cannot by electrophysiological means directly measure transitions between different states with the same conductance. The kinetic diagrams is therefore a way to fit data more than a way to obtain information of the physical nature of conformational states. For more details

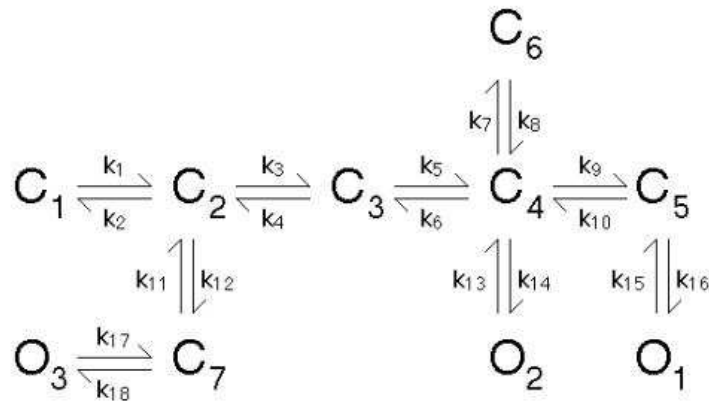


Figure 14: Example of a kinetic diagram used to model a chloride channel. Closed and open states are represented by C_i and O_i . The kinetics is described by rate constants k that is given by the probability of switch per second. Figure taken from [47]

see [47] and references therein.

Information about the design of proteins can be found by a combination of patch clamp and site directed mutations. By changing specific parts of the amino acid chain one can measure the effect on for example selectivity and gating and this way locate functional parts. But in general there is a lack of information about the complex protein channels described above. As an alternative many studies have tried to gain insight by the use of model channel structures, such as gramicidins.[8, 48, 49] Some of the advantages of gramicidin is that it is small, experimentally accessible, and well characterized and shows the same behavior as biological ion channels as for example opening and closing, ion selectivity and single file conductance. It has been shown with X-ray crystallography that the channel lumen of gramicidin and the KcsA K^+ -channel have similar diameter and a common structure of carbonyl groups of the polypeptide backbone, which is responsible for ion interactions.[49] So even though the gramicidin is unnatural with respect to some of its amino acids, it exhibits 3D structures representative of more complex channels and therefore serves as a reasonable model.

Gramicidin consists of a β -strand that forms a helical structure with 6.3 amino acids per turn. The standard conformation is therefore known as $\beta^{6.3}$. Gramicidin channels appear when monomers in each leaflet of the bilayer diffusing in the plane of the membrane meet and form a transmembrane dimer with a length of 25 Å (see figure 15). Opening and closing is a result of

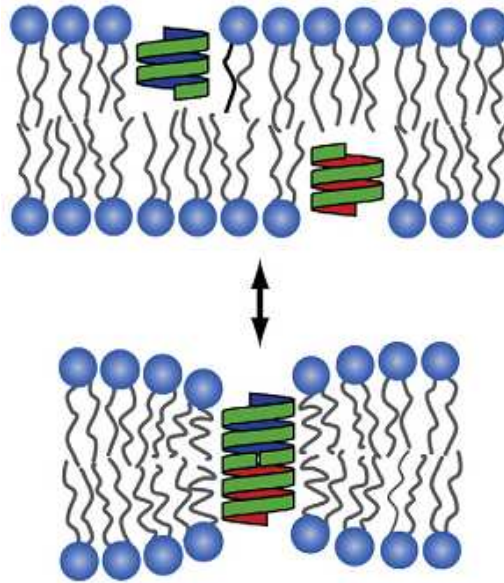


Figure 15: Opening and closing of gramicidin channels are the result of an equilibrium between monomer and dimer conformation. From [115]

dimer association and dissociation. The monomers are bound together by six intermolecular hydrogen bonds i.e. a binding energy of the order of $1-2 k_B T$ per bond. The channel is however subject to a disjoining force as hydrophobic mismatch (see section 5) induce local thinning of the membrane. This is reflected in varying channel lifetimes at different membrane thicknesses.[45, 115] The internal pore diameter is $3-4 \text{ \AA}$, which only allows for a single ion to pass at a time.

4.2 Selection of previous permeability studies

This section will go through some of the previous studies of permeability in mainly pure lipid membranes, which lay the ground of this thesis. More people than the ones mentioned here have been involved in this area. These are some of the highlights in the history of experimental investigation of macroscopic permeability and single channel events.

One of the early experiments to relate permeability and the lipid state where made by Papahadjopoulos et al in 1973.[51] They demonstrated an up to 100-fold increase in permeability for radioactively labeled $^{22}\text{Na}^+$ ions diffusing out of dipalmitoyl phosphatidylglycerol (DPPG) and dipalmitoyl phosphatidylcholine (DMPC) vesicles in their main phase transition regimes.

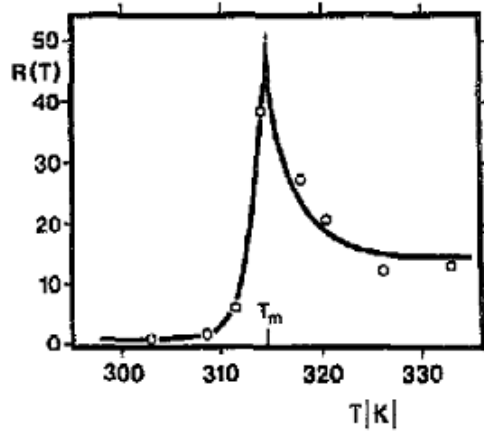


Figure 16: Relative permeability $R(T)$ of radioactive $^{22}\text{Na}^+$ as a function of temperature T in a DPPG vesicle with main transition temperature T_m . The permeability scale is relative to the permeability at $T = 298$ K. Circles represent the experimental data by Papahadjopoulos et al [51] (without error bars) and the line is calculated by Cruzeiro-Hansson and Mouritsen by Monte Carlo simulations [65] (see section 4.3.1). Figure taken from [65].

Some of the data are shown in figure 16.

The first channel events in pure lipid membranes were reported by Yafuso et al. in 1974.[52] Their experiments showed spontaneous conductance changes and multilevel conductance states in BLM experiments (see section 4.5) with oxidized cholesterol films. This was two years before Neher and Sakmann published their famous article that ascribed the quantized current events they measured to the activity of protein channels.[46]

Later experiments coupled the current fluctuations to the lipid transition. For example in 1980 Antonov et al [53] and Boheim et al [54] measured transmembrane current fluctuations at various temperatures and showed that channel events could be induced reversibly in pure lipid membranes. Kaufmann and Silman showed that they could also form reversible channels by changing pH.[55] This and similar results with transmembrane potential, pH and lateral tension lead Kaufmann et al to suggest that any mechanism causing large fluctuations in the membrane could generate lipid ion channels and they provided thermodynamic arguments that all intensive variables can influence the lipid ion channel behavior.[56] The intensive variables are in addition known to affect the transition temperature (see section 3.2). The early experiments were accused of observing channel events due to impurities in the membrane (see for example [57]). But the ability to switch permeation

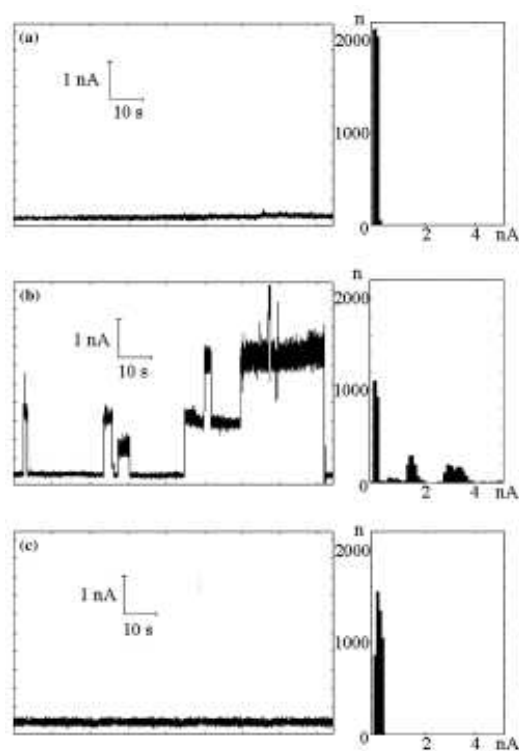


Figure 17: Electric current fluctuations and corresponding histograms in DPPC membranes in 1 M LiCl and transmembrane potential of 50 mV as presented by Antonov et al.[58] The main transition temperature of DPPC is 43°C. Currents are measured at 50°C (a), 43°C (b) and 35°C (c). n is the number of current values determined with a frequency of 80 Hz.

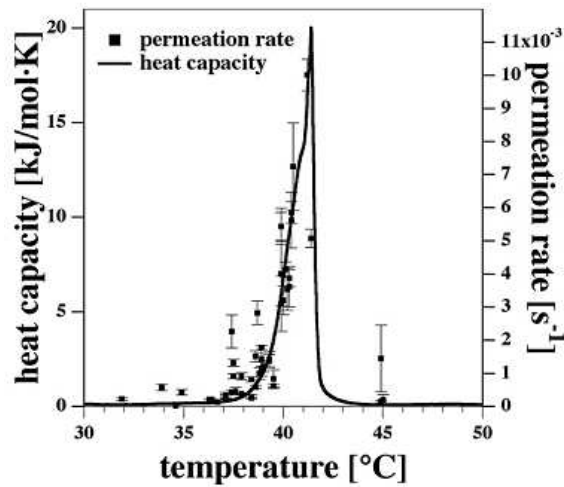


Figure 18: Heat capacity profile of 95:5 DPPC:DPPG and the permeation rate of rhodamine as a function of temperature. From [61]

on and off by changing the temperature (or other variables) speaks against it. Further experiments are nowadays made with synthetic lipids which are made to be clean.

A number of following studies have subsequently related permeability to the transition regime and/or demonstrated the channels to display quantized current steps (e.g. Antonov et al [58], Woodbury [59], Wunderlich et al [60]). Figure 17 shows an example. The lipid ion channels have been demonstrated to have similar pore radii as protein ion channels i.e. 0.7-2nm.[58, 61] Several studies have even indicated that the lipid ion channels display selectivity.[59, 62]

In the recent years our group have shown that yet another intensive variable change the permeability. Addition of anesthetics was demonstrated to make changes as predicted by their effect on the heat capacity profiles.[61, 63] It was further shown that not only ions but also the larger fluorescent molecule rhodamine leaks out of vesicles in the transition regime with a conductance that correlates within experimental error with the heat capacity profile (see figure 18).[10, 61]

Antonov et al [58] choose to name the process of quantized channel events occurring at low voltages *soft perforation* in contrast to *electroporation* that is a known and medically used increased permeability induced by pulses of high voltage [4]. Blicher et al [61] have suggested that it is actually the same phenomenon with the difference that the pore sizes are larger at high voltage.

This however requires further investigation to become a solid statement.

As a last little interesting curio the transport across primitive cells could not have relied on protein channels. Protein channels are simply too complex. Instead they have had to depend on some simple mechanism involving the membrane alone. Experiments have shown that under the right conditions simple cells are able to acquire critical nutrients from the outside.[64]

4.3 Models for lipid ion channels

As described, experiments have shown the permeability to increase vastly in the transition regime. There are two dominating views in the debate of the origin of membrane permeability. One is that it is most likely to find a channel or pore through the membrane in the interfaces between domains, which form in the transition. The other view is that to form a channel work has to be performed that is proportional to the lateral compressibility. The corresponding models are here called the domain interface model and the fluctuation model, respectively. Both models are thermodynamically founded and relate the permeability to the transition. They are minimalistic in the sense that both try to incorporate as few assumptions as possible, but they are still largely founded on assumptions. None of them suggest a detailed structural model for the defects. Such will instead be presented in the subsection about pore structure models.

4.3.1 Domain interface model

That it is the domain interfaces that were responsible for the increased permeability was suggested already by Papahadjopoulos et al.[51] Cruzeiro-Hansson and Mouritsen later followed up on the idea with Monte Carlo simulations.[65] The statement is that in the interfaces defects occur due to mismatch between gel and fluid domains which prevent optimal packing of the lipids. These defects facilitate diffusion of water and ions through the membrane. So the permeability is proportional to the fractional area of domain interfaces, which is shown to peak in the transition. In the simulation it is assumed that the probability of an ion passing the membrane $P(T)$ can be written as

$$P(T) = a_f(T)p_f + a_g(T)p_g + a_i(T)p_i \quad (28)$$

where a_f , a_g and a_i represent the fractions of membrane area occupied by fluid, gel and interfaces respectively. p_f , p_g and p_i are the corresponding probabilities of transfer for the three types of regions. It is further assumed

that $p_i \gg p_f, p_g$ for the reasons given above. There is no way of calculating the transfer probabilities from basic principles and no relevant experimental results. Instead numbers are chosen to fit the experimental results of Papahadjopoulos. The simulation compared to experimental data is shown in figure 16.

The domain interface model predicts that more cooperative transitions will have lower permeability. When the cooperativity is high the domains are larger and fewer and the total domain interface is smaller.

4.3.2 Fluctuation model

The idea of Nagle and Scott [66] is that lateral density fluctuations in the membrane create pores or cavities that ions can enter into and through. The fluctuation is here defined as an area where half of the molecules increase their area with ΔA and the other half decrease their area with the same amount. According to Nagle and Scott the change in free energy ΔF of a fluctuation compared to the equilibrium state is given by the relation below.

$$\Delta F = \frac{1}{2} \frac{(\Delta A)^2}{A\kappa_T^A}. \quad (29)$$

where κ_T^A is the lateral area compressibility defined in section 3.2.1. The probability of such fluctuation is proportional to $\exp(-\Delta F/kT)$, where k is the Boltzmann constant. This means that the probability is the same when $(\Delta A)^2/\kappa_T^A$ is the same. In other words larger κ_T^A gives larger fluctuations.

$$\kappa_T^A \propto (\Delta A)^2 \quad (30)$$

It is now assumed that the permeability P is related to the size of the fluctuations. Thus a series expansion of the permeability as a function of area change can be made

$$P = P_0 + C_1\Delta A + C_2(\Delta A)^2 + \dots \quad (31)$$

where P_0 is the permeability in the absence of fluctuations. As the permeability is an average and fluctuations are assumed to be positive and negative with equal probability, the linear term disappears.

$$P = P_0 + C_2\kappa_T^A = P_0 + C_2'\Delta c_p \quad (32)$$



Figure 19: Hydrophobic (left) and hydrophilic (right) pore as proposed by Glaser et al. Figure taken from [68]

The last equality stems from eq. 27. The equation reflects that one expects the largest permeability when the heat capacity is high i.e. in the phase transitions. It is a very simple expression directly coupled to calorimetric experiments. The theory predicts that the maximum permeability will decrease if the cooperativity of the system is lowered since low cooperativity manifests itself in lower and broader heat capacity profiles. It can for example be done with addition of anesthetics.[67] Opposed to the Cruzeiro-Hansson and Mouritsen model this model doesn't contain any adjustable parameters and it presents testable predictions.

4.3.3 Pore structure models

None of the above models provide detailed information about the nature of the pore. This is however done by Glaser et al [68]. They suggest a model where thermal motion of the lipids spontaneously create hydrophobic pores (figure 19, left). If such pore reach a critical radius of 0.3-0.5 nm it becomes energetically favorable to reorient the lipid molecules which result in conversion into a hydrophilic pore with headgroups forming the walls of the pore (figure 19, right). The hydrophilic pore is suggested to be stable with a radius of approximately 1 nm.

Molecular dynamics simulations performed by Böckmann et al [69] also suggest formation of hydrophilic pores trough intermediates (figure 20). The first intermediate is a state with tilted headgroups and the second, called a prepore, involves a state almost similar to the hydrophobic pore. However here the radius of the pore is only wide enough for a single water molecule - also known as a water file [3]. It is created by a perturbation where protruding headgroups drag their water shells with them into the membrane interior. Simulation and experiment arrive at a hydrophobic pore radius of 0.5 nm. It should be noted that the simulations are performed with the membrane exposed to a rather high voltage of 2V.

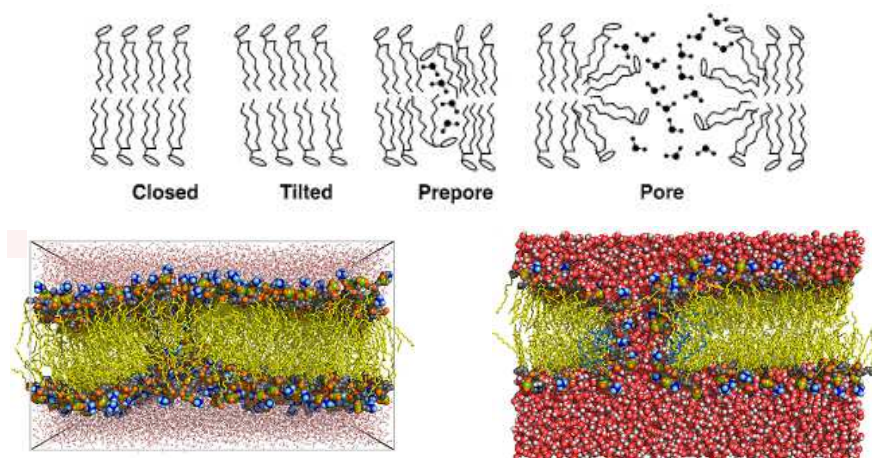


Figure 20: *Top* Schematic representation of the events leading to a hydrophobic pore suggested by molecular dynamics simulation. *Bottom* Molecular dynamics simulation of prepore (or water file) (left) and hydrophilic pore (right) in a POPC membrane with a transmembrane voltage of 2 V. Figures are taken from [69]

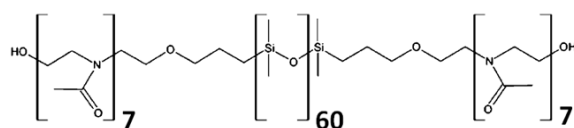


Figure 21: Chemical structure of the amphiphilic triblock copolymer poly(2-methyl-2-oxazoline)-*block*-poly(dimethylsiloxane)-*block*-poly(2-methyl-2-oxazoline) (PMOXA-PDMS-PMOXA).

4.4 Copolymer membranes as an alternative?

For years the only possibility for making electrophysiological studies of protein channels have been with the protein incorporated in lipid membranes. This raises the obvious question of whether the measured channel events arise from the protein channel or from lipid channels. In the recent years a possible alternative have emerged. Block copolymers are polymer chains linked in a series of two or more "blocks". They can be made such that they resemble the amphiphilic nature of lipids that make them self-assemble.

In this thesis I present a preliminary study of the permeability of a copolymer membrane to test its usability as a matrix for protein channel measurements. The used copolymer is made of the three blocks PMOXA₇-PDMS₆₀-

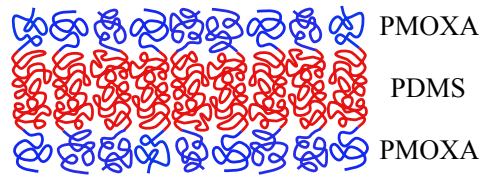


Figure 22: Triblock copolymer membrane with blocks of hydrophilic PMOXA and hydrophobic PDMS.

PMOXA₇, where PMOXA is hydrophilic and PDMS is hydrophobic. See figure 21 for the chemical structure. The copolymer form lamellar structures [70] and is therefore suitable as an alternative to the lipid bilayer (see figure 22).

Freestanding planar lipid bilayer and lipid vesicles meant for drug delivery are mechanically unstable.[70, 71] This disadvantage is claimed to be overcome by the copolymer membranes which show both higher mechanical and electrical stability.[72, 73] They additionally hold the possibility to be made even more stable by cross linking the polymers.[70] The stability and possibility of synthesizing polymers of ones needs (e.g. molecular weight, length, chemical constitution) lead to a spiring hope for copolymer membranes to be applicable in areas like screening devices, sensor technology and drug delivery.

4.5 Methods for electrophysiological measurements

There exists a variety of methods that makes it possible to place an electrode on each side of a lipid bilayer and measure single-channel events. Below I will describe a number of them, some of which I have tried myself (i.e. Montal-Mueller and tip pf pipette) and some which are widely used by others (i.e patch clamp).

4.5.1 Montal-Mueller

The Montal-Mueller setup consists of two chambers separated by a thin teflon foil (around 25 μ m thick) with a small aperture in it (typically 50-100 μ m in diameter)(see figure 23). Each chamber contains a salt solution and an electrode. After lowering the solution surface below the aperture (A) one place a drop of lipids in a volatile solvent on top of the solution. The solvent evaporates leaving lipid monolayers in the interface between salt solution and air (B). These monolayers can now be folded up around the aperture by

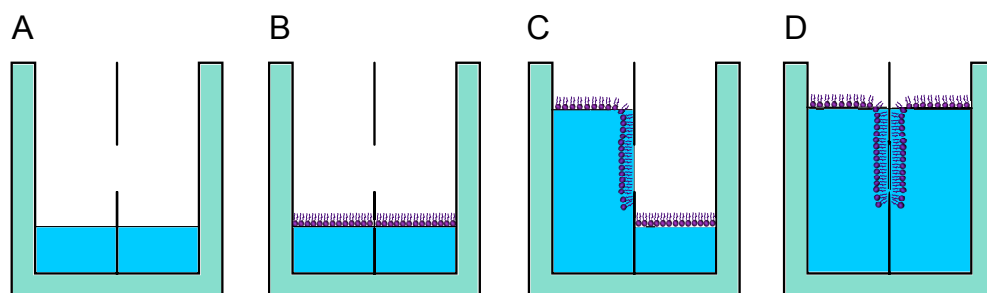


Figure 23: Schematic drawing of the Montal-Mueller technique. See text for details. The figure is not drawn to scale.

rising the salt solution level and a bilayer is formed (C-D). Most often the aperture is pre-painted with an organic solvent (e.g. [54]) possibly containing lipids (e.g. [58]) as the membranes otherwise turn out to be unstable. The membranes formed by this method is unlikely to be completely free of solvent residues.[74, 75]

This method is known as the Montal-Mueller technique after the persons who first described it.[76] The setup is also sometimes referred to as a BLM-cell. BLM is an acronym for bilayer lipid membrane or black lipid membrane. The last refers to the fact that the bilayer membrane appears dark when lit on.

4.5.2 Patch clamp

The patch clamp technique has become the standard method for single-channel measurements on protein channels in real cells after it was introduced by Neher and Sakmann in 1976 and continuously improved.[46, 77]

The name of the technique refers to a pipette with μm diameter which encloses a small area (or patch) of the surface while an electronic device maintains (or clamps) the membrane potential while recording ionic currents (see figure 24).

The configuration in figure 24 (left) is the *cell-attached* or *on-cell* mode. It allows measurements on single ion channels within the patch without disrupting the interior of the cell. Other configurations also exist (see figure 24, right). If sufficient suction is applied it is possible to break the patch while the pipette is still sealed and thereby giving access to measure on the entire area of the cell. This configuration is known as *whole-cell*. Alternatively one can detach the patched area from the cell with the patch intact and sealed

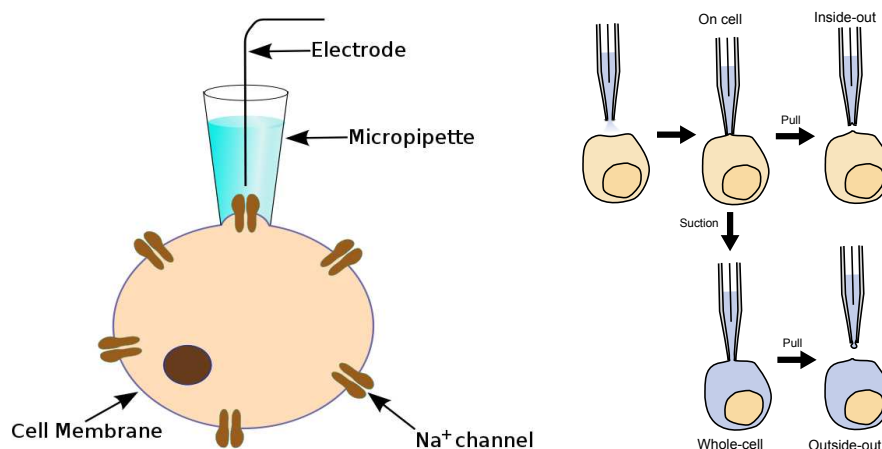


Figure 24: *Left* Schematic drawing of the patch-clamp technique. *Right* Different patch-clamp recording methods. The blue color of the cell in the whole-cell configuration indicate that solution from the pipette with time will diffuse into the cell. Figures are taken from wikipedia.org

to the pipette. This can be done with the membrane interior turning either into or out of the pipette and thereby giving direct access to either side of an asymmetric membrane. The configurations are called *inside-out* and *outside-out*.

Instead of measuring on real cells the patch-clamp technique can be applied to more controlled objects such as giant unilamellar vesicles (GUVs). These can be created with or without proteins and diameters from 1 to more than 100 μm .

4.5.3 Tip of pipette

Alternatively membranes can be formed directly on the tip of a patch-clamp pipette. One of the major advantages of this procedure is that no pretreatment of the pipette is necessary and one can therefore avoid solvent in the resulting bilayer. Two different methods can be used when creating membranes on pipettes. Both are described carefully by Hanke et al [78] including procedures for incorporation of proteins.

Droplet method The simplest way to produce a membrane covered pipette is by the droplet method. One simply dips the pipette into a beaker with water and lets a drop of lipids in a volatile solvent run down the shaft of the pipette (see figure 32). Within short time a lipid bilayer spontaneously

forms near the tip. This method will be described in details in the methods section.

Tip-dip method The other method is known as the tip-dip method referring to the tip of the pipette being dipped several times through a monolayer on the air-water interface. The monolayer can be created from lipids in a volatile solvent (e.g. hexane) similar to the monolayer in the BLMcell. Alternatively the monolayer can be formed from liposomes suspended in bath solution. Contact between monolayer and pipette has to be made very gently and the method is therefore more difficult than the droplet method.

5 Lipid-protein interactions

The people that study protein channels and the people that study membranes are to a large extent not the same. This results in explanations based on the various parts of the system instead of the interplay. This discrepancy is also seen in especially the way proteins have been described so far in this thesis. If the ultimate goal is to understand living systems it necessary to also investigate even more complex systems. In the cell membrane both protein and membranes are present. This section is devoted to looking at proteins and membranes as a whole and how they may interact.

First as an example of the clash between the protein and membrane scientist one can look at general anesthetics. Some of the first experiments within this field showed that the effect of anesthetics is proportional to its solubility in fatty substances. This was first shown around 1900 by Meyer and Overton who investigated the critical dose at which tadpoles stopped swimming and related it to the solubility in oil. This has later been described on thermodynamic grounds by Heimburg and Jackson [67] who related the anesthetic action to the state of the membrane and provided means to predict and confirm the effect of other thermodynamic variables (such as pressure, pH, and calcium concentration).

Today however focus is mainly on the proteins as the site of action as they are believed to be responsible for conductance of nerve signals. Patch clamp experiments are used to show that protein channels are inhibited by anesthetic compounds (e.g. [79] and references therein) and are used as evidence for the protein oriented view. The specific target that the anesthetic should bind to is though often unclear as known anesthetics include a range of molecules with a broad diversion in sizes and chemical properties as for example ether, laughing gas, chloroform, procaine and even the noble gas xenon.

Cantor have build a bridge between the two points of view by recognizing the alleged importance of protein channels but suggesting the blocking to be membrane mediated.[80] The idea is that that substances solved in the membrane alter the transmembrane pressure profile and that way can affect the conformation of proteins. The membrane has a non-uniform distribution of lateral pressure due to repulsion between the headgroups, attraction in the hydrophobic-hydrophilic interface and entropic repulsion between the chains (see figure 25). The hypothesis of the Cantor model is that addition of anesthetics results in an increase of the lateral pressure near the aqueous interface accompanied by a decreased pressure in the center of the bilayer. This should result in inhibition of ion channels since greater mechanical work is then needed to open them.

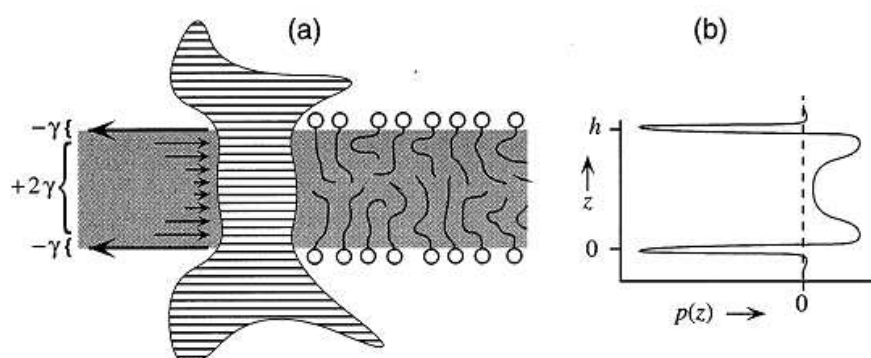


Figure 25: The transmembrane pressure profile of membranes is non-uniform due to repulsion between the head and tail regions and attraction in the interface between them. If the pressure profile is changed due to anesthetics dissolved in the membrane, the conformation of transmembrane proteins might be affected. (a) Length and direction of arrows indicate the magnitude and sign of the local lateral pressures that act on an embedded protein. (b) The corresponding lateral pressure density p through the membrane. Figure adapted from [81].

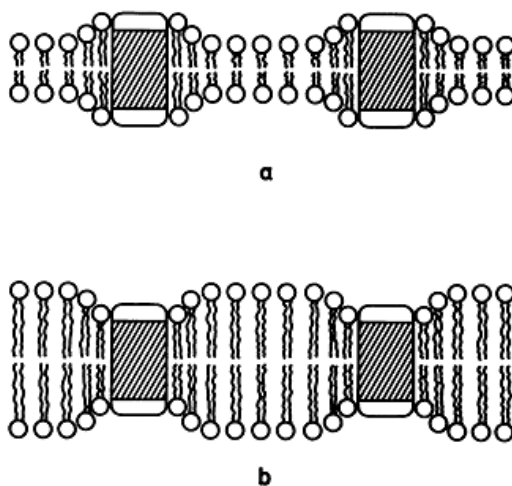


Figure 26: Hydrophobic mismatch. The boxes imitate proteins with a hydrophilic (white) and a hydrophobic (cross-hatched) part embedded in a membrane. Short lipids have to stretch (a) and long lipids have to contract (b) to avoid exposure of hydrophobic parts to the surroundings. Figure taken from [82].

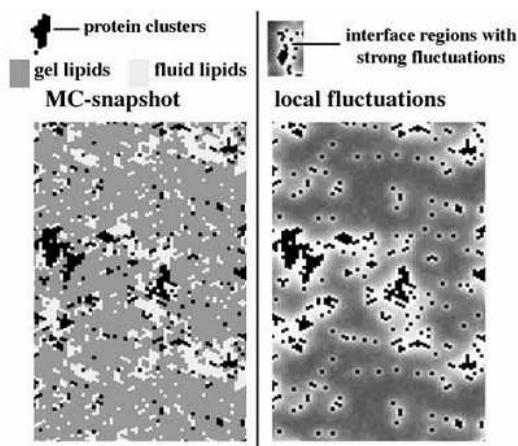


Figure 27: Monte Carlo simulations of gramicidin A in a DPPC membrane. *Left:* Snapshot of a simulation slightly below the transition of DPPC. Lipids are found mainly in gel state (grey). gA (black) aggregates in the fluid domains (white). *Right:* Magnitude of local fluctuation for the same snapshot. Dark grey are small fluctuations and white is large fluctuations. The largest fluctuations are found around the proteins. Figure adapted from [3].

Integral or transmembrane proteins all possess a central hydrophobic part which is shielded from the aqueous environment by the surrounding lipids. There can however be a mismatch between the hydrophobic part of the protein and the hydrophobic part of the lipids as described in the mattress model by Mouritsen and Bloom.[5, 82] For energetic reasons this can result in deformations of the membrane (figure 26). If the length of the protein is long the mismatch can be compensated by a stretching of the nearby lipids. The result is a perturbed region around the protein characterized by increased thickness and conformational order. If in contrast the protein is short the nearby lipid chains contract causing a thinner membrane. In a membrane with several lipid species the result of mismatch could instead be a local demixing such that species with a better hydrophobic match inhabit the vicinity. This way the protein can perform a sorting of the lipids.

The results of mismatch might be a controlling mechanism for proteins. For instance a number of integral proteins is found to function optimally in a certain thickness range.[5, 115, 83] Alterations of thickness induced by internal or external stimuli can therefore function as a trigger for enhancement or suppression of function. As example the function of gA is found to be affected by the lengths of the chains in the membrane.[84]

Another possible controlling mechanism is attraction between the proteins because of a lowering of the energetic costs by sharing a perturbed region.

One could imagine this to be important in signaling processes within the cell. Protein aggregation have been demonstrated by Ivanova et al [17] who have made Monte Carlo simulations of gA in DPPC membranes. gA is shorter than DPPC which gives an unfavorable hydrophobic mismatch in the gel phase. Figure 27 shows a snapshot from a simulation made a bit below the transition temperature of DPPC. Due to mismatch the peptides prefer lipid domains and aggregate into clusters. In addition the peptides it is shown to induce fluctuations at the interfaces of the clusters. The peptides consequently alter the elastic constants in their vicinity which increase the probability of pore formation.

Interestingly there is also indications that the activity of protein ion channels is related to the transition of the membrane they are embedded in. Seeger et al [85] have demonstrated the conductance of the pH-gated KscA K^+ -channel to follow the heat capacity profile of two different lipid mixtures. Also the open probability and dwell times seems to be altered in the transition region. Similar observations have been made by Cannon et al [86] with an other well-characterized protein channel.

A last example of lipid-protein interactions are the effect of curvature. Even though cell membranes are lamellar they also contain a considerable amount of lipids with a propensity for inverted hexagonal structures as the one shown in figure 3,C.[5] Such curved structures typically arise from lipids with a headgroup with a small cross-section compared to the chain region. These lipids induce stress in the membrane. It was suggested by Kinnunen that a way of releasing this stress is if a lipid adopt the so-called extended conformation where one of the chains extends out from the bilayer while the other chain remains within the membrane.[87] This is naturally counteracted by the hydrophobic effect but if the packing pressure within the membrane is high enough it is possible. Another possibility is to hide the chain inside a hydrophobic crevice of a protein as pictured in figure 4,D and thereby create an anchoring site for specific proteins.

An enzyme with such crevice is protein kinase C (PKC).[83] PKC is important for cellular signal transmission and is activated upon binding to the membrane. Requirements for binding are lipids with negatively charged headgroups and the presence of calcium ions. This combination result in large curvature stress. The activity of PKC is enhanced by PE lipids which have small headgroups and therefore increase curvature stress. This supports the hypothesis that PKC binds by anchoring to an extended chain. Cytochrome c have also been suggested to be able to bind this way.[88] The suggestion is among other encouraged by the finding that cyt c can bind to uncharged PEs.

6 Materials and methods

6.1 Preceding considerations about experiments with cytochrome *c* and DMPG

One of the purposes of this thesis is to observe how a non-channel protein affects the permeability of the membrane. According to previous experiments and theories described in sections 4.2 and 4.3, the permeability is strongly related to the transition of the membrane. Cyt *c* is a widely used model for peripheral protein-membrane interactions ([89] and references therein) which is known to shift the transition. Further there exist previous experiments concerning its binding to lipid membranes elucidating why it is a suitable choice for this experiment.

The effect of cyt *c* on the phase transition was investigated by Heimburg and Biltonen [41] as shown in figure 28. The more cyt *c* bound to the membrane the more the transition is shifted towards higher temperatures and the profile becomes increasingly flat. To observe a change in the permeability, it is preferential to change the heat capacity profile as much as possible i.e. having the surface saturated with cyt *c*.

In the described experiment a pure DMPG membrane was used. Such a membrane is assumed to be too unstable for the permeability measurements because of repulsion between the charged headgroups. However, high charge density is necessary for cyt *c* to bind. To increase the stability of DMPG, it is mixed with the similar but uncharged lipid DMPC. This is done in a ratio of 6:4 DMPG:DMPC (mol:mol) in search for a compromise between a highly charged membrane and structural stability. In addition, prior work on the binding of cyt *c* to membranes also employ this ratio between charged and uncharged lipids.[90] The relevant data is shown in figure 29. It is seen that the curve starts to flatten around 20 μ M cyt *c* added to 210 μ M DMPG. So in order to obtain almost full saturation the ratio of cyt *c* to lipid should be of the order 1:10. Figure 29 also shows that increasing the salt concentration lowers binding due to screening. So a low salt concentration is preferable.

Another consideration to be made for this experiment is regarding the salt solution. Firstly, it is important to ensure that the salt solution is buffered as the transition of DMPG is pH dependent.[15] Secondly, salt is necessary to measure currents but it is required to work with a low salt concentration to avoid screening effects. The Debye length κ^{-1} , which is the distance at which the membrane surface potential has decreased by a factor $1/e$, is proportional to $1/\sqrt{c_0}$, where for monovalent salts the ionic strength c_0 is equal to the salt concentration.[6] On the other hand, high salt concentrations are assumed to stabilize the charged membrane. In the experiments presented here are

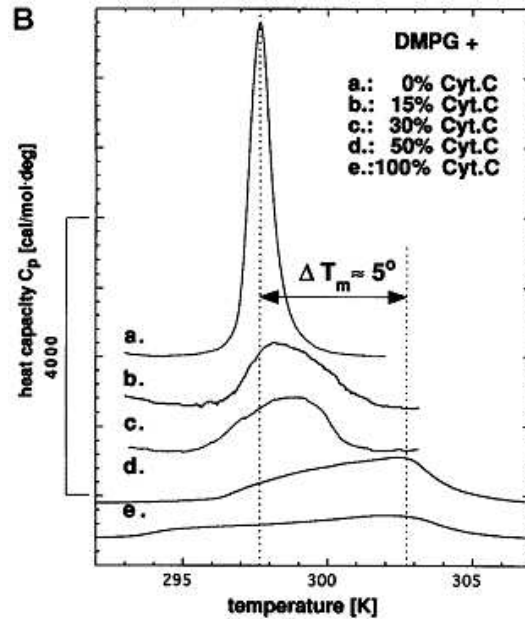


Figure 28: Heat capacity profiles of different surface fillings of cytochrome c on a DMPG membrane. Upon binding of cyt c the transition shifts to higher temperatures and the heat capacity profile becomes flatter. From [41]

performed at a salt concentration of 50mM as a start. This corresponds to a screening length of 1.4nm.

6.2 Sample preparation

6.2.1 Materials

The lipids 1,2-Dimyristoyl-*sn*-Glycero-3-Phosphocholine (DMPC) and 1,2-Dilauroyl-*sn*-Glycero-3-Phosphocholine (DLPC) and 1,2-ditetradecanoyl-*sn*-glycero-3-phospho-(1'-rac-glycerol) (sodium salt) (DMPG) were purchased from Avanti Polar Lipids, USA) and used without further purification. Copolymers of the type PMOXA₇-PDMS₆₀-PMOXA₇ (Biocure, USA) was a present from Alfredo González-Pérez. The mixtures were prepared from stock solutions of the individual lipids solved in 2:1 (vol:vol) dichloromethane:methanol. Stock solutions were kept in a -25°C freezer. All mentioned lipid mixtures are in molar ratios. All water used was MilliQ water (18.1 MΩ).

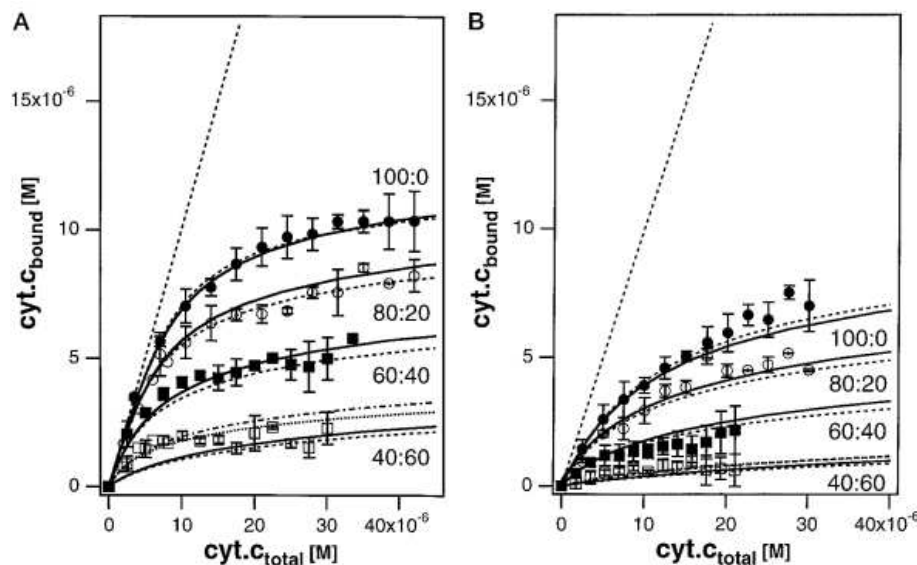


Figure 29: Binding isotherms of cytochrome *c* for mixed lipid membranes of 210 μ M DOPG:DOPC (mol:mol) mixtures at ionic strengths of (A) $[\text{Na}^+] = 45\text{mM}$ and (B) $[\text{Na}^+] = 90\text{mM}$. The higher the ratio of charged lipids the more *cyt c* binds. If the ionic strength is increased less *cyt c* binds due to screening. Adapted from [90]

6.2.2 Samples for calorimetry

After mixing of the stock solutions to the desired ratios the solvent was evaporated under a nitrogen flow. Thereafter the samples meant for calorimetry were kept under vacuum for several hours or preferentially overnight. Before adding salt solution (50mM-1M NaCl, KCl or LiCl) to the dried lipids, the salt solution was heated to above the main transition temperature. Then lipids and salt solution were stirred on a magnetic stirrer for at least 30 minutes at the same temperature. Samples were usually put in the calorimeter immediately after. Lipid concentrations for calorimetry were 10mM.

Salt solutions for measurements on mixtures with DMPG were buffered with 10mM HEPES (Sigma-Aldrich, Germany), 1mM EDTA (Fluka, Switzerland) and pH adjusted to 7.4 with NaOH. When including the counterions of HEPES and EDTA they contribute with a ionic strength corresponding to 12mM Na^+ .

To mimic the setup with a membrane in a pipette only accessible from one side, the experiments with cytochrome *c* (purchased from Sigma-Aldrich, Germany) were made on unilamellar vesicles where the protein was added to

the buffer afterwards so that cyt c only binds to one side of the membrane. Vesicles were made unilamellar by extrusion. The extruder (Mini-Extruder, Avanti Polar Lipids, Alabaster, AL) is a setup with two mechanized syringes pressing the dispersion through a polycarbonate filter with a pore size of 100nm. One of the syringes was filled with 1ml 8.3mM lipid dispersion. The extruder was placed in a heated brass block ($T=45^{\circ}C$) for about 50 minutes. The time for emptying one syringe into the other was about 2 minutes. After extrusion the lipid solution was taken from the initially empty syringe to ensure that all the vesicles had been through the filter at least once. The extruded sample was first scanned in the calorimeter. Then cyt c was added in a protein to lipid ration of approximately 1:10, stirred gently and scanned again.

6.2.3 Samples for permeability experiments

After mixing the stock solutions, the solvent was evaporated under a nitrogen flow and put in vacuum for half an hour. The lipids were then dissolved in 4:1 (vol:vol) hexane:ethanol to a concentration of 1-2mM. Beaker and pipette were filled with the same salt solutions as those used for calorimetry.

gA was added as as a 1:1 mixture of 1mM 10:1 DMPC:DLPC in 4:1 (vol:vol) hexane:ethanol and 1nM gA in ethanol i.e. a solution of 0.5mM lipids and 0.5nM gA.

Polymer experiments were made with a 1.2mM solution where the polymer powder was dissolved directly in 4:1 (vol:vol) hexane:ethanol. gA was added as 50 μ l 10nM gA in ethanol to 500 μ l of the polymer solution i.e. a concentration of approximately 1 nM gA.

6.3 Calorimetry

A differential scanning calorimeter (DSC) was used to measure the heat capacity during phase transitions. The calorimeter used was of the type VP-DSC produced by MicroCal (Northhampton/MA, USA). The DSC consists of two cells with capillaries in an adiabatic box isolated from the surroundings (figure 30) One cell contains the sample and the other one is a reference, which in this case contains whatever solution the lipids are dispersed in.

The DSC can be set to continuously change the temperature T of the cells and simultaneously maintain the temperature difference between the cells at zero. The excess power $\Delta P = P_s - P_r$ necessary to heat the sample cell compared to the reference cell is recorded. The excess heat ΔQ is then found by integration of the excess power with respect to time t .

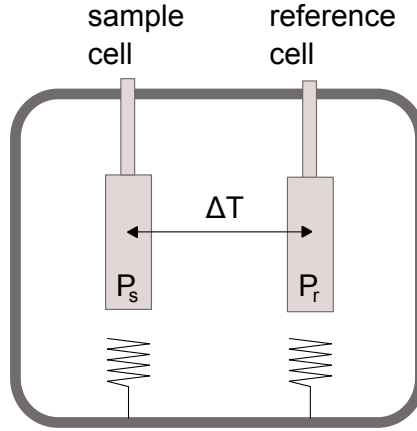


Figure 30: Schematic representation of a differential scanning calorimeter (DSC). The two cells are encapsulated in an adiabatic shield. Each cell is heated at a constant rate such that they both have the same temperature. During scanning the difference in heating power between the two cells is recorded.

$$\Delta Q = \int_t^{t+\Delta t} \Delta P(t') dt' \simeq \Delta P \cdot \Delta t \quad (33)$$

At constant pressure and volume the (excess) heat capacity C_p is given by

$$C_p = \left(\frac{\partial Q}{\partial T} \right)_p \simeq \left(\frac{\Delta Q}{\Delta T} \right)_p = \frac{\Delta P}{\frac{\Delta T}{\Delta t}} \quad (34)$$

where $\frac{\Delta T}{\Delta t}$ is the scan rate. That way the DSC provide information about the heat capacity of the sample as a function of temperature. A temperature induced transition in the system (e.g. lipid melting or protein denaturation) requires extra heat and therefore a higher power in the sample cell. This turns out as a peak in the heat capacity profile.

6.4 Permeability experiments

6.4.1 Setup

The central part of the setup is a beaker with salt solution in a brass block with water circulation (Haake DC30-K10, Biolab) for temperature control (see figure 31). The temperature is measured either with a thermometer (P650, Dostmann Electronics, Germany) or a home-build thermocouple with

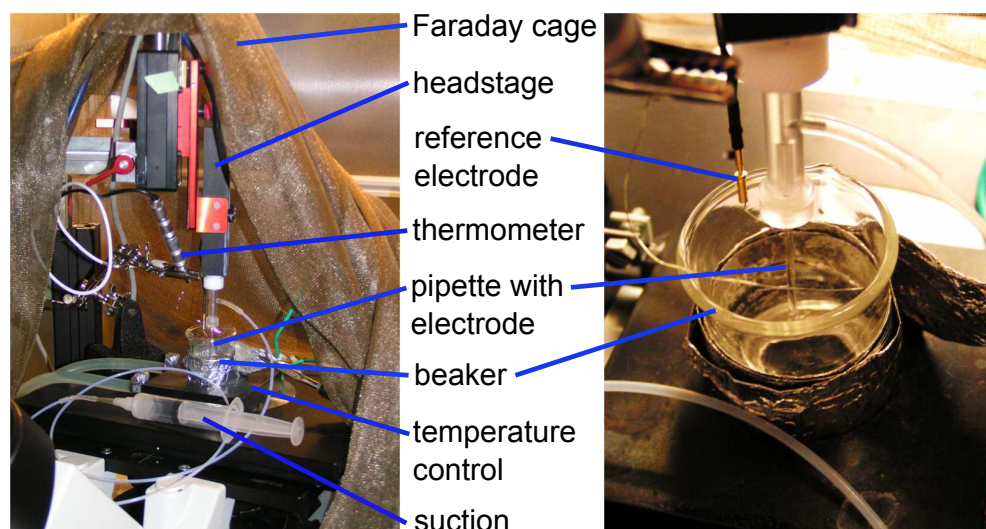


Figure 31: Pictures of the setup for permeability experiments.

automatic data recording. The precision of the thermometer is within 0.1°C . Unfortunately it turned out that there were some drift in the calibration of the thermocouple so that the temperature is only true within $1\text{-}2^{\circ}\text{C}$. Temperatures measured with the thermocouple is therefore given without decimals. Above the beaker is placed a pipette containing an electrode. The electrode is connected to an axon headstage (Molecular Devices, USA) which preamplifies the signal. Another electrode is connected to ground on the headstage and placed in the beaker. One has to make sure that the reference electrode does not touch the pipette as this can result in a membrane-like capacitance response. The headstage amplifier was mounted on a micromanipulator (model SM1; Luigs and Neumann, Germany) so that the pipette can be dipped slowly into the bath solution. The membrane conductance was further amplified with an Axopatch 200B patch clamp amplifier (Molecular Devices, USA) run in voltage clamp whole cell mode. The currents were filtered with 2kHz internal 8-pole Bessel filter of the Axopatch 200B. Signals were digitized with a sampling frequency of 10 or 20 kHz which corresponds to a time resolution of 0.1 or 0.05ms. The currents were filtered with a 2kHz Bessel filter build into the the Axopatch 200B.

Software used for recording of current traces was Clampex 9.2 (Axon Instruments) with the use of a 12-bit AD converter (DigiData 1200 series, Molecular Devices, USA).

The gain⁷ was set as high as possible as this reduces the noise and in-

⁷Gain is the ratio of the signal output to the signal input. A gain of 10 means that

creases the resolution. Too high gain however leads to saturation of the AD board. Gain set above 10 did not have any visible effect on the noise level, so this was the gain used when possible. The data was adjusted to the gain setting automatically.

Data is analyzed and graphs produced in IgorPro with the help of procedures written by Andreas Blicher.

6.4.2 Pipette preparation

Pipettes were pulled from 1.5mm glass capillaries (World Precision Instruments, USA) in a vertical PC-10 puller from Narshige, Japan. A two-step pull was performed: First step with a distance of 8mm and heat setting of 80% of max. In the second step the heating coil was lowered 4mm and heat was set to 45% which pulled the capillary apart. The ideal is the narrowest part to be short in order to lower the resistance and thereby reduce noise.[?]

Subsequently the pipettes were fire polished. Fire polishing of the tip is not essential, but makes bilayer formation easier.[78] Typical diameters of the tip were 5-15 μm . The pipette diameters were estimated by eye on a 10 μm scale. In some experiments the unpolished pipette is used. These will be referred to as mini pipettes. Their diameter is less than 1 μm .

The pipettes can be reused immediately after membrane breakage for a couple of times. The reuseability of the mini pipettes is less than for the fire polished ones as they have a higher tendency to clog after repeated use. The stability of the membranes are typically from minutes to hours. In some cases membranes made on a mini pipette have been stable until the next day.

Pipettes were only filled half with the salt solution as overfilling can cause solution to spill over into the pipette holder, which introduce additional background noise.[91] Possible air bubbles were removed before an electrode was inserted. The electrodes were made of chlorinated silver wires, which were rechlorinated frequently to prevent baseline drift and additional noise.[91]

6.4.3 Silanization

Some of the pipettes to be used with DMPG mixtures were silanized in an attempt to make the charged membranes more stable. The silanization was done after a protocol made for mica sheets from SPI Supplies⁸ but adjusted to capillaries. Capillaries were stored in 2% 3-aminopropyltriethoxysilane (3APTS) in acetone at 50°C for 24h in a closed glass container. Afterwards

you take one tenth of the original input and use the original number of bits to describe it. This means you get a higher resolution.

⁸www.2spi.com/catalog/submat/silanize-mica.html

the were cleaned by dipping the capillaries in acetone and flushing them through by attaching a syringe in one end. The same procedure was done with water after which the entire cleaning procedure was repeated.

Pipettes were pulled as described above after drying the capillaries under vacuum for half an hour. Capillaries not to be used right away were stored in a water filled container.

6.4.4 Bilayer formation and capacitance test

As the membrane is not directly visible in the pipette a capacitance test is made simultaneous to the membrane formation. This makes it possible to follow and confirm the formation. The background for this method is that the membrane consist of an insulating layer of lipids that separate two conducting ionic solutions and therefore acts as a capacitor with a capacitance of 0.5-1 μ F/cm². [4, 92, 93]. The formation technique and the capacitance test is shown in figure 32.

In general for a capacitor the electric charge Q that accumulates on the plates in response to applied voltage U is given by

$$Q = C \cdot U \quad (35)$$

where C is the capacitance. Assuming a constant capacitance, differentiation of the above with respect to time gives

$$\frac{dQ}{dt} = I = C \frac{dU}{dt}. \quad (36)$$

It is now seen that the current I is proportional to C . Therefore applying a triangular voltage pulse i.e. having $|dU/dt|$ a constant, makes it easy to read of the capacitance. The triangular voltage used had a slope of 100mV/5ms. An ideal capacitor would provide a rectangular response to the triangular voltage pulse. The membrane however is non-ideal meaning that it is not completely insulating. This results in a resistive current overlapping the capacitative response with a slope $I = U/R$.

When the pipette is above the water surface a pure capacitative response from the headstage is seen as a squared current pulse with an amplitude of 110pA (corresponding to a capacitance of 5.5pF). As the pipette hits the surface and the electrode gets in contact with water the system short circuits giving an infinite current amplitude as seen in figure 32, second column. When the solvent is evaporated a capacitative response is again seen somewhat higher than before. The slope arises because the seal is not completely tight giving the overlapping ohmic response. Only membranes with seals

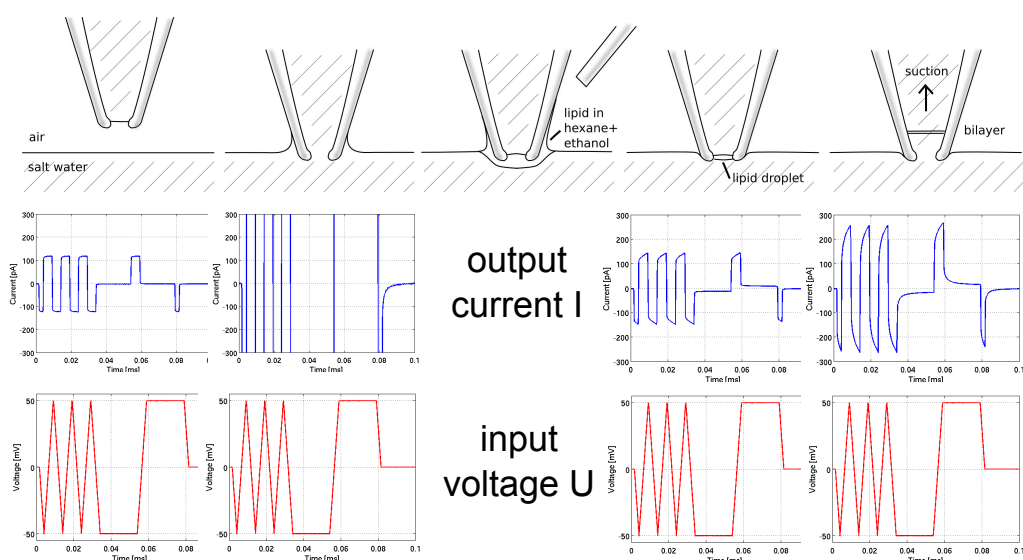


Figure 32: *Top* Procedure for bilayer formation: The pipette is dipped slightly below the surface of a salt solution. A few microliters of lipids dissolved in a mixture of hexane and ethanol are let to run down the side of the pipette. The solvent is highly volatile and evaporates which leaves only lipids at the tip. The droplet might consist of several layers but by applying a bit of suction get the lipids to thin out into a single bilayer. *Mid and bottom* Measurements of current as a function of time (output) induced by a triangular voltage pulse (input) made simultaneous with the membrane formation. Before the pipette enters the salt solution a squared current is seen corresponding to a perfect capacitor. Dipping the tip into the solution results in short circuiting seen by the vertical lines in the current trace. When one or more membranes are formed the current response is again capacitive but this time with a slope on top due to leak through the membrane or at the rim.

above $1\text{G}\Omega$ are accepted. They do however often loosen during the experiment. Very high seals are often an indication of multiple membranes. If the capacitance is too low suction is applied and in the end a reasonable capacitance is achieved. After membrane formation the pipette was sunken 2mm below the surface to prevent loss of water contact caused by evaporation.

It is not a problem to see that something has formed, but one drawback of this method is that it is difficult to see if it is a single or multiple membranes. The reason is that with these small pipettes the capacitive contribution from the bilayer is small and the exact contribution from the pipette in water is impossible to measure. Assuming a membrane capacitance of $1\mu\text{F}/\text{cm}^2$ a pipette of $5\mu\text{m}$ diameter will only result in a 4pA current increase and the double for a double bilayer. This is very small compared to the total current. However when I see events I assume it to be a single membrane. Membranes not showing events at certain conditions have always been shown to be able to show events at other.

6.4.5 Addition of cytochrome c

Cyt c was added by letting a 15 μl drop of 2mM cyt c in buffer run down the shaft in the same way as when forming a membrane but after formation of and a membrane displaying activity. To ensure that the effect of cyt c is not purely mechanical from the impact of the drop on the surface control or due to a different chemical potential across the membrane, experiments with 2mM glycerol in buffer were performed prior to cyt c addition.

7 Results and discussions

In this section I will present the results obtained during the experiments. The results have been divided into sections with the associated discussions directly following.

7.1 Membrane formation techniques

During the work with this thesis I tried some of the different techniques described in section 4.5. Here is given my experience together with some advantages and disadvantages that I have become aware of.

The Montal-Mueller technique might be the most used method when studying channel events in artificial membranes. However for me formation of membranes with this technique turned out to be problematic. That this technique is not always reliable to function is also claimed by Erhlich [94] who first cites Finkelstein for stating:

”... that some manipulation of variables is required before everything is working properly. Then, one can make stable membranes quickly and reliably for week after week until, as happens for everyone I know who works with this system, one day a stable membrane cannot be formed. After a few agonizing days of changing and permuting the lipid, the septa, the brush, the distilled water source, and your socks, everything works properly again. Most likely, the conditions are the same as before.” I have been asked many times if it is truly necessary to change your socks. The answer is yes.

Apparently I never changed to the right pair of socks during the couple of months I tried getting the Montal-Mueller technique to work. I tried with a number of different holes in the teflon foil made by lasers, heated needles, unheated needles and/or sparks, I tried different lipid mixtures, different concentrations, different prepainting procedures and different temperatures, but never got any reproducibly stable membranes. The mixtures, concentrations and prepainting procedures I used were all described in the literature. The only thing I never got to change was the lipid solvent, which is the one used by Antonov [58] who has worked with this technique for more than 30 years.

As always with experimental work there are days where nothing works. But in comparison with the Montal-Mueller technique it is very easy to form membranes with the droplet technique - at least for some lipid mixtures. Especially a 10:1 (mol:mol) DMPC:DLPC mixture was pretty reliable and

fulfill requirements of not having a too narrow main transition near room temperature. Mixtures of DMPC with at least half DMPG was unfortunately less trustworthy. Others have reported that unsaturated lipids should make especially stable membranes in BLM-cells [75] but they didn't show extraordinary results in my experiments.

When it comes to solvent residues in the membrane, which surely affect its behavior (e.g. [63]), the patch-clamp technique and tip-dip made from vesicle suspension are the only ones that definitely can be claimed to be solvent free. With the patch-clamp technique one is however limited to work with lipids that can form large, stable, unilamellar vesicles opposed to tip-dipping. The fact that membranes formed with the Montal-Mueller technique are only stable when pre-painted with a usually non-volatile hydrocarbon solvent indicates that solvents are at least present at the rim of the membrane.[74] Another indication is that the thickness of a BLM-membrane is found to change depending of the solvent and independent of the lipid.[95] The same investigation have not been performed on droplet formed membranes. Both when using the Montal-Mueller technique and creating membranes with the droplet method the membrane forming lipids are initially dissolved in some solvent which is expected to evaporate or dissolve in the surrounding water. Hexane is highly volatile but possible non-evaporated residues have a partition coefficient that vastly favors solution in the membrane.⁹ Ethanol shows a slight preference for the aqueous phase. Membranes formed with the droplet technique however probably contain less solvent than those formed with the Montal-Mueller technique as no pre-painting is required.

The bilayer created with the tip-dip method should be less stable than one made by the droplet method.[78] This could again indicate that droplet formed membranes are not completely solvent free but it could also be caused by a less protected position of the membrane. According to Hanke [78] the tip-dip membrane is positioned on the extreme tip of the pipette while the droplet membrane is formed inside the pipette.

Advantages of the tip-dip method and the BLM-cell are that one can make bilayers with different lipids in each layer. If one needs to change the environment on both sides of the membrane or change it after a membrane is formed the Montal-Mueller method seems to be the easiest choice. It is difficult to access a pipette solution after membrane formation, but asymmetric conditions can be made prior to membrane creation.

Temperature control is essential when investigating channel events in pure

⁹Partition coefficients K are defined as the substance's concentration in octanol divided with its concentration in water in equilibrium. For ethanol $K = 0.5$ and for hexane $K = 7940$. Values can be found at <http://logkow.cisti.nrc.ca/logkow/>.

lipid membranes. When using "tip of pipette"-techniques it is impossible or undesirable to bring the tip lower than just below the surface. This position might not have the exact same temperature as the rest of the solution. On the other hand pressure control is a possibility when using pipette based methods.

A very significant part of the noise especially in BLM-cells is related to the capacitance of the membrane which is again proportional to the area.[96, 97] That means that the larger the membrane area the larger the width of the noise as seen on the current measurement. In the pipette based setups the membrane contribution to capacitance is negligible compared to the rest of the system which is mostly the same as in the BLM-cell. The only exception is the pipette, whose capacitance increases almost linearly with the depth.[96] Sylgard which is normally used in patch-clamp experiments to reduce noise (among others by reducing capacitance) cannot be used for the droplet technique as the lipid solvent also dissolves the sylgard when floating down the shaft.[78] So using the Montal-Mueller technique limits the resolution. On the other hand the negligible capacitance also makes it impossible to use this as a verification of a single bilayer.

Another obvious consequence of the membrane area in droplet versus Montal-Mueller technique is that smaller amounts of potentially expensive lipids and proteins that are necessary in the first mentioned.

The last things to be aware of have to do with the geometry of the setup. In the Montal-Mueller technique one can use the same aperture for a long time while recycling of pipettes is limited. It might affect the reproducibility of an experiment that the area changes from one experiment to another. Especially when one can not correct for it as the area inside the pipette is unknown. Experiments have been performed with fluorescent lipids to see where in the pipette the membrane actually formed but lipids at the pipette surface glowed too much compared to the membrane.

It is not uncommon that membranes formed with the droplet method behaves differently at a certain voltage if the sign is changed. There is even examples of shifting voltage have had a stabilizing effect on the membrane. This is immediately unexpected from a supposedly symmetric membrane. Symmetry of lipid ion channel current have been reported with the Montal-Mueller setup.[58, 63] Berestovsky et al [24] on the other hand report of an unspecified structural asymmetry and sensitivity to the sign of the voltage after long duration of a constant voltage in a Montal-Mueller-like setup. It is likely to be the same observation made with the pipette setup. That membranes in a pipette show asymmetry may also be explained by the asymmetry of the setup. The sides of the pipette tip are inclined. It is conceivable that an altered voltage is associated with a physical movement of the membrane

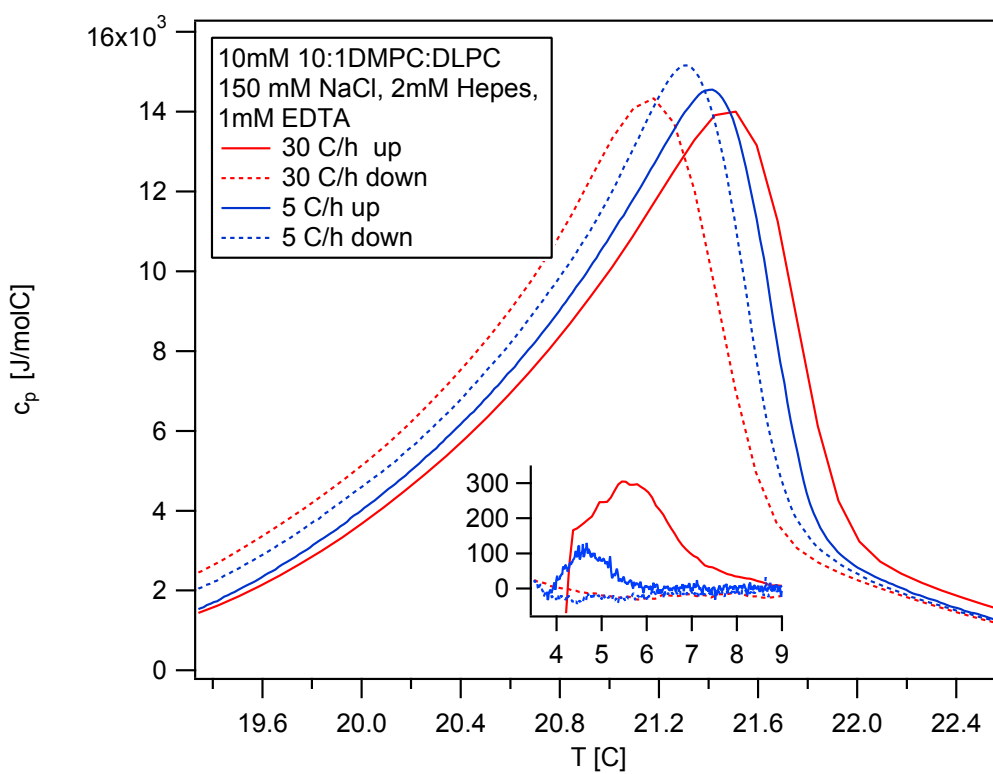


Figure 33: Detail of the main transition in the heat capacity profile of 10:1 DMPC:DLPC. Both up and down scans and scans at 5°C/h and 30°C/h are shown. There is no considerable hysteresis. The inset shows the position of the pretransition.

especially for charged lipids.

7.2 Calorimetry

Figure 33 shows the heat capacity profile of 10:1 DMPC:DLPC. The profile have been made at different scan rates of 5 and 30°C per hour and in both scanning directions in order to examine possible hysteresis effects. For the high scan rate the peak is found at 21.2°C for the downscan and at 21.5°C for the upscan. For the low scan rate the difference is less. The hysteresis effect for the main transition is thereby found to be almost negligible compared to the precision of the temperature measurements. The pretransition is more sensitive to scan direction and disappears in the downscans.

During the extrusion procedure of the 6:4 DMPG:DMPC dispersion there

was a loss of lipid solution. Whether it leaked out or evaporated is not clear, so the exact concentration subsequently scanned in the calorimeter is unknown. The initial 1ml of 8.3mM solution was reduced to 0.65ml which gives a concentration between 8.3mM and 12.8mM. To be sure to have enough protein cyt c was added to reach a concentration of 1.5mM which should be sufficient for saturation cf. figure 29. The exact concentrations are anyway not that important as it is the transition temperatures that are of interest. So when looking at the heat capacities one should note that only the relative numbers are exact. The heat capacities have been calculated assuming a lipid concentration of 10mM.

Figure 34 shows consecutive scans of cyt c bound to the outside of unilamellar vesicles. 4 peaks are observed. The first two with peak temperatures at 17.6°C and 23.35°C can be related to the pre- and main transition of the membrane respectively. The pretransition is very sensitive to scan direction and moves to lower temperatures at downscans. The main transition is at practically the same temperature at all scans. The third peak at 62.5°C is attributed to the denaturation of cyt c bound to the membrane and the peak at 78.5°C to denaturation of free cyt c in the solution. Denaturations are irreversible opposed to the lipid transition. It is seen that the lipid transition changes when cyt c is denatured. When only the bound cyt c is denatured one still sees a narrow peak on top of a peak that have become broader towards lower temperatures. Maybe a bit surprising the denaturation of free cyt c also affect the lipid transition by eliminating the narrow peak.

That the protein denatures at different temperatures depending on if it is bound or not and that the lipid transition is influenced by the state of the protein are examples of how membrane and protein influence each other. This is further demonstrated by the fact that the lipid transition is affected by cyt c being bound or not. Figure 35 shows heat capacity profiles of the same extruded vesicles with (red) and without (blue) cyt c added to the outside of the extruded vesicles.

The splitting of the peak in the protein free 6:4 DMPG:DMPC mixture was initially thought to be due to a separation of the two lipid species. But care was taken that the stocks of the two lipids were mixed properly before drying and PG and PC with equal chain length are known to mix almost ideally [90, 98]. A similar splitting have previously been observed for extruded vesicles of DMPC [11] but I also see it for non-extruded vesicles (data not shown).

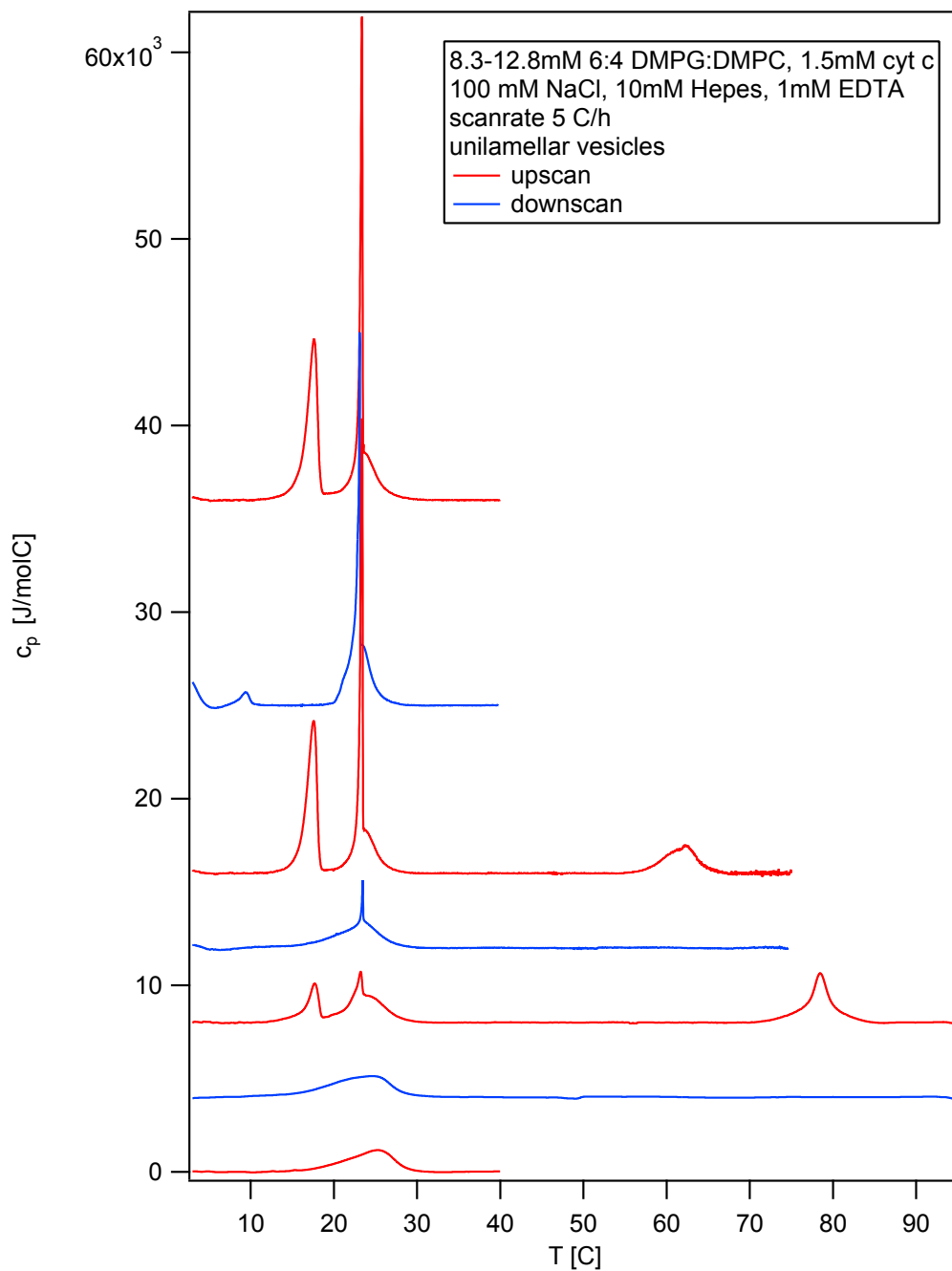


Figure 34: Consecutive scans of 8.3-12.3mM 6:4 DMPG:DMPC, 1.5mM cyt c in 100mM NaCl. The top trace is the first scan. The numbers of the y-axis is calculated assuming a concentration of 10mM.

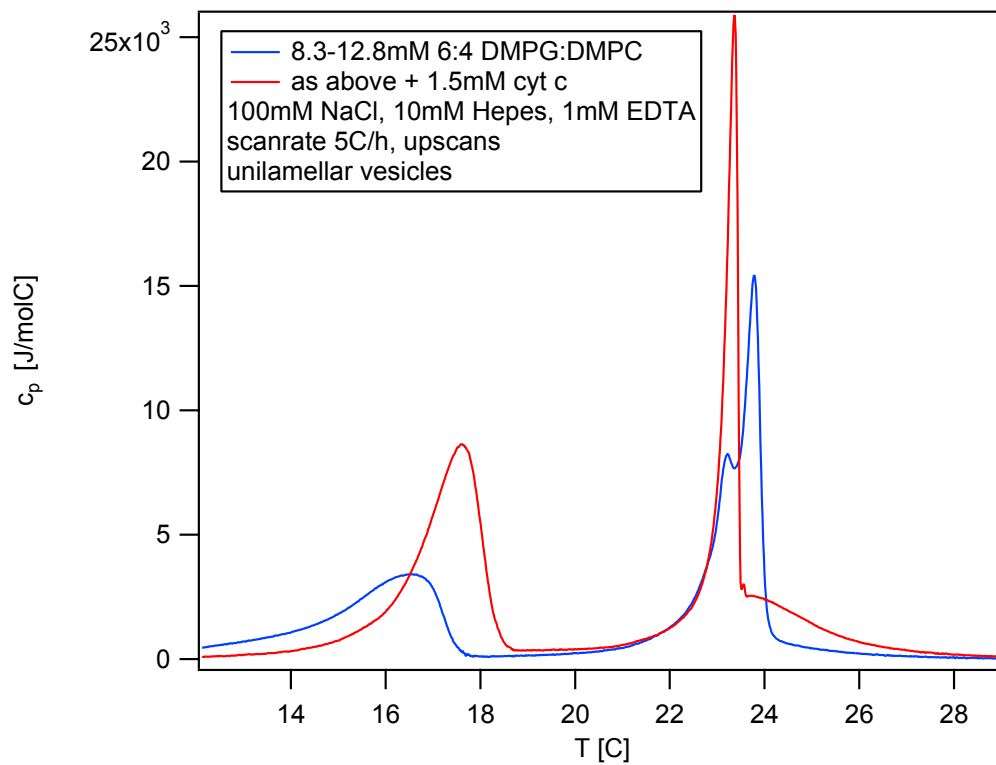


Figure 35: Heat capacity profile of extruded vesicles of 6:4 DMPG:DMPC with and without cyt c bound to the outside.

7.2.1 Discussion

The main purpose of making the heat capacity profiles is to be able to relate the permeability to the state of the membrane and possibly directly to the heat capacity profile as suggested by the fluctuation model. Other interesting results can however also be extracted from these profiles. But first a discussion considering the main objective.

Figure 33 show that one do not have to be very careful about making slow temperature changes and in which direction temperature is changed. gA is known to have little influence on the lipid transition except at high concentrations [17] so the same heat capacity profile is valid for experiments with gA added.

Figure 36 is a zoom in on the main transition in the scan shown in figure 35. If the permeability of the membrane is proportional to the heat capacity as stated in the literature one would expect a significant change if the experiment of adding cyt c to a preformed membrane is made at 23.8°C. This will

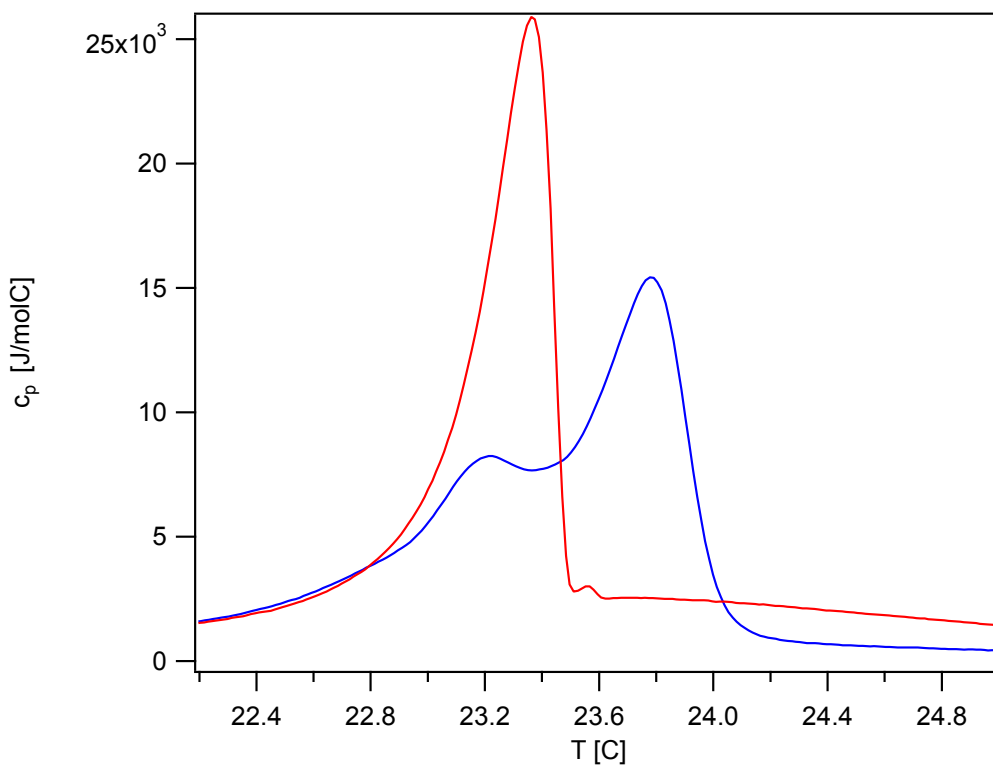


Figure 36: Detail of main transition from the scan shown in figure 35 with the same color code.

therefore be the temperature used.

As described previously the transition is sensitive to a number of thermodynamic variables. Of significance here is the transmembrane voltage which is present in the permeability experiment but not in the calorimetry experiments. In principle the voltage can change the heat capacity profile but it is not certain exactly how the membrane is affected and if there is a significant effect on the transition temperature cf. section 3.3.

The transition of the single membranes in the pipette setup may be expected to have a bit wider transition than the multilamellar vesicles shown in figure 33 because the multilamellar vesicle profile is affected by additional inter layer cooperativity.

The heat capacity profile of unilamellar vesicles with cyt c shown in figure 34 is a nice example of the interaction between protein and membrane. The denaturation temperature of free cyt c in buffer is reported to have a midpoint of 82-83°C.[99, 100] The temperature found here is a bit lower. It is well

established that the denaturation temperature of *cyt c* is lowered by around 20-30°C when it is bound to a charged membrane.[99, 100, 101] How much it is decreased depend on the membranes surface density of charges i.e. the fraction of DMPG.[99] Linear interpolation of the data presented in reference [99] gives a denaturation temperature of bound *cyt c* of 65°C which is again slightly higher but close to the value found in this study.

That bound *cyt c* denatures at a lower temperature is explained by what happens upon binding. Several studies indicate a loosening or destabilization of the tertiary structure¹⁰ of the protein when it binds to a charged surface.[7, 100, 101] This changed bound state is suggested to be important for the function of *cyt c* in the mitochondria.[99, 102]

The protein binding is found to not only affect the protein itself but also the membrane. In the presented experiments it is found that without *cyt c* one gets a splitted peak in the main transition. With *cyt c* there is a higher peak where the first peak was before and a smeared out peak where the second peak was before. At saturation previous publications describes a single smeared out peak ranging from some degrees below to 5 degrees above the protein free transition cf. figure 28, trace e. As expected a smaller effect is seen here as this study is made with a mixture with DMPC opposed to the data presented in figure 28 which are made with pure DMPG.

With a purely electrostatic interaction between *cyt c* and the membrane one would expect an increased transition temperature when the protein is bound.[6] This is because the charge density is higher in the gel state than the liquid and the electrostatic binding therefore will be stronger to gel state lipids. As seen both in the present data and in figure 28 the interaction is not that simple so other kinds of interactions must also be present.

The origin of the first high peak with *cyt c* is unknown but have been observed in several similar heat capacity profiles made from different stock solutions (data not shown). The changed membrane transition upon denaturation is probably related to the finding that *cyt c* aggregates on the lipid surface when it denatures.[89]

7.3 Different membrane behaviors

Even though articles normally only show the nice quantized current events, this is not the general behavior of membranes in the real world. A considerable amount of data consists of artifacts and more or less explainable incidents. Quite often you even see a number of different behaviors and a

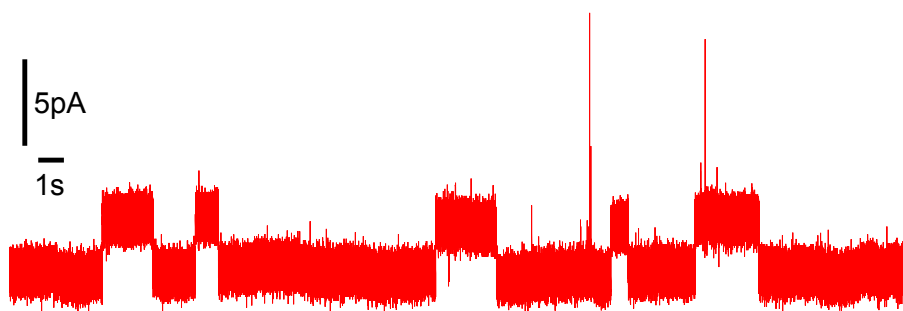
¹⁰The tertiary structure of a protein refer to the three dimensional structure of the entire polypeptide chain. The tertiary structure is closely related to the function of the protein.

variety of conductances performed by the same membrane. An example of this is shown in appendix A. Below is an attempt to draw out some of the typical behaviors. These are standard examples. In practice they are not well defined and all kind of combinations are just as likely which sometimes makes it difficult to distinguish them. I have tried to find the most illustrative examples which is why the illustrations are made under different conditions. They are however representative for all membranes unless otherwise stated. All the shown traces are measured under positive voltages. It means that opening of a channel corresponds to an increased current.

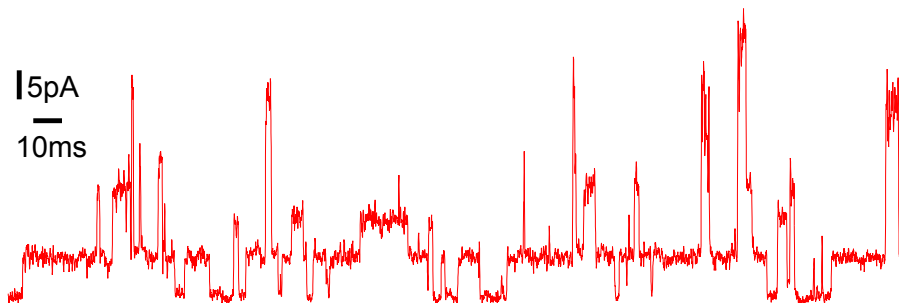
Stable quantized events The quantized events are reversible changes in current in a step-like manner. Sometimes several steps can be observed on top of each other. The quantization is however only within limited periods of time as the conductances change from patch to patch and even during measurements on the same patch. Conductances between less than 10pS and at least 2000pS have been measured. Examples of high conductance events are shown in appendix B.

Within the same trace there may be periods with openings of different current amplitudes. Some of them can be interpreted as multiple channels with the same conductance but stable current levels that can not be explained this way can also be found. The less occurring current amplitudes are denoted subconductance. A trace with these substates is displayed in appendix B.

As also shown in appendix A the same membrane can show different timescales for the events. The two examples below are from the same membrane in one case displaying open times of seconds and later showing openings with a duration of milliseconds.



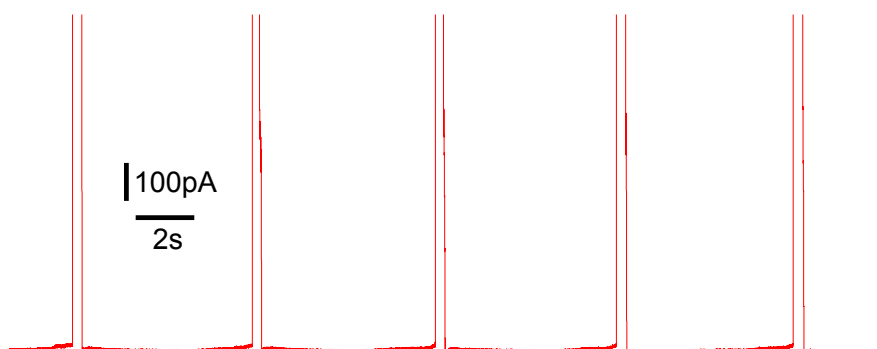
10:1 DMPC:DLPC, 150mM KCl, U=200mV, T=20.6°C, baseline drift subtracted.



10:1 DMPC:DLPC, 150mM KCl, $U=200\text{mV}$, $T=20.6^\circ\text{C}$

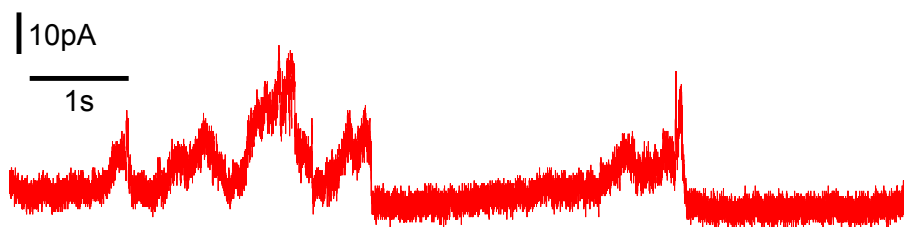
Overload events Overload events are events with a conductances so high that they are above the range possible to measure with the usual settings i.e. a current above 1000pA. Openings and closings are apparently instantaneous. The lowest voltage at which they have been observed is 100mV. Most often the measurement have been stopped or the voltage changed when these events occurred so the amount of data is not tremendous. They have however been observed several times especially in charged membranes. In a few cases the gain setting have been decreased in order to allow higher currents. In some case the top became visible. The data is shown in appendix B. The top turned out to be asymmetric with a conductance between 10000pS and 50000pS. They are not necessarily periodic as those shown below.

It have been investigated whether the overload events were associated with a low seal resistance ($<1\text{G}\Omega$). It turned out only to be the case for the charged membranes, which in general often have bad seals.



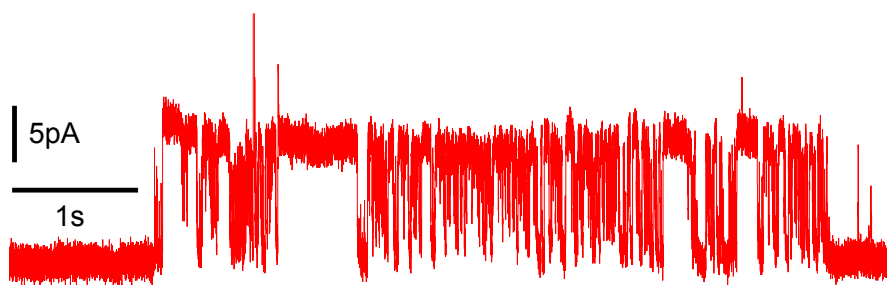
6:4 DMPG:DMPC, 100mM NaCl, 10mM HEPES, 1mM EDTA, $U=50\text{mV}$
 $T=23.8^\circ\text{C}$

Non-quantized events Events similar to described above can also present itself in a non-quantized manner. They are mostly distinguishable from random fluctuations due to a tendency to return to a relatively stable baseline level. Sometimes it is just a deviation from white noise with an asymmetry towards open states. It can be very difficult to see from a small section of a trace but becomes more clear when the general behavior over longer time. Additional figures can be found in appendices A and B.



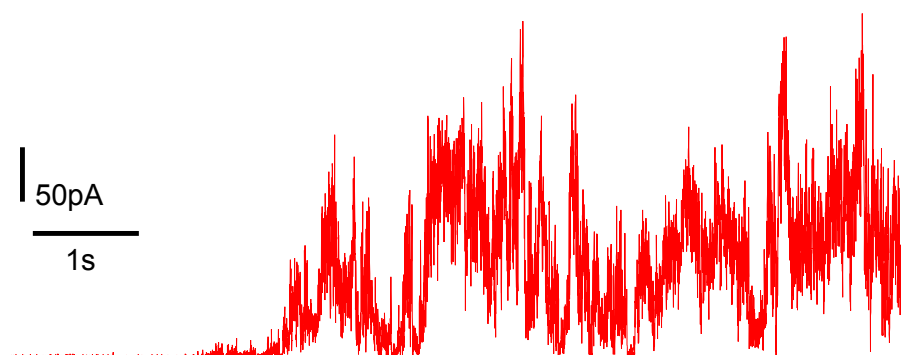
1:1 DMPG:DMPC, 150mM KCl, $U=70\text{mV}$ $T=22^\circ\text{C}$

Flickering Often one observes periods with a frequent occurrence of very brief closings of an otherwise open channel. This will be denoted flickering.



10:1 DMPC:DLPC, 150mM KCl, $U=350\text{mV}$, $T=20.8^\circ\text{C}$

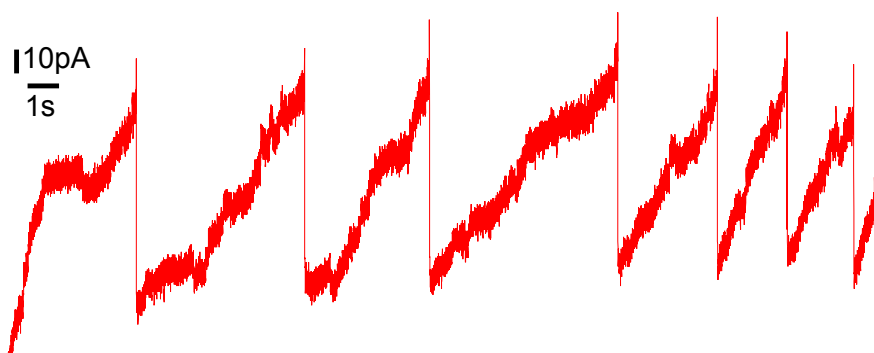
Bursts Activity happens to suddenly appear in bursts of fast fluctuating current. They are normally not quantized but they can turn out to be if one zooms adequately. Amplitudes can be from few pA to more than hundred pA and most often several amplitudes are observed in a single burst. The non-quantized appearance can in principle be caused by openings being faster than the time resolution of the recording.



4:1 DMPC:DLPC, 150mM KCl, $U=100\text{mV}$, $T=19.9^\circ\text{C}$

Inactivation It is not unusual that the channel activity shows up in periods of large activity with long periods (up to minutes or more) of inactive periods in between.

Sawteeth Sawteeth shaped current events are not uncommon. Most often they show a continuous increase and then an abrupt fall, but there have been observed a few that do it the other way around. They can be very periodical but it is not necessarily the case. More examples are shown in figure 51 in appendix A and in appendix B.

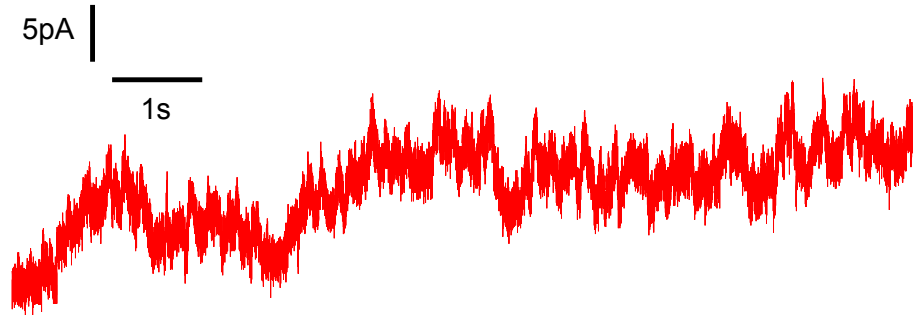


1:1 DMPG:DMPC, 150mM KCl, $U=70\text{mV}$, $T=22^\circ\text{C}$

Baseline drift Unless the seal is very tight some drift of the baseline is common appearing as a continuous change in conductance. This behavior was especially pronounced and catastrophic for mixtures with charged lipids at low salt concentrations where it typically accelerated when the voltage exceeded 100 to 150mV or -80 to -130mV. An example is shown in appendix B.

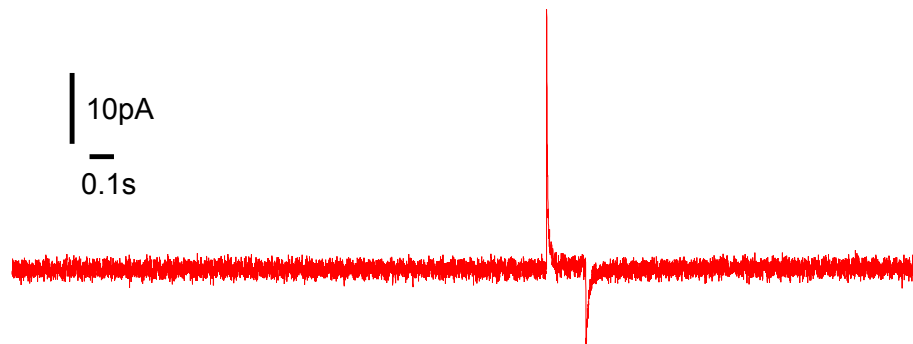
Baseline jump It sometimes happens that the baseline jumps to a new level. Jumps can be both ways and there is therefore no good way to differentiate between baseline jumps and quantized event. The closest one gets to a discrimination is that baseline jumps are longer lasting (or better not returning) and often higher than a typical event. Sometimes consecutive jumps are seen making the current trace resemble a stair. Figures can be seen in appendix B.

Uneven baseline The baseline can be more or less fluctuating. This can make it difficult to distinguish and/or analyze channel activity. In some cases one can assign the fluctuations to one or more constantly open channels. The distinction between an uneven baseline and non-quantized events are not always clear.



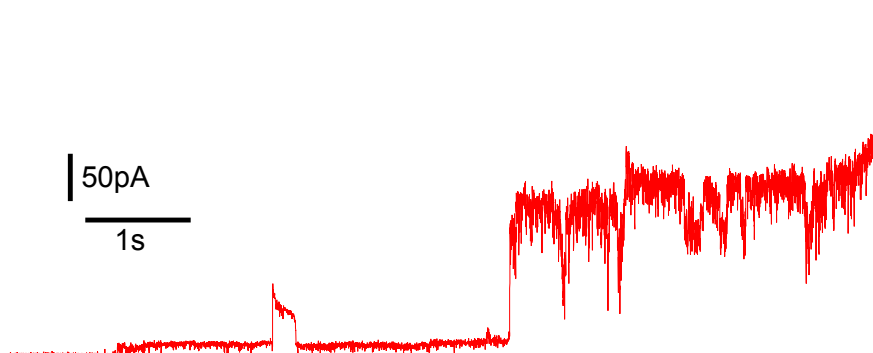
1:1 DMPG:DMPC, 150mM KCl, $U=10\text{mV}$, $T=23^\circ\text{C}$

Spikes Spikes are fast (ms), single standing events. They can point both ways but most commonly have the same sign as the voltage. In a few cases it has been possible to attribute the high spikes ($>50\text{pA}$) to outside noise directly. Another example is shown in appendix B.



6:4 DMPG:DMPC, 50mM KCl, 10mM Hepes, 1mM EDTA, $U=200\text{mV}$, $T=23.3^\circ\text{C}$

Breakage It is common to see activity prior to membrane breakage. This also happens without any previous activity and hence it is considered atypical for the behavior of the specific membrane. The activity is quite often quantized events preceded by bursting activity and rapidly increasing baseline drift. The membrane can also break without any preceding activity. See also appendix B



6:4 DMPG:DMPC, 50mM KCl, 10mM Hepes, 1mM EDTA, $U=100\text{mV}$, $T=21.6^\circ\text{C}$

Unbreakable membranes Normally some kind of activity (channel activity or breakage) can be induced by increasing the voltage. It happens that the membrane is completely unresponsive to voltages up to 1V which is the maximum possible with the used setup. Such membranes normally don't show any kind of the above mentioned activities except for sometimes a highly irregular baseline. The behavior is most often seen with pipettes that have been used several times.

7.3.1 Discussion

That a single membrane can display a large variety of behaviors makes it difficult to point out a typical behavior and identify changes in behavior due to addition of some substrate. What you see in articles is almost always the stable quantized events. These are also the most interesting as they most obviously confront protein scientist with an interpretation problem. But whether these are representative for the behavior of pure lipid membranes is according to my results questionable. Most others (including Antonov) making permeability measurements on pure lipid membranes use the Montal-Mueller technique. In contrast to the droplet technique one there uses the same aperture each time. This might explain the variation between experiments but not within single experiments as that shown in appendix A.

Similar for all the behaviors described above is the difficulty of knowing what is actually going on as it can not be inspected visually. I will anyway try to discuss explanations for some of them.

It is a bit surprising that pure lipid membranes exhibit quantized channel events. This all-or-nothing behavior means that a pore with a fixed size opens and closes almost instantaneously. The quantization makes sense if

there exist a certain radius at which the pore is stable as suggested by Glaser et al [68]. But unless something in the membrane changes with time this does not explain why one can observe repeated channel events with the same conductance and later the conductance is changed as demonstrated in appendix A.

One have to question if what is seen is currents through the membrane or if it is something happening at the rim. On one hand Kaufmann et al [56] have found the channel activity of a pure lipid membrane to correlate with the area of the patch and not the circumference. On the other hand quantized channel events that showed selectivity and voltage-dependent kinetics have been demonstrated with a patch made of impermeable, hydrophobic rubber by Sachs et al.[103] Likewise quantized events and subconductance states, selectivity and inhibition are found in plastic sheets with narrow pores of a fixed size.[104] Sachs suggests that the gating is a result of ordered water. Calculations have showed that when water is ordered in certain ring structures the centers can provide low energy binding sites for specific ions. If a pore contains a stack of these rings, ions can pass through the pore by moving from ring to ring. A cooperative change of conformation of the water will result in an abrupt end of the permeation.

It turns out that not all events are quantized. The nature of this kind of pores must be different as they open and close slowly and have no stable conformation. It cannot be excluded to be just a temporary loosening of the seal due to some kind of for example mechanical disturbance.

The non-quantized events can be very difficult to distinguish from an uneven baseline. Uneven baselines may be caused by large scale fluctuations in the membrane causing mechanical instability. In some cases the uneven baselines is suspicioned to be explained by pores being open the entire time. The distinction is difficult but an indication can be increased noise level as there is often more noise when a channel is open due to the stochastic flow of ions through the channel or maybe also due to conformational fluctuations as described for the acetylcholine receptor by Sigworth [105]. The figures in appendix B, part B.1 show clear examples of increased noise level in the open state.

Gallaher et al [106] provide a possible explanation for the difference between stable openings and flickering. In accordance with the fluctuation model they suggest that pores of a hydrophilic nature most readily form at gel-fluid interfaces (see section 4.3). Freezing of the lipids involved in the formation will stabilize the pore while freezing of the surrounding lipids will stabilize it even further and make it long lived. If however the pore lining melts partially, some of the lipids may move more freely and possibly clog up the pore. With the rest of the pore construction being intact it is likely

for the pore to reopen and refreeze. The stability of the pore is hence a question of in which kind of domain it is positioned and flickering should be an incidence of interfaces.

Hanke et al [78] describes observation of "bursts of spike-like current events" when the pipette tip-water interface is interrupted caused by evaporation. In my experiments the tip is sunken 2mm below the surface to avoid evaporation to cause problems so I find the explanation unlikely in my experiments.

Baseline drift may in some cases be explained by the bad chlorination which can result in shifts in the electrode potential.[91] Drift might also be because of movement of membrane inside the pipette. This is possible if the pipette surface contains a reservoir of lipids. Attempts to observe the membrane inside the pipette by making it with fluorescent lipids turned out to be impossible as the pipette itself glowed too much compared with the membrane. This indicates that a reservoir is actually present. It is not clear whether the baseline conductance is due to leak at the rim or from the membrane itself. Anyway a change in area would result in an altered baseline conductance. Baseline jumps could then be a sudden sudden movement for example initiated by the release of some tension.

In the case of DMPG-mixtures instability may be more pronounced because the glass surface is also negatively charged (personal conversation with T. Heimburg). This made it quite difficult to perform experiments with DMPG. Attempts on overcoming this have been made with silanization and increased salt concentrations. These experiments will be described later.

Unbreakable membranes can not be single membranes as these should break at around 500mV.[73, 78] Rather it is assumed to be a build up of lipids or air bubbles that clog the pipette. That the occurrence is most likely to happen for pipettes used several times speaks for this explanation.

7.3.2 Comparison with protein channels

As stated previously what you see in literature both about protein ion channels and lipid ion channels is in most cases the quantized events. In some cases conductances and radii of these data of the lipid ion channels are compared to the protein data with the conclusion that they are indistinguishable (e.g. [3]). There have never made a comparison of the different membrane behaviors described above and raw protein data. I have sent a draft of the above section to K. Witschas who as a ph.d. student work with patch clamp experiments on protein channels at the University Hospital Aachen and asked her how much she recognizes from her experiments and how they are normally explained by a protein scientist.

The protein channel experiments are made with different types of human transient receptor potential (hTRP) channels. A common function of TRP channels is to mediate sensation. The data is recorded in voltage-clamp mode with a sample rate of 20kHz and lowpass filtered at 2kHz with an Axopatch 200B at room temperature (22-23°C). This part of the setup is thus the same as used for measurements of lipid channels. The protein data is not previously published.

The protein data is divided into two categories: specific and unspecific events. The specific events are characteristic of a certain kind of channel while the unspecific events can occur in any patch. The unspecific events found when investigating proteins are noise spikes, sawteeth, drift, baseline jumps, uneven baseline, non-quantized events and breakage. Figures of these can be found in appendix C. Except for the sawteeth these events are very similar to what is observed with pure lipid membranes and can probably be explained the same way. In the patch clamp data sawteeth are only observed as noise from the cooling circuit of the headstage and always looks the same (see figure 56) opposed to the large variety found in my measurements.

Most of the other unspecific events have to do with the seal. According to Witchas uneven baseline is seen if the seal resistance is low or because of background channel activity. Baseline drift is attributed to loosening of the seal. Non-quantized events are ascribed to mechanical disturbances. Complete breakdown of the seal produces irregular events like those often seen in breakage of pure lipid membranes. An example of breakage from an inside-out patch is shown in figure 57. The quantized events prior to breakage is apparently only typical for pure lipid membranes. This indicates that pre-breakage quantized events could have to do with the way the membrane is attached to the pipette. Where conventional patch clamp experiments are made on preformed membranes the droplet technique build up the membranes inside the pipette. One could imagine that the last method gives a higher amount of defects at the rim.

In the category of specific events one finds the quantized events with specific conductances, substates, and timescales. Very short openings can result in spike-like events (figure 37) while long openings gives a stair-like current with each step being a new channel opening (figure 38). Flickering and bursts are also found in the specific events category.

Examples of quantized protein channel events are given in figure 39. A comparison with the traces from lipid ion channels shown above reveals comparable conductance and timescales. In the protein data the different timescales are attributed to different channels after addition of ligands. In the lipid data both timescales are displayed in the same membrane patch under unchanged conditions.

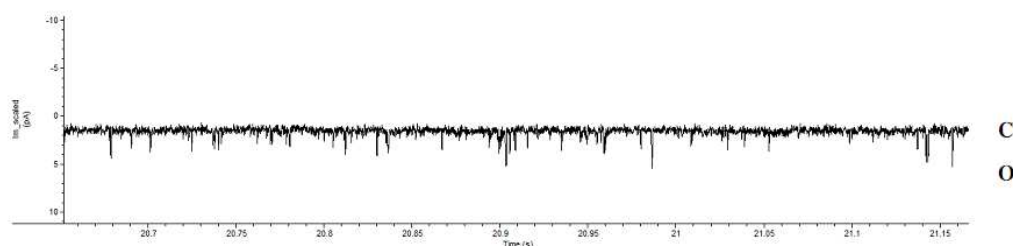


Figure 37: Spikes from hTRPM8 in HEK293 cell in on-cell configuration. $U = -60\text{mV}$. Courtesy K. Witschas.

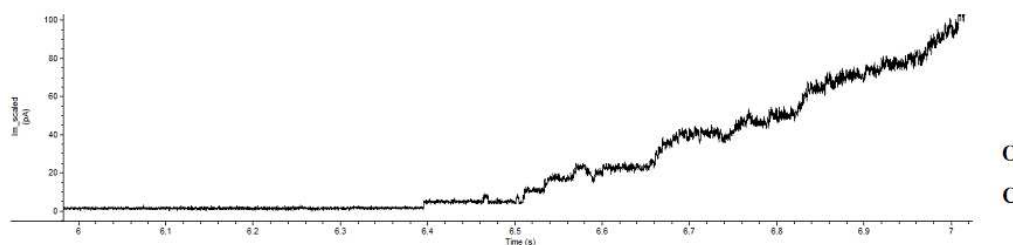


Figure 38: Stair found in HEK293 cell with hTRPM2 incorporated after addition of ADP-ribose. Made in inside-out configuration at $U = 60\text{mV}$. Compare with the figure in appendix B, section B.7. Courtesy K. Witschas.



Figure 39: Quantized channel events in two different types of human TRPM channels with 40% sequence homology. Both traces are recorded at $U = 60\text{mV}$. Notice the different time scales. A) hTRPM2 after addition of H_2O_2 . B) hTRPM8 after addition of icilin. Courtesy K. Witschas.

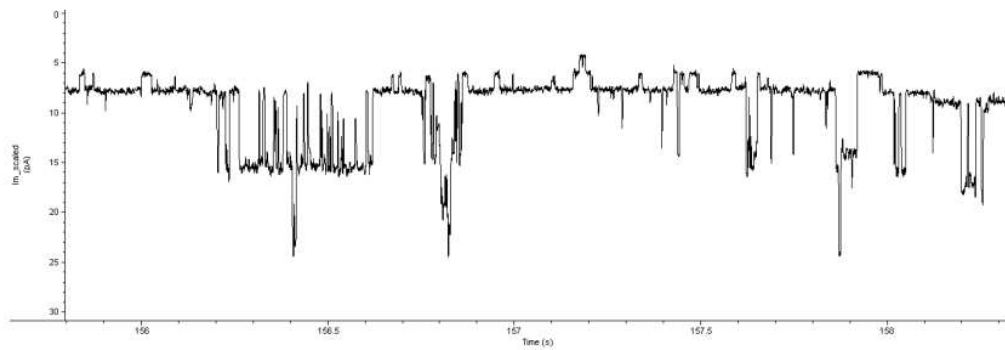


Figure 40: Subconductance states seen in hTRPA1 in HEK293 cell after suction is applied. Made in inside-out configuration at $U=-60\text{mV}$. The trace is low-pass filtered at 300 Hz. Courtesy K. Witschas.

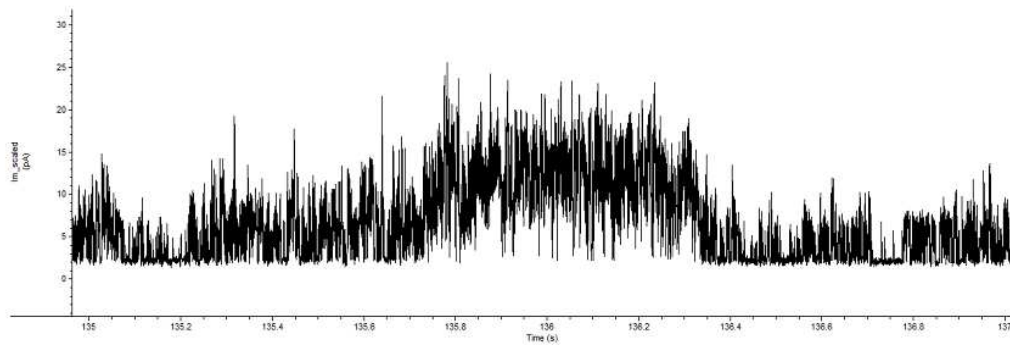


Figure 41: Bursts from hTRPM8 channel in HEK293 cell after addition of WS-12 (i.e. a synthetic cooling agent). Made in on-cell configuration at $U=60\text{mV}$. Courtesy K. Witschas.

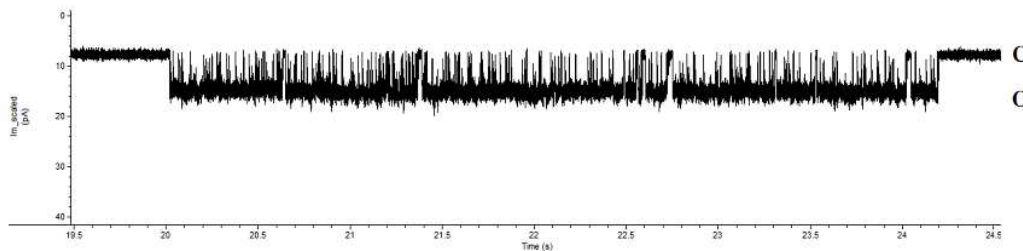


Figure 42: Flickering made by hTRPA1 in HEK293 cell in on-cell configuration. $U=-60\text{mV}$. Courtesy K. Witschas.

Subconductance states are also a characteristic of certain proteins as seen in figure 40. A subconductance state (i.e. a different conformation) is defined as a state with a conductance different from the one occurring most frequently.[107] The criteria for distinction of the extra states from an extra protein of a different type are [107]: 1) One should observe direct transitions between the substate and the main state. 2) The substate should only be observed in the presence of channel main-state activity. 3) One must exclude the possibility that the main state is a superposition of two independent channels.

Examples of pure lipid membranes that fulfill all the criteria can be found. If one follows the same logic as given for the proteins it must be a single lipid channel that gives rise to several conductance levels. For proteins subconductance is claimed to be caused by some alteration in the conformation of the protein. This is not different from stating that a lipid channel can have several stable states solely based on the current trace. Neither in the case of lipid or protein ion channels detailed structural data exist. More than one stable lipid channel state does not fit with the theoretical consideration about hydrophilic and hydrophobic pores with only one stable state presented by Glaser [68]. But it could be that more than one conformation is not necessary. It appears that substates can also be found in a perforated plastic foil with a fixed pore size (figure 3 in [104]). This indicates that the explanation of substates is different from stating changed conformations of the channel.

As mentioned bursts (figure 41) and flickering (figure 42) is also seen in protein data. Again the data from pure lipid membranes and protein containing membranes look very similar. For the protein data the behaviors are suggested to be due to a stable closed state and very unstable openings in the case of bursts, while flickering is the result of long openings and a short-lived closed state. Flickering is in other cases attributed to high concentrations of low-affinity blockers.[108]

The comparison of data from protein channels and pure lipid membranes shows that qualitatively all kinds of protein behaviors can be reproduced in pure lipid membranes. The sawtooth patterns are only found in the pure lipid membranes. The major difference between the pure lipid system and the protein containing system is that a single lipid membrane can show all kinds of behavior while for proteins the behaviors are characteristics of specific types of channels or combinations of channel and ligand.

It has so far not been possible to deduce what it is that control the different kinds of behavior in pure lipid membrane. Apparently all kinds of behavior can be found under the same set of conditions (cf. appendix A). This means that it is difficult to reproduce certain types of events opposed

to protein data where each channel has its own characteristics. There is the possibility that it is the droplet method that is the source of the large variation as this variation is not reflected in previous publications and most of the published data on pure lipid membranes is made with Montal-Mueller-like setups. The reproducibility of these can however also be a problem according to a personal conversation with Heiko Seeger. He has worked with both pure lipid membranes and protein channels incorporated in artificial membranes in a BLM-cell and found the reproducibility to be better when proteins were incorporated. This however does not hide the fact that all the types of behavior of protein channels can also be found in protein-free membranes. It means that protein scientists still have a problem with stating that all activity is due to the proteins. Also it has not been proved that the currents actually go through the proteins. It could be that the proteins induce perturbations in the membrane that create an environment for lipid pores by increasing the fluctuations (cf. figure 27) or causing defects.

7.4 Charged membranes

The occurrence of channel events is used as an indication of having only a single membrane. This turned out to be very problematic for the charged membranes. With low salt concentration (50mM NaCl) whenever increasing the voltage in order to see channel events the baseline current most often started drifting catastrophically. Channel events have been seen but most often in relation to breaking of the membrane. An estimate would be that out of hundred tries quantized channels have been seen a few times without following breakage.

The instability may arise because of interactions between the charged lipids and negatively charged glass. Therefore it was tested if the problem could be conquered by silanization. Silanization is a process that chemically makes the surface hydrophobic.[109]

In total 19 silanized pipettes were tested with 6:4 DMPG:DMPC in 50mM KCl. Two of these were minipipettes on which it wasn't possible to form a membrane. Membrane formation succeeded on most of the fire polished pipettes but in general drift was also here a considerable problem. In addition the baseline was more uneven compared to the non-silanized pipettes. In a few cases some mostly non-quantized activity was observed but it was rare and it mostly drowned in baseline noise. An example is shown in figure 43.

As the silanization didn't work it was instead tried to increase the ionic strength. 75mM NaCl wasn't successful but with 100mM NaCl it was sometimes possible to make stable membranes. With this concentration drift was still a returning problem but if I were lucky to obtain a good seal (seal

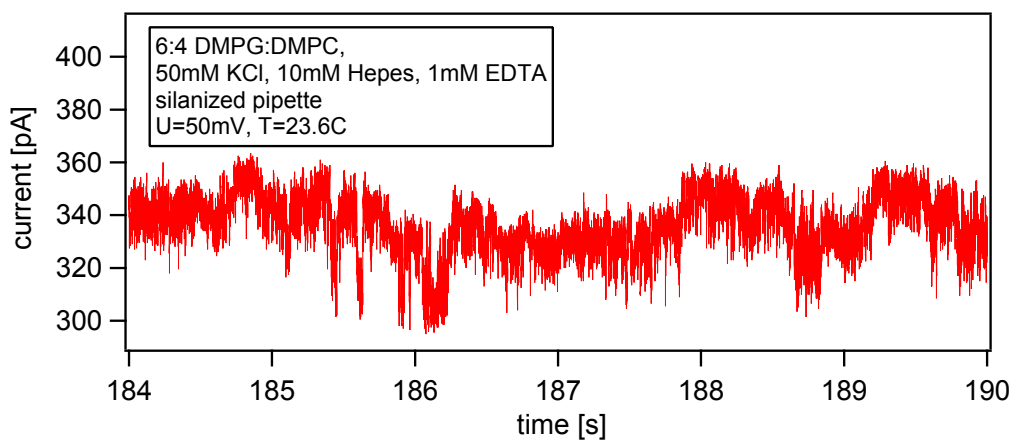


Figure 43: 6:4 DMPG:DMPC, 50 mM KCl in silanized pipette. There is a clear tendency of short closing events but the baseline is unstable and the noise level high. Normal noise level is around 2pA peak-to-peak.

strength $> 1G\Omega$) channel activity could be observed. These experiments were performed at room temperature (21.6-22.4°C).

7.4.1 Discussion

The procedure used is originally meant for cover glass so it has been necessary with a few adjustments. It is possible that these have damaged the silanization. This could for example happen when doing the firepolishing as it might not be the original surface glass that is still the surface after heating the tip. If this is the explanation one would have expected that it would work with the minipipettes, which wasn't the case. It could also be the pulling procedure itself that was the problem. With another similar coating described by Lin et al [110] it is however done in the same way by first coating the capillaries and then turning them into pipettes. There is also the possibility that the hexane:ethanol solvent destroys the coating but there definitely is an effect of the silanization as a strong tendency of more uneven baselines is observed.

Whatever the reason for the instability of DMPG mixtures at low salt concentrations is, silanization doesn't seem to be the solution. The membrane is stabilized by screening the charged headgroups by means of increased salt concentration. But the higher ionic strength also screens for cyt c and decreases its binding (cf figure 29).

7.5 Cytochrome c

The preliminary studies of stability at different salt concentration resulted in cyt c experiments to be made with 100mM NaCl. These experiments were performed just below the transition temperature. It turned out that in the transition at 23.8°C the membranes were less stable, which limited the success rate of this experiment severely.

The procedure was to first add 2mM glycerol and if the membrane survived then add 2mM cyt c to the same membrane and observe possible changes. All membranes showed activity prior to addition of glycerol. The experiment was performed with the pipette tip at different depths below the surface. All membranes less than 2mm below broke within a minute upon addition of the glycerol solution. At 2mm about half stayed unaffected and the rest broke. This is therefore assumed to be the limit where one can be sure that the drop reach the membrane without destroying by it by the impact.

The membranes that survived until the point of cyt c addition either broke or showed no changes within the first minutes upon addition (data not shown). A few membranes afterwards turned out to be unbreakable and were therefore neglected.

7.5.1 Discussion

The odds are against succeeding with this experiment. First, the membranes are extremely unstable despite attempts to surmount this problem. Second, the experiment builds on the assumption that the activity of the membrane scale with the heat capacity. In the following section it is questioned if this is true with this setup. If assuming the correlation then even when taking most care the necessary certainty of $\pm 0.1^\circ\text{C}$ is at the limit of what is possible with the available temperature control. It is here also assumed that the transition temperature is not affected by the transmembrane voltage, which may not be the case as described in section 3.3. The transition can also be slightly different due to possible solvent residues in the membrane. Third, as described in section 7.3, the activity may change even without changing the conditions. So possible changes would not necessarily be due to interactions with cyt c.

7.6 Temperature dependence

Figure 44 shows a number of plots of the current as a function of temperature made on 3 different membranes in 3 different minipipettes. The plots provide both the baseline dependence of temperature and an indication of the channel

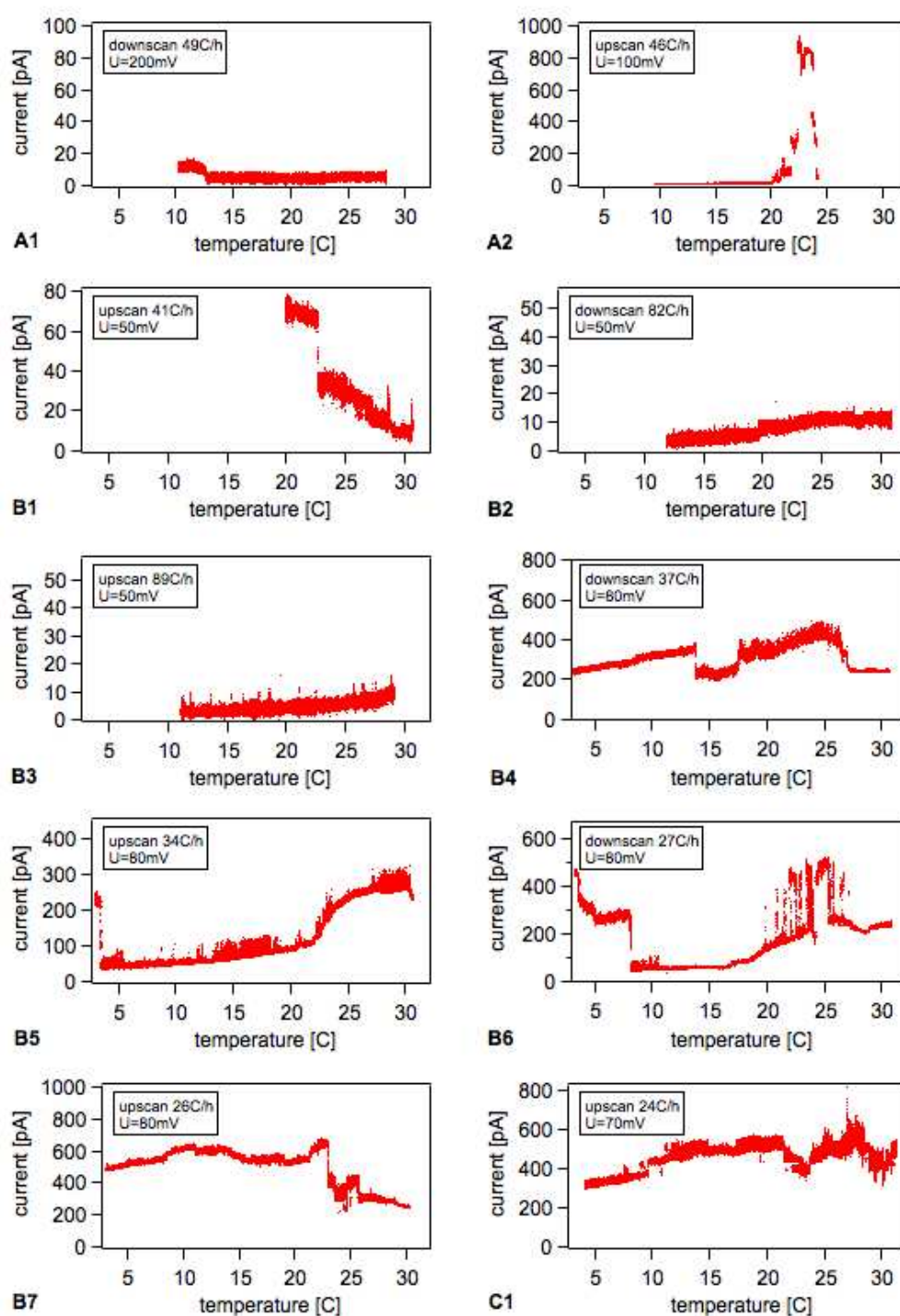


Figure 44: Scans of the current as a function of temperature. All membranes are 10:1 DMPC:DLPC in 150mM NaCl, 2mM HEPES, 1mM EDTA made on minipipettes. A, B, and C are different pipettes. The numbers denote the order of the scans made on each pipette. Only every 100th point is plotted.

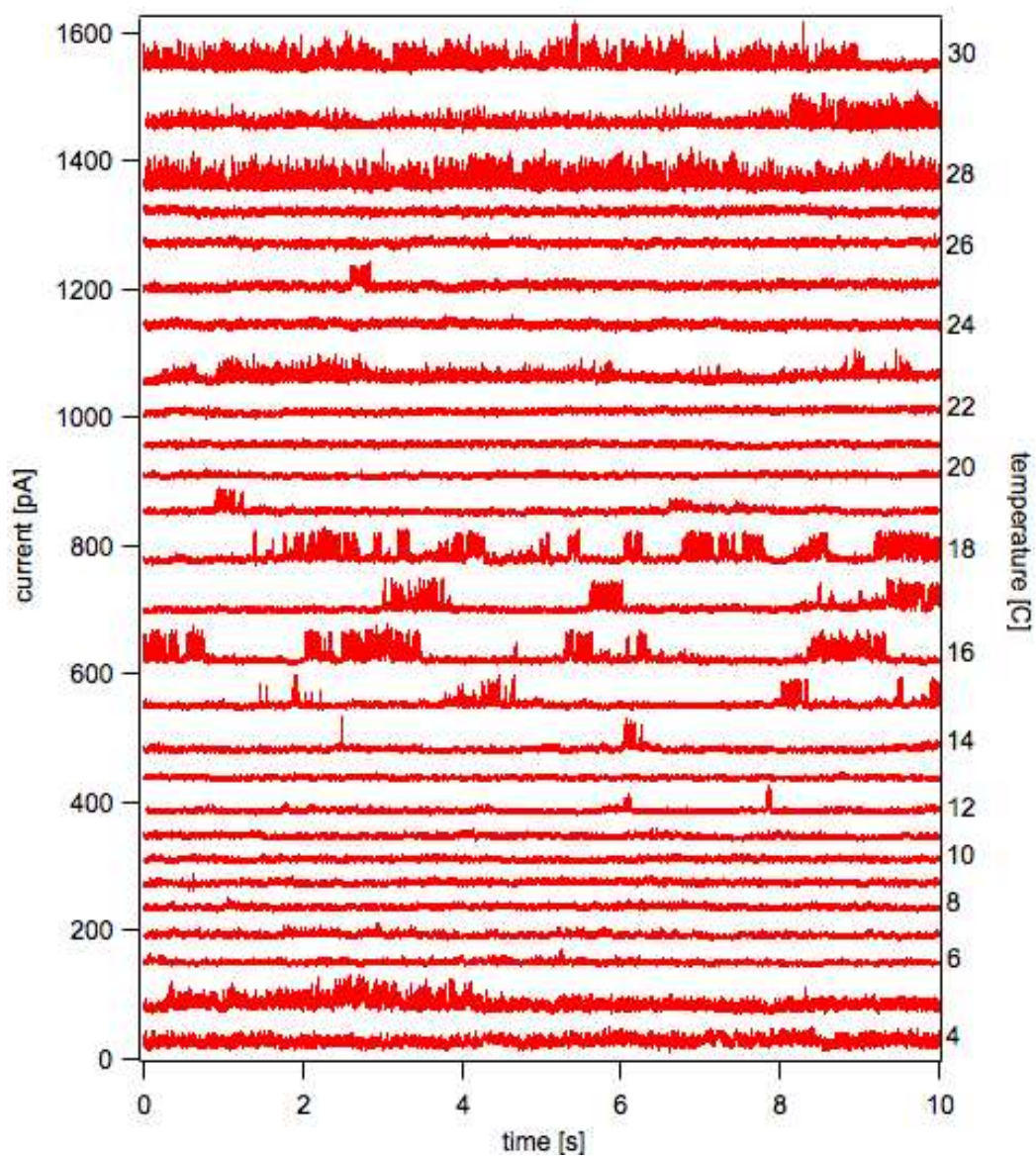


Figure 45: Current traces of 10:1 DMPC:DLPC in 150mM NaCl, 2mM Hepes, 1mM EDTA at integer temperatures from 4 to 30°C and $U=80\text{mV}$. The temperature is only written next to every second trace. Baselines have been shifted. The traces are from a temperature scan made at a scanrate of 34°C/h.

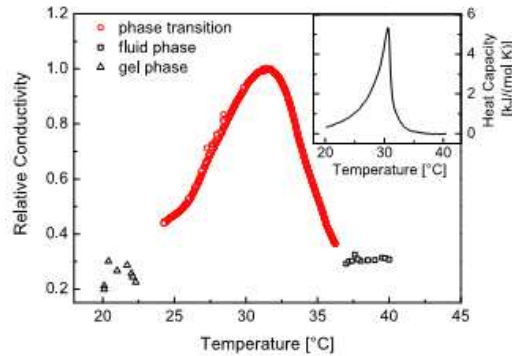


Figure 46: Average conductivity as a function of temperature. The heat capacity profile shown as an inset. Made on a 95:5 D15PC:DOPC membrane at $U=400\text{mV}$ with a Montal-Mueller setup. Measurements in the transition, gel, and fluid phase are made on different membranes. Scanrate= $0.2^\circ\text{C}/\text{min}$. From [60].

activity reflected in the variance of the traces. As seen, a single membrane can behave very different from scan to scan. For example membrane B goes from peaking at the main transition to showing no peaks to showing peaks below, above, or at the main transition temperature.

Previous publications have stated that channel activity is a feature coupled to the phase transition of the membrane. My data demonstrates that events are not solely observed in the transition. Figure 45 shows some traces taken from scan B5 in figure 44. These traces are examples of that channel activity can be found at arbitrary temperatures. Additionally it is not uncommon with membranes showing no activity for long periods even though they should be in the transition (see for example B2 and B3 in figure 44 and figure 45).

7.6.1 Discussion

There are two possible contributions to the permeability, whose temperature dependence is inspected here. One is the leak current giving the baseline of a current trace. The other is fluctuations in the current showing up as channel activity. None of them correlate with the transition temperature of the membrane opposed to what has previously been published.

Figure 46 is a scan of the conductivity versus temperature from an article by Wunderlich et al [60]. It shows the average conductivity to peak around the main transition. Several other experiments on vesicle ensembles show

unambiguous relations between the average permeability of membranes and the gel-fluid transition (cf figures 16 and 18).[51, 61, 111] In my small patches the reproducibility is lacking. Only 4 out of 10 graphs in figure 44 show a clear baseline peak around the main transition and it is not even consistent within the single membrane.

The peaks that do turn up are wider than the transition found in the DSC scans. Given there is a relation to the transition, this might be because the pipette tip is closer to the surface than the thermocouple. Therefore the temperature near the membrane may be closer to room temperature (around 22°C) than the thermocouple. This would result in a broadening of temperatures close to the main transition compared to what is shown on the scale.

It is not certain what the origin of the baseline current is. It is normally attributed to an unspecified leak due to constantly open channels or imperfect sealing between membrane and pipette. If it related to the transition one could imagine a contribution from channels with a conductance that is too small to be resolved.

The activity of the single membrane does not correlate with the transition either. Activity can be observed both far below and far above, while there is no guarantee for observing activity in the transition. In previous publications people have succeeded in relating the activity in single channel measurements to the transition.[58, 61] Others have reported additional activity in the fluid phase, but claim it to be more spiky than quantized.[60] The activity above the transition shown in figure 45 is mostly spiky but can just as well be quantized as demonstrated in figure 47.

There is of course the possibility that the transition temperature is different from that measured in the calorimetric scans. This could be because of solvent residues, or increased curvature of the membrane in the pipette membranes. But both of these variables lower the transition temperature.[6, 112] Nevertheless activity is observed repeatedly about 10 degrees above the assumed transition temperature. The only thermodynamic variable that shifts the temperature upwards is increased hydrostatic pressure which is not in play here as there is access from the inside of the pipette to the outside.

Even if the transition was shifted it does not explain why channel activity is observed in at least three temperature ranges (i.e. 4-5°C, 15-18°C, and 28-30°C) in figure 45. One could try to relate one temperature to the main transition and a second to the pretransition but there is no third heat capacity peak for 10:1 DMPC:DLPC within the relevant temperature range.

The big question is why do my experiments contradict the previous publications. In the case of single channel activity it could also be that others

simply haven't looked for long enough outside the transition. It is striking that often very few data is shown. For example the article by Antonov et al [58] only presents 100 second traces (figure 17). If estimating the number of counts and relate it to the counting frequency, it appears that the histogram is just made over approximately the same time interval (see figure 17). The ensemble experiments however provides much better statistics.

All the cited previous publications are made with either the Montal-Mueller technique or vesicles. This leads to the thought that it is the pipette setup that gives rise the contradictions. One major difference is the size of the system. The larger areas gives a better statistics. Further, if there is some edge effects these are expected to play a larger role in the pipette setup, where the rim surroundings represent a larger fraction of the total area.

From atomic force microscopy it is known that the bilayer closest to a surface is strongly affected by the proximity and don't show the same transitions.[113] One could imagine similar interactions between the membrane and the edge of the pipette. Defects could arise in the interface between lipids close to the edge and lipids free of interaction. If edge effects dominate the lipid interactions the consequences of phase transition may become impossible to observe.

Whatever the cause it is found that channel events can be found at all temperatures when the membrane is formed in a pipette. It is likely that the same effects are present in patch clamp experiments. The consequence is one always have to be careful with the interpretation of protein data. The possibility of confusing protein events with lipid events is not necessarily something one can get rid of by making experiments outside the membrane phase transition.

7.7 Voltage dependence

In some experiments channels have reversibly opened and closed in response to changes in the transmembrane voltage. Figure 47 shows two examples made at two different temperatures. To the right is shown examples of 15 seconds traces made at various voltages while the histograms to the left represents 5 minutes at each voltage. Two things can be deduces from the histograms: Voltage affects the probability of a channel being open and it shifts the baseline conductance.

Each peak corresponds to an open or closed state of a channel. The histograms are normalized such that the area under each of them is equal to one. The area under each peak therefore gives the probability of being in the given state. It can be seen that with increasing voltage the channels go from being closed to being more and more open. In appendix D more data is

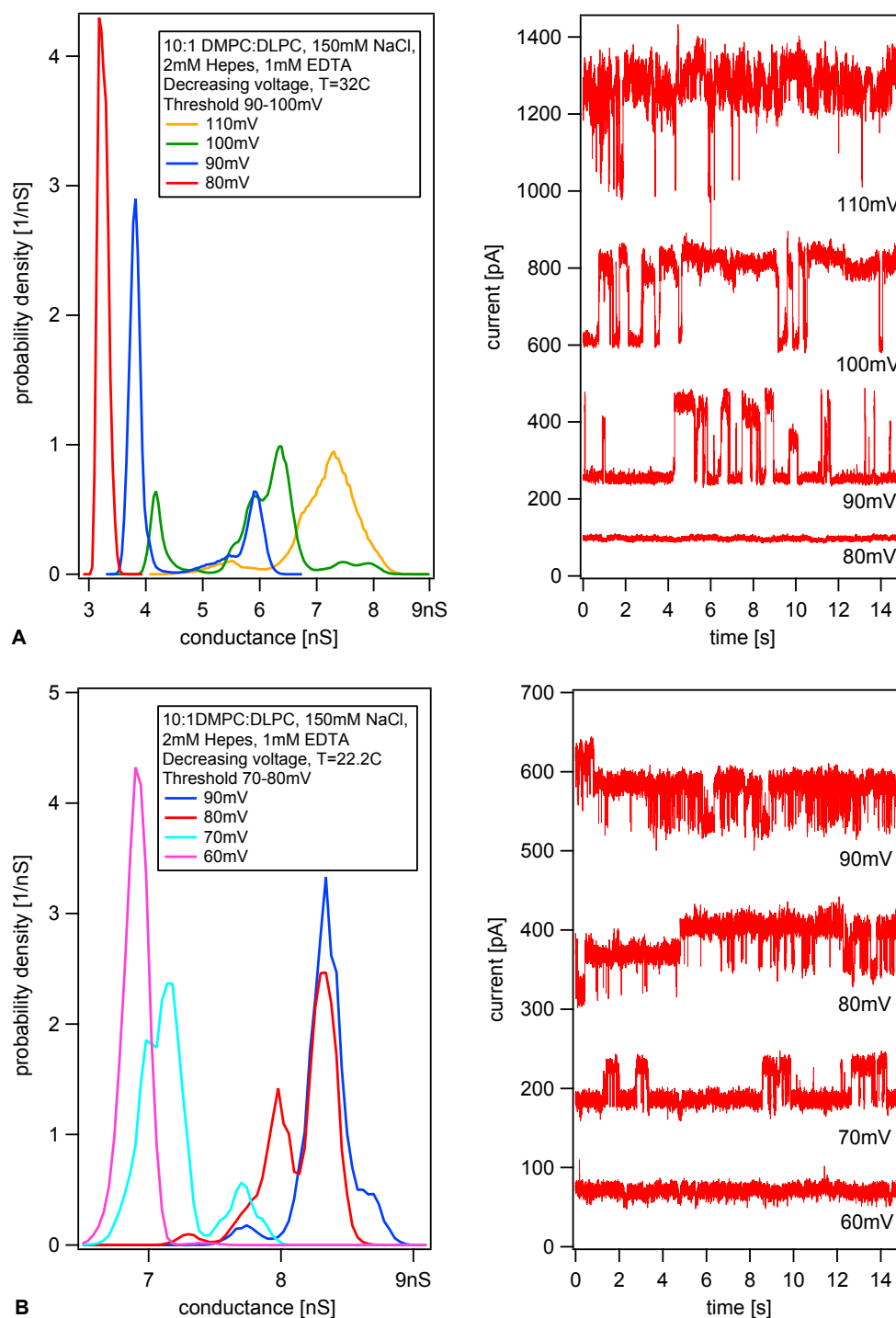


Figure 47: Histograms (left) of the conductance at different transmembrane voltages for two membranes. To the right is shown representative examples of the corresponding current traces. Each trace is based on approximately 5 minutes measurements. The baselines have been shifted. The histograms are normalized such that the area under each histogram is equal to 1. The bin width is 0.04nS. Both membranes consist of 10:1 DMPC:DLPC in 150mM NaCl, 2mM Hepes, 1mM EDTA, pH 7.4. The top figures are made at 22.2°C and bottom figures at 32°C.

presented that all show the same trend. Assuming a 2 state model a threshold can be defined as the voltage where the probability of a channel being open or closed is the same. Thresholds are found to be between 70 and 80mV for the measurements made at 22.2°C and around 100mV for the measurements made at 32°C.

At a first glance the increased threshold found at the high temperature could be interpreted as that a higher voltage is required the further the membrane is from its phase transition temperature. However, the measurements are based on only two different membranes and a comparison with similar (not yet published) measurements made by Andreas Blicher indicates that the threshold depends more of the single membrane than of the temperature. But further experiments are required to settle this.

By further examination of the histograms it becomes clear that the peak corresponding to the baseline or closed state (i.e. the lower peak given that a closed state exist at the given voltage) is shifted upwards as the voltage is increased. Figure 48 is a plot of the baseline conductance as a function of voltage based on the data from figure 47 and appendix D. Within the narrow voltage range the baseline conductance seems to exhibit a linear relation with almost the same slope in both sets, which differ by being different membranes measured at 22.2°C and 32°C.

7.7.1 Discussion

It should be clear by now that the membranes are difficult to control. Also the voltage thresholds are something that is only observed sometimes and it is not established what it is that stimulates the feature. Here only a limited set of data is presented. The findings shall therefore rather be taken as a proof of principles than exact results. It is though still interesting that the channel activity in these pure lipid membranes is capable of displaying voltage thresholds. In the world of protein channels it is known as voltage gating when the open probability increases with voltage.[114] The voltage thresholds for channel activity is thereby yet another feature of protein channels that can also be found in pure lipid membranes.

For protein channels voltage gating is explained by the protein having a charged part that moves in response to voltage.[114] The movement causes a conformational change that opens the channel. How voltage gating can arise in pure lipid membranes requires further investigation. In the view that gating is due to ordered water one can easily imagine that it requires a certain electric field strength to keep the arrangement of the dipolar water molecules regardless of thermal fluctuations.

To my knowledge it is the first time that the concept of voltage gating

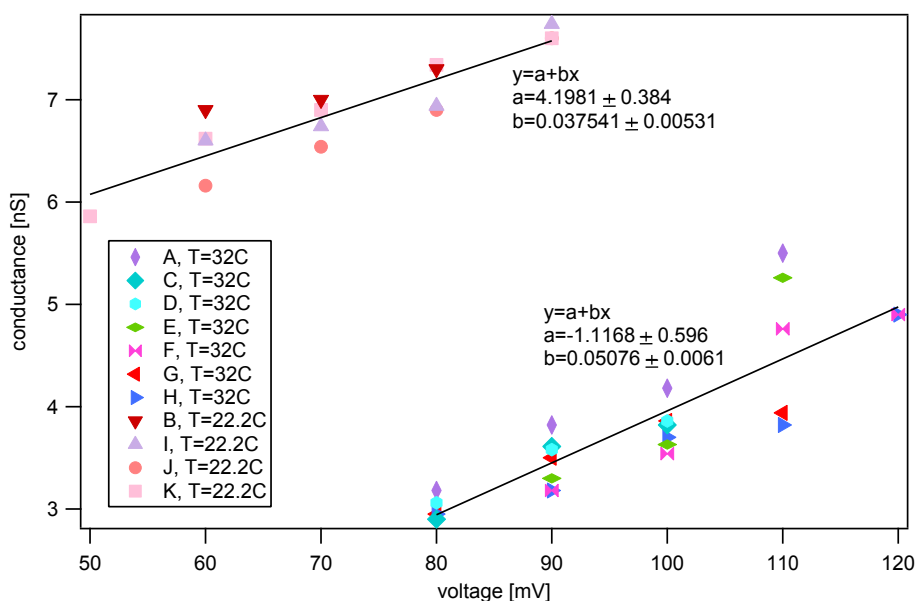


Figure 48: Plot of the baseline conductance as a function of voltage. The letters refer to the graphs in figure 47 and appendix D. Error bars is omitted for clarity. The lines are average fits of the two groups.

is reported for protein free membranes. Rather previous published channel current-voltage relations have been proportional for voltages below 100mV.[58, 63] It should again be emphasized that voltage gating is not always observed. Other experiments on membranes not showing voltage gating could probably have confirmed the proportionality.

As written in section 7.6.1 the origin of the baseline conductance is unknown, but as demonstrated here it shows a linear voltage dependence within the measured voltage range. If the baseline conductance is due to unresolved channels it means that more of these channels open with increasing voltage. If the baseline is rather due to defects at the rim it can be interpreted as the defects become larger with increasing voltage.

7.8 Copolymer membranes

In a preliminary study it have been tested if the use of triblock copolymer membranes could be an alternative to lipid membrane for the investigation

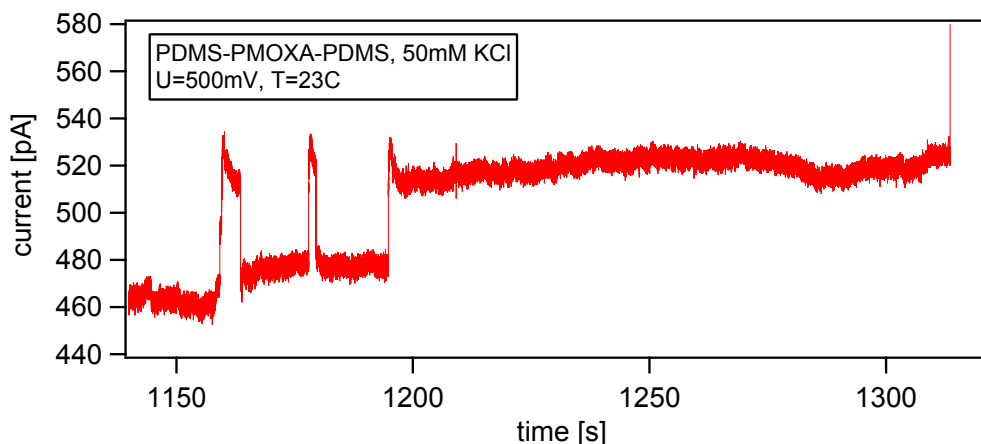


Figure 49: Breakage of polymer membrane in 50mM KCl, 10mM Hepes, 1mM EDTA, pH 7.4, $U=500\text{mV}$.

of protein channel activity. The purpose is to test if the pure polymer membranes show channel events and if gA can be incorporated and show activity similar to what is seen in lipid membranes. The copolymer show no phase transition (personal conversation with Alfredo González-Pérez) so experiments are performed at room temperature (21-23°C).

It has supposedly never been tried to make polymer membranes with the droplet method before. This is possible but the success rate is lower than with lipids. However, tip dipping occurred more often compared to lipids and around half of the successful membranes were formed this way.

In this study it was managed to form 5 pure polymer membranes that were stable for more than a few minutes. 3 of the membranes showed completely stable baselines for up to 30 minutes after which the pipette was changed. An example is shown in the top trace in figure 50, A. They were unbreakable at voltages up to 1V. One was also completely stable but broke after 14 minutes at a voltage of 1V. The last pure polymer membrane showed minor fluctuations in the baseline of the type one often sees in the baseline of single lipid membranes. It broke after a bit more than 20 minutes and showed some channel-like events with a conductance of $\sim 80\text{pS}$ in the minutes before breakage (see figure 49).

The general trend in copolymer membranes with gA was that they were less stable in the sense that the baseline had a tendency to drift and the current (including baseline) fluctuated. In 5 out of the 9 membranes, that survived more than the first 5 minutes, the current fluctuations were un-

doubtedly channel events. The most common type of activity is shown in figure 50, A. The current amplitude has some variation giving a conductance of $60\text{pS}\pm 40\text{pS}$. In a single patch the activity shown in figure 50, B appeared with a much larger conductance of $200\text{pS}\pm 60\text{pS}$. Some of the membranes with channel events didn't break for hours.

7.8.1 Discussion

In a test of inactivity it is of course necessary to abandon the requirement of channel events as an indication of a single membrane. This rises the problem of knowing whether the pipette is just clogged up with several membranes or if it is the desired single membrane. If it had been a lipid membrane I would have ascribed the extremely stable membranes without any sign of activity to the category of unbreakable membranes i.e. probably several layers of membranes. It should here be noted that polymer membranes are reported to be able to resist voltages up to 1.5V [73] which is above the possible voltage range of used setup. Only in one case there where small undirected fluctuations which maybe can be seen as a sign of a single membrane. But the point of the polymer membranes is that they are more stable, so the completely flat baseline may just be the way a single polymer membrane behaves. There is as stated previously no way to distinguish single and multiple membranes (with this setup) except from the occurrence of channel activity.

One membrane did show channel events but not until a few minutes before breakage. In general prebreakage events are not considered as representative. At least in lipid membranes the activity prior to breakage is very different from the rest as described in section 7.3.

There is a clear change of membrane behavior when gA is added to the system. The baseline fluctuates and channel events take place regularly. The conductance is however much higher than what is normally reported for gA. At optimal conditions such as high ($\sim 1\text{M}$) salt concentration and type of salt the conductance is up to 50pS . [45, 115, 116] With the salt concentration used here a more realistic channel conductance is $< 10\text{pS}$. At voltages below $\sim 400\text{mV}$ such a low conductance corresponds to a current amplitude similar to the noise level. The fluctuating baseline can be a sign of unresolved channel events.

The incorporation of gA in the same type of copolymer membrane has been done before by González-Pérez et al [72]. They find channel events with a conductance of around 160pS , which is close to the high conductance events found here, but made in a 1M HCl solution. Their noise level is of the order of 60pS peak-to-peak even after heavy filtering, so possible low conductance

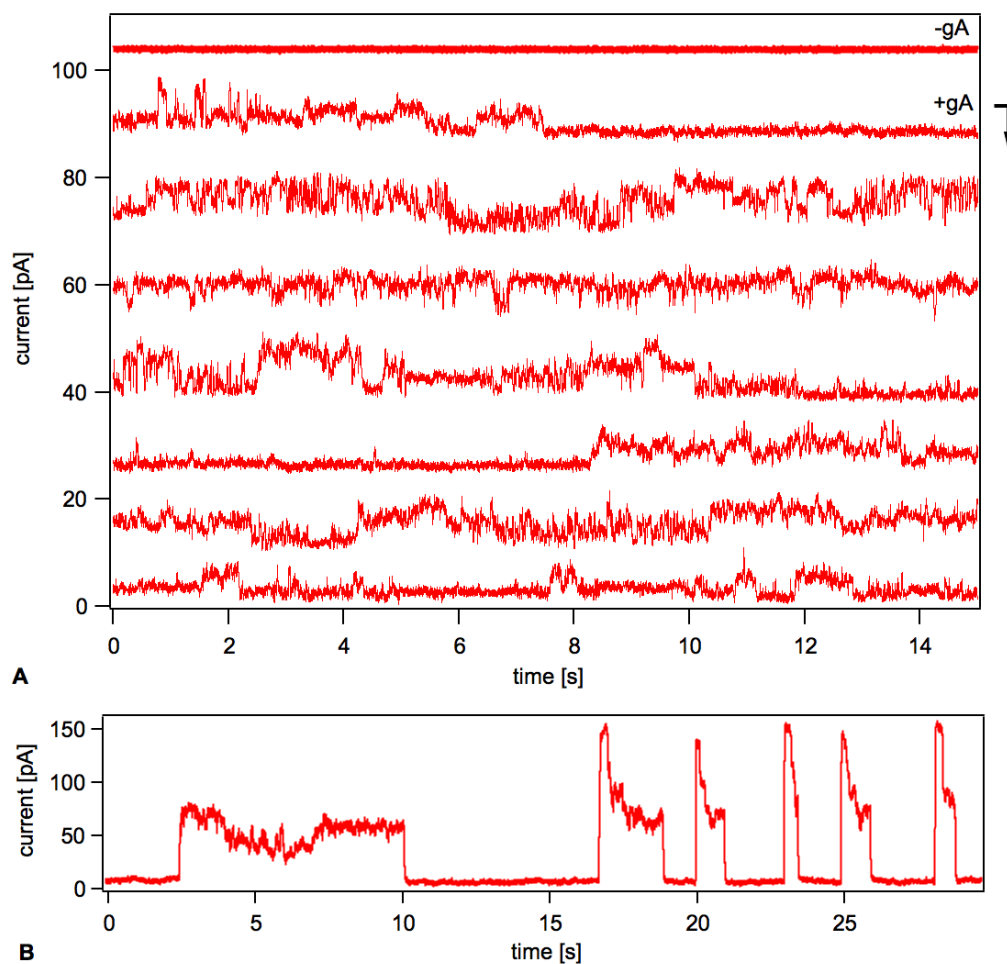


Figure 50: Current traces of copolymer membranes with gramicidin incorporated. A) A single trace (top) without gA for comparison to the traces with gA (rest). This was the most common type of channel activity with conductances of $60\text{pS} \pm 40\text{pS}$. The traces are measured at $U=100\text{mV}$. B) Less commonly occurring where large quantized events with a conductance of $200\text{pS} \pm 60\text{pS}$. Here measured at $U=300\text{mV}$. All membranes are made of 10:1 PMOXA-PDMS-PMOXA:gA in 50mM KCl, 10mM Hepes, 1mM EDTA, pH 7.4. Baselines are shifted and corrected for drift. The data is filtered with a Kaiser-Bessel filter with a cutoff frequency of 100Hz.

events would probably not have been detected.

Both González-Pérez et al [72] and I find channel events in the copolymer membranes with gA, while nothing is observed in the peptide free membranes. This demonstrates that protein channels can be incorporated in an active form. The found channel conductance is in general higher than that reported for gA in a lipid environment. It can be that the peptides aggregates due to hydrophobic mismatch or it can be that their conformation is altered in the unfamiliar environment.

In experiments with bacterial porins they are shown to have the same characteristic conductance as in a lipid membrane.[70] This is despite the fact that the hydrophobic thickness of the copolymer membrane in this study is about twice of that found in typical lipid membranes.

Even though the functionality of some proteins are preserved this is unlikely to be the case for all of them as a number of factor might influence the protein conformation. However, it is probably possible to synthesize polymers that mimics for example the lateral pressure profile of a lipid membrane.

The copolymers may therefore be an alternative to lipid membranes for the investigation of protein channels. But more experiments especially on the lack of activity in the protein free membrane should be carried out. This could by benefit be done on a Montal-Mueller setup. A capacitance test with the larger aperture provides a way to ensure that there is actually only one membrane.

8 Conclusions

The standard tests when exploring a new protein channel is ion selectivity, conductance, ligand sensitivity, and voltage dependence. With lipid ion channels there have previously been indications of selectivity.[59, 62] It has in this thesis been shown that the lipid channel conductance spans a wide range including those typical of protein channels. Previous experiments have demonstrated that the lipid channels are also affected by anesthetics (i.e. ligands).[63] Now for the first time it is demonstrated that in some cases the lipid channels can additionally exhibit voltage gating. That means that all types of standard characteristics of a given protein channel can be found in lipid ion channels as well. Further it has here been demonstrated that several types of channel activity such as quantized current steps, flickering, bursts, and subconductance states are common to lipid and protein ion channels.

Caution is therefore required for interpretation of protein channel data. Previous experiments have shown that lipid ion channels are only found in the membrane phase transition (e.g. [58, 61]). This could not be confirmed by my experiments. It is suggested that the deviation from previous publications is found because the membrane behavior is dominated by edge effects. It is not unlikely that the same edge effects are present in patch clamp experiments. One can therefore not necessarily avoid lipid channel activity by measuring far from the transition. Polymer membranes might be an alternative. One however have to remember that the protein channels are affected by their environment. A thin amphiphilic layer is not in itself enough to mimic a natural protein environment.

There seems though to be one major difference between lipid and protein ion channels, namely the reproducibility. Apparently a single membrane can exhibit any kind of behavior without change of the conditions. In contrast protein scientists are able to attribute certain behaviors to certain protein channels.

That one can observe quantized events in rubber [103] and in plastics pores [104] reveals that there is still a lot that is not understood both concerning lipid and protein channels. It indicates the normally assumed gating mechanisms are not a necessity.

9 Future research

One of the unsolved questions is how the membrane is attached inside the pipette and how this influences the membrane. There are several possible approaches to get closer to this insight. As a start one could use a microscope to try to look at the membrane optically. I have tried to see a membrane by making it of fluorescent lipids. It didn't succeed because lipids at the edge of the pipette glowed too much compared to the membrane. As an alternative one could try with stretch sensitive fluorophores or other kinds that could be expected to glow only in the bilayer. This kind of experiment can provide information about where in the pipette the membrane is positioned. Further one could possibly follow the formation of a membrane.

More detailed information about the structure of the membrane and particularly interesting, edge effects, can maybe be obtained with atomic force microscopy. In practice the experiment is probably impossible to make with a pipette but one could try to mimic the inside of a pipette with a hole in a mica sheet. It requires though that one can form a freely behaving membrane close to the surface if the cantilever shall be able to reach the membrane.

In this thesis it has been tried to compare different types of events in pure lipid membranes with that attributed to protein channels. For a more careful comparison one would have to do, or at least watch, the patch clamp experiments self. This would give a better insight into similarities and differences including the reproducibility.

If one wants to proceed with experiments on the effect of non-channel proteins on the permeability another setup is required. First of all one needs a setup where the permeability actually correlates with the membrane phase transition. This could be the Montal-Mueller setup but vesicles would be closer to a biological system and one can avoid solvents. The permeability can be measured either on an ensemble of vesicles with fluorescence spectroscopy as in [61, 111] or on single vesicles with the patch clamp technique.

In well behaving membranes with stable quantized activity over longer times one can gain information about the nature of the lipid pores by use of kinetic analysis. Preliminary results indicate that the closing probability is not purely stochastic. Rather that there seems to exist a stabilizing effect on long-lived pores.

10 Bibliography

References

- [1] Jordan, P.C., 2007. *Ion Channels, from Fantasy to Fact in Fifty Years*. In S. Chung, O. S. Andersen, & V. Krishnamurthy, eds. *Biological Membrane Ion Channels: Dynamics, Structure, and Applications*. New York: Springer, pp. 3-32.
- [2] Gorter, E. & Grendel, F., 1925. *On bimolecular layers of lipoids on the chromocytes of the blood*. *Journal of Experimental Medicine*, 41(4), 439-443.
- [3] Heimburg, T., 2010. *Lipid ion channels*. *Biophysical Chemistry*, 150(1-3), 2-22.
- [4] Tien, H. & Ottova, A., 2003. *The bilayer lipid membrane (BLM) under electrical fields*. *IEEE Transactions on dielectrics and electrical insulation*, 10(5), 717-727.
- [5] Mouritsen, O.G., 2005. *Life - as a matter of fat* 1st ed., Berlin: Springer.
- [6] Heimburg, T., 2007. *Thermal biophysics of membranes* 1st ed., Weinheim: Wiley-VCH.
- [7] Pinheiro, T., 1994. *The interaction of horse heart cytochrome c with phospholipid bilayers. Structural and dynamic effects*. *Biochimie*, 76(6), 489-500.
- [8] Kelkar, D.A. & Chattopadhyay, A., 2007. *The gramicidin ion channel: A model membrane protein*. *Biochimica et Biophysica Acta (BBA) - Biomembranes*, 1768(9), 2011-2025.
- [9] Khandelia, H., Ipsen, J. & Mouritsen, O., 2008. *The impact of peptides on lipid membranes*. *Biochimica et Biophysica Acta (BBA) - Biomembranes*, 1778(7-8), 1528-1536.
- [10] Blicher, A., 2007. *Permeability studies of lipid vesicles by Fluorescence Correlation Spectroscopy and Monte Carlo simulations*. Master thesis. University of Copenhagen. Available at: www.membranes.nbi.dk.

- [11] Heimburg, T., 1998. *Mechanical aspects of membrane thermodynamics. Estimation of the mechanical properties of lipid membranes close to the chain melting transition from calorimetry.* Biochimica et Biophysica Acta (BBA) - Biomembranes, 1415(1), 147-162.
- [12] Heimburg, T., 2000. *A model for the lipid pretransition: Coupling of ripple formation with the chain-melting transition.* Biophysical Journal, 78(3), 1154-1165.
- [13] Lamy-Freund, M.T. & Riske, K.A., 2003. *The peculiar thermostructural behavior of the anionic lipid DMPG.* Chemistry and Physics of Lipids, 122(1-2), 19-32.
- [14] Heimburg, T. & Biltonen, R., 1994. *Thermotropic behavior of dimyristoylphosphatidylglycerol and its interaction with cytochrome c.* Biochemistry, 33(32), 9477-9488.
- [15] Riske, K., Dobereiner, H. & Lamy-Freund, M., 2002. *Gel-fluid transition in dilute versus concentrated DMPG aqueous dispersions.* Biophysical Journal, 82(1), 767.
- [16] Nielsen, L.K., Bjornholm, T. & Mouritsen, O.G., 2000. *Critical phenomena: Fluctuations caught in the act.* Nature, 404(6776), 352.
- [17] Ivanova, V. et al., 2003. *Analyzing heat capacity profiles of peptide-containing membranes: Cluster formation of gramicidin A.* Biophysical Journal, 84(4), 2427-2439.
- [18] Kondepudi, D. & Prigogine, I., 1998. *Modern thermodynamics: from heat engines to dissipative structures,* Chichester: John Wiley & sons.
- [19] Dill, K.A. & Bromberg, S., 2002. *Molecular Driving Forces: Statistical Thermodynamics in Chemistry & Biology.* 1st ed., Garland Science.
- [20] Ebel, H., Grabitz, P. & Heimburg, T., 2001. *Enthalpy and volume changes in lipid membranes. I. The proportionality of heat and volume changes in the lipid melting transition and its implication for the elastic constants.* Journal of physical chemistry B, 105(30), 7353-7360.
- [21] Träuble, H. & Eibl, H., 1974. *Electrostatic Effects on Lipid Phase Transitions: Membrane Structure and Ionic Environment.* Proceedings of the National Academy of Sciences of the United States of America, 71(1), 214-219.

- [22] Seeger, H., 2006. *Kinetics of domain formation processes in lipid membranes*. PhD thesis. Göttingen: Georg-August-Universität. Available at: www.membranes.nbi.dk.
- [23] Anthony, F.H., Biltonen, R.L. & Freire, E., 1981. *Modification of a vibrating-tube density meter for precise temperature scanning*. Analytical Biochemistry, 116(1), 161-167.
- [24] Berestovsky, G.N. et al., 1978. *Voltage-induced reflectivity relaxation of bilayer lipid membranes: On changes of bilayer thickness*. The Journal of Membrane Biology, 43(2-3), 107-126.
- [25] Crowley, J., 1973. *Electrical Breakdown of Bimolecular Lipid Membranes as an Electromechanical Instability*. Biophysical Journal, 13(7), 711-724.
- [26] Stulen, G., 1981. *Electric field effects on lipid membrane structure*. Biochimica et Biophysica Acta (BBA) - Biomembranes, 640(3), 621-627.
- [27] Sugár, I.P., 1979. *A theory of the electric field-induced phase transition of phospholipid bilayers*. Biochimica et Biophysica Acta (BBA) - Biomembranes, 556(1), 72-85.
- [28] Cotterill, R., 1978. *Field effects on lipid-membrane melting*. Physica Scripta, 18(3), 191-192.
- [29] Antonov, V., Smirnova, E. & Shevchenko, E., 1990. *Electric field increases the phase transition temperature in the bilayer membrane of phosphatidic acid*. Chemistry and Physics of Lipids, 52(3-4), 251-257.
- [30] Thürk, M. & Porschke, D., 1991. *Phase-transition of dimyristoylphosphatidylglycerol bilayers induced by electric-field pulses*. Biochimica et Biophysica Acta, 1067(2), 153-158.
- [31] Weaver, J.C. & Chizmadzhev, Y., 1996. *Theory of electroporation: A review*. Bioelectrochemistry and Bioenergetics, 41(2), 135-160.
- [32] Hazel, J.R. & Eugene Williams, E., 1990. *The role of alterations in membrane lipid composition in enabling physiological adaptation of organisms to their physical environment*. Progress in Lipid Research, 29(3), 167-227.

- [33] Sinensky, M., 1974. *Homeoviscous Adaptation A Homeostatic Process that Regulates the Viscosity of Membrane Lipids in Escherichia coli*. Proceedings of the National Academy of Sciences of the United States of America, 71(2), 522-525.
- [34] Marr, A.G. & Ingraham, J.L., 1962. *Effect of temperature on the composition of fatty acids in Escherichia coli*. J. Bacteriol., 84(6), 1260-1267.
- [35] DeLong, E. & Yayanos, A., 1985. *Adaptation of the membrane lipids of a deep-sea bacterium to changes in hydrostatic pressure*. Science, 228(4703), 1101-1103.
- [36] Macdonald, A.G., 1988. *Application of the theory of homeoviscous adaptation to excitable membranes: pre-synaptic processes*. Biochemical Journal, 256(2), 313-327.
- [37] Fox, C., 1972. *Structure of cell-membranes*. Scientific American, 226(2), 30-38.
- [38] Parmahamsa, M., Reddy, K. & Varadacharyulu, N., 2004. *Changes in composition and properties of erythrocyte membrane in chronic alcoholics*. Alcohol and alcoholism, 39(2), 110-112.
- [39] Stibler, H. et al., 1991. *Biophysical and biochemical alterations in erythrocyte membranes from chronic alcoholics*. Scandinavian Journal of Clinical & Laboratory Investigation, 51(4), 309-319.
- [40] Aloia, R.C. et al., 1985. *Effect of chronic alcohol consumption on rat brain microsome lipid composition, membrane fluidity and Na⁺-K⁺-ATPase activity*. Life Sciences, 36(10), 1003-1017.
- [41] Heimburg, T. & Biltonen, R., 1996. *A Monte Carlo simulation study of protein-induced heat capacity changes and lipid-induced protein clustering*. Biophysical Journal, 70(1), 84-96.
- [42] Grainger, D. et al., 1989. *An enzyme caught in action: Direct imaging of hydrolytic function and domain formation of phospholipase A2 in phosphatidylcholine monolayers*. FEBS Letters, 252(1-2), 73-82.
- [43] Gudmand, M. et al., 2010. *Influence of Lipid Heterogeneity and Phase Behavior on Phospholipase A2 Action at the Single Molecule Level*. Biophysical Journal, 98(9), 1873-1882.

- [44] Biltonen, R.L., 1990. *A statistical-thermodynamic view of cooperative structural changes in phospholipid bilayer membranes: their potential role in biological function*. The Journal of Chemical Thermodynamics, 22(1), 1-19.
- [45] Hladky, S. & Haydon, D., 1972. *Ion transfer across lipid membranes in the presence of gramicidin A: I. Studies of the unit conductance channel*. Biochimica et Biophysica Acta (BBA) - Biomembranes, 274(2), 294-312.
- [46] Neher, E. & Sakmann, B., 1976. *Single-channel currents recorded from membrane of denervated frog muscle-fibers*. Nature, 260(5554), 799-802.
- [47] Liebovitch, L.S. & Krekora, P., 2002. *The physical basis of ion channel kinetics: The importance of dynamics*. In H. E. Layton & A. M. Weinstein, eds. Membrane transport and renal physiology. New York, Berlin, Heidelberg: Springer, pp. 27-52.
- [48] Andersen, O.S., 1984. *Gramicidin Channels*. Annual Review of Physiology, 46(1), 531-548.
- [49] Wallace, B., 2000. *Common structural features in gramicidin and other ion channels*. Bioessays, 22(3), 227-234.
- [50] Andersen, O.S. & Koeppe, R.E., 2007. *Bilayer Thickness and Membrane Protein Function: An Energetic Perspective*. Annual Review of Biophysics and Biomolecular Structure, 36(1), 107-130.
- [51] Papahadjopoulos, D. et al., 1973. Phase transitions in phospholipid vesicles Fluorescence polarization and permeability measurements concerning the effect of temperature and cholesterol. Biochimica et Biophysica Acta (BBA) - Biomembranes, 311(3), 330-348.
- [52] Yafuso, M., Kennedy, S.J. & Freeman, A.R., 1974. *Spontaneous conductance changes, multilevel conductance states and negative differential resistance in oxidized cholesterol black lipid membranes*. Journal of Membrane Biology, 17(1), 201-212.
- [53] Antonov, V. et al., 1980. *Appearance of single-ion channels in unmodified lipid bilayer-membranes at the phase-transition temperature*. Nature, 283(5747), 585-586.
- [54] Boehm, G., Hanke, W. & Eibl, H., 1980. *Lipid Phase Transition in Planar Bilayer Membrane and Its Effect on Carrier- and Pore-Mediated*

- Ion Transport*. Proceedings of the National Academy of Sciences of the United States of America, 77(6), 3403-3407.
- [55] Kaufmann, K. & Silman, I., 1983. *Proton-induced ion channels through lipid bilayer membranes*. *Naturwissenschaften*, 70(3), 147-149.
- [56] Kaufmann, K., Hanke, W. & Corcia, A., 1989. *Ion channel fluctuations in pure lipid bilayer membranes: Control by voltage*. Available at: membranes.nbi.dk/Kaufmann/publications.html
- [57] Gögelein, H. & Koepsell, H., 1984. *Channels in planar bilayers made from commercially available lipids*. *Pflügers Archiv European Journal of Physiology*, 401(4), 433-434.
- [58] Antonov, V. et al., 2005. *Soft perforation of planar bilayer lipid membranes of dipalmitoylphosphatidylcholine at the temperature of the phase transition from the liquid crystalline to the gel state*. *European Biophysics Journal with Biophysical Letters*, 34(2), 155-162.
- [59] Woodbury, D.J., 1989. *Pure lipid vesicles can induce channel-like conductances in planar bilayers*. *Journal of Membrane Biology*, 109(2), 145-150.
- [60] Wunderlich, B. et al., 2009. *Phase-State Dependent Current Fluctuations in Pure Lipid Membranes*. *Biophysical Journal*, 96(11), 4592-4597.
- [61] Blicher, A. et al., 2009. *The Temperature Dependence of Lipid Membrane Permeability, its Quantized Nature, and the Influence of Anesthetics*. *Biophysical Journal*, 96(11), 4581-4591.
- [62] Papahadjopoulos, D., 1971. *Na⁺-K⁺ discrimination by pure phospholipid membranes*. *Biochimica et Biophysica Acta*, 241(1), 254-259.
- [63] Wodzinska, K., Blicher, A. & Heimburg, T., 2009. *The thermodynamics of lipid ion channel formation in the absence and presence of anesthetics. BLM experiments and simulations*. *Soft Matter*, 5, 3319-3330.
- [64] Mansy, S. et al., 2008. *Template-directed synthesis of a genetic polymer in a model protocell*. *Nature*, 454(7200), 122-126.
- [65] Cruzeiro-Hansson, L. & Mouritsen, O.G., 1988. *Passive ion permeability of lipid membranes modelled via lipid-domain interfacial area*. *Biochimica et Biophysica Acta (BBA) - Biomembranes*, 944(1), 63-72.

- [66] Nagle, J. & Scott Jr., H., 1978. *Lateral compressibility of lipid mono- and bilayers. Theory of membrane permeability.* Biochimica et Biophysica Acta (BBA) - Biomembranes, 513(2), 236-243.
- [67] Heimburg, T. & Jackson, A., 2007. *The thermodynamics of general anesthesia.* Biophysical Journal, 92(9), 3159-3165.
- [68] Glaser, R.W. et al., 1988. *Reversible electrical breakdown of lipid bilayers: formation and evolution of pores.* Biochimica et Biophysica Acta (BBA) - Biomembranes, 940(2), 275-287.
- [69] Böckmann, R.A. et al., 2008. *Kinetics, Statistics, and Energetics of Lipid Membrane Electroporation Studied by Molecular Dynamics Simulations.* Biophysical Journal, 95(4), 1837-1850.
- [70] Meier, W., Nardin, C. & Winterhalter, M., 2000. *Reconstitution of Channel Proteins in (Polymerized) ABA Triblock Copolymer Membranes.* Angewandte Chemie (International Ed. in English), 39(24), 4599-4602.
- [71] Discher, D.E. & Eisenberg, A., 2002. *Polymer Vesicles.* Science, 297(5583), 967-973.
- [72] González-Pérez, A. et al., 2009. *Biomimetic Triblock Copolymer Membrane Arrays: A Stable Template for Functional Membrane Proteins.* Langmuir, 25(18), 10447-10450.
- [73] Ho, D. et al., 2004. *Hybrid protein-polymer biomimetic membranes.* IEEE Transactions on Nanotechnology, 3(2), 256-263.
- [74] Hanke, W. & Miller, C., 1985. *Reconstitution of ion channels.* Critical Reviews in Biochemistry and Molecular Biology, 19(1), 1-44.
- [75] Fidorra, M., 2007. *Confocal Microscopy, Calorimetry and Permeability Studies on Giant Lipid Vesicles Containing Ceramides.* PhD thesis. University of Southern Denmark. Available at: www.membranes.nbi.dk.
- [76] Montal, M. & Mueller, P., 1972. *Formation of bimolecular membranes from lipid monolayers and a study of their electrical properties.* Proceedings of the National Academy of Sciences of the United States of America, 69(12), 3561-3566.

- [77] Hamill, O.P. et al., 1981. *Improved patch-clamp techniques for high-resolution current recording from cells and cell-free membrane patches*. Pflügers Archiv European Journal of Physiology, 391(2), 85-100.
- [78] Hanke, W. et al., 1984. *Ion channel reconstitution into lipid bilayer membranes on glass patch pipettes*. Bioelectrochemistry and Bioenergetics, 12(3-4), 329-339.
- [79] Grant, A. et al., 1989. *Blockade of cardiac sodium-channels by lidocaine - single-channel analysis*. Circulation Research, 65(5), 1247-1262.
- [80] Cantor, R., 1997. *The lateral pressure profile in membranes: A physical mechanism of general anesthesia*. Biochemistry, 36(9), 2339-2344.
- [81] Cantor, R., 1998. *The lateral pressure profile in membranes: a physical mechanism of general anesthesia*. Toxicology Letters, 101, 451-458.
- [82] Mouritsen, O. & Bloom, M., 1984. *Mattress model of lipid-protein interactions in membranes*. Biophysical Journal, 46(2), 141-153.
- [83] Jensen, M.Ø. & Mouritsen, O.G., 2004. *Lipids do influence protein function - the hydrophobic matching hypothesis revisited*. Biochimica et Biophysica Acta (BBA) - Biomembranes, 1666(1-2), 205-226.
- [84] Martinac, B. & Hamill, O.P., 2002. *Gramicidin A channels switch between stretch activation and stretch inactivation depending on bilayer thickness*. Proceedings of the National Academy of Sciences of the United States of America, 99(7), 4308-4312.
- [85] Seeger, H. et al., 2010. *Changes in single K⁺ channel behavior through the lipid phase transition*. submitted to Biophysical Journal.
- [86] Cannon, B. et al., 2003. *Regulation of Calcium Channel Activity by Lipid Domain Formation in Planar Lipid Bilayers*. Biophysical Journal, 85(2), 933-942.
- [87] Kinnunen, P.K.J., 1996. *On the molecular-level mechanisms of peripheral protein-membrane interactions induced by lipids forming inverted non-lamellar phases*. Chemistry and Physics of Lipids, 81(2), 151-166.
- [88] Tuominen, E.K.J., Wallace, C.J.A. & Kinnunen, P.K.J., 2002. *Phospholipid-Cytochrome c Interaction*. Journal of Biological Chemistry, 277(11), 8822-8826.

- [89] Heimburg, T. & Marsh, D., 1995. *Protein surface-distribution and protein-protein interactions in the binding of peripheral proteins to charged lipid membranes*. *Biophysical Journal*, 68(2), 536-546.
- [90] Heimburg, T., Angerstein, B. & Marsh, D., 1999. *Binding of peripheral proteins to mixed lipid membranes: Effect of lipid demixing upon binding*. *Biophysical Journal*, 76(5), 2575-2586.
- [91] Penner, R., 1995. *Practical guide to patch clamping*. In B. Sakmann & E. Neher, eds. *Single-Channel Recording*. New York, London: Plenum Press, pp. 3-30.
- [92] Antonov, V. et al., 2003. *Electrical capacitance of lipid bilayer membranes of hydrogenated egg lecithin at the temperature phase transition*. *European Biophysics Journal with Biophysics Letters*, 32(1), 55-59.
- [93] Tien, H. & Diana, A., 1968. *Bimolecular lipid membranes - a review and a summary of recent studies*. *Chemistry and Physics of Lipids*, 2(1), 55-101.
- [94] Ehrlich, B., 1992. *Planar lipid bilayers on patch pipettes: Bilayer Formation and ion channel incorporation*. In B. Rudy & L. Iverson, eds. *Methods in Enzymology*. New York, San Francisco, London: Academic Press, pp. 463-470.
- [95] Hianik, T., 2006. *Structure and physical properties of biomembranes and model membranes*. *Acta Physica Slovaca*, 56(6), 687-806.
- [96] Molecular Devices, 2008. *The Axon Guide - A guide to electrophysiological & biophysics laboratory techniques*. Available at: http://www.moleculardevices.com/pdfs/Axon_Guide.pdf.
- [97] Wonderlin, W., Finkel, A. & French, R., 1990. *Optimizing planar lipid bilayer single-channel recordings for high resolution with rapid voltage steps*. *Biophysical Journal*, 58(2), 289-297.
- [98] Garidel, P. et al., 1997. *The mixing behavior of pseudobinary phosphatidylcholine-phosphatidylglycerol mixtures as a function of pH and chain length*. *European Biophysics Journal*, 26(6), 447-459.
- [99] Muga, A., Mantsch, H.H. & Surewicz, W.K., 1991. *Membrane binding induces destabilization of cytochrome c structure*. *Biochemistry*, 30(29), 7219-7224.

- [100] Heimburg, T. & Marsh, D., 1993. *Investigation of secondary and tertiary structural changes of cytochrome c in complexes with anionic lipids using amide hydrogen exchange measurements: an FTIR study.* Biophysical Journal, 65(6), 2408-2417.
- [101] Hudecek, Y. et al., 1997. *Spectroscopic Studies of cytochrome c interaction with lipid membranes.* In P. Carmona, ed. Spectroscopy of Biological Molecules: Modern Trends. The Netherlands: Kluwer Academic Publishers.
- [102] Hamachi, I., Fujita, A. & Kunitake, T., 1997. *Protein Engineering Using Molecular Assembly: Functional Conversion of Cytochrome c via Noncovalent Interactions.* Journal of the American Chemical Society, 119(39), 9096-9102.
- [103] Sachs, F. & Qin, F., 1993. *Gated, ion-selective channels observed with patch pipettes in the absence of membranes: novel properties of a giga-seal.* Biophysical Journal, 65(3), 1101-1107.
- [104] Lev, A.A. et al., 1993. *Rapid Switching of Ion Current in Narrow Pores: Implications for Biological Ion Channels.* Proceedings: Biological Sciences, 252(1335), 187-192.
- [105] Sigworth, F., 1985. *Open channel noise. I. Noise in acetylcholine receptor currents suggests conformational fluctuations.* Biophysical Journal, 47(5), 709-720.
- [106] Gallaher, J. et al., 2010. *Ion-channel-like behavior in lipid bilayer membranes at the melting transition.* Physical Review E, 81(6). 061925
- [107] Fox, J.A., 1987. *Ion channel subconductance states.* The Journal of Membrane Biology, 97(1), 1-8.
- [108] Neher, E. & Steinbach, J., 1978. *Local-anesthetics transiently block currents through single acetylcholine-receptor channels.* Journal of Physiology-London, 277, 153-176.
- [109] Sandison, M.E. et al., 2007. *Micromachined glass apertures for artificial lipid bilayer formation in a microfluidic system.* Journal of Micromechanics and Microengineering, 17(7), S189-S196.
- [110] Lin, D. et al., 2007. *Characterization of mRNA Expression in Single Neurons.* In T. Borsello, ed. Neuroprotection Methods and Protocols. Totowa, NJ: Humana Press

- [111] Sabra, M.C., Jørgensen, K. & Mouritsen, O.G., 1996. *Lindane suppresses the lipid-bilayer permeability in the main transition region.* Biochimica et Biophysica Acta (BBA) - Biomembranes, 1282(1), 85-92.
- [112] Brumm, T. et al., 1996. *The effect of increasing membrane curvature on the phase transition and mixing behavior of a dimyristoyl-sn-glycero-3-phosphatidylcholine/distearoyl-sn-glycero-3-phosphatidylcholine lipid mixture as studied by Fourier transform infrared spectroscopy and differential scanning calorimetry.* Biophysical Journal, 70(3), 1373-1379.
- [113] Leidy, C. et al., 2002. *Ripples and the Formation of Anisotropic Lipid Domains: Imaging Two-Component Supported Double Bilayers by Atomic Force Microscopy.* Biophysical Journal, 83(5), 2625-2633.
- [114] Bezanilla, F., 2007. *Voltage-Gated Ion channels.* In S. Chung, O. S. Andersen, & V. Krishnamurthy, eds. Biological Membrane Ion Channels: Dynamics, Structure, and Applications. New York: Springer, pp. 81-118.
- [115] Andersen, O.S., Koeppe, R.E. & Roux, B., 2007. *Gramicidin Channels: Versatile tools.* In S. Chung, O. S. Andersen, & V. Krishnamurthy, eds. Biological Membrane Ion Channels: Dynamics, Structure, and Applications. New York: Springer, 33-80.
- [116] Busath, D. & Szabo, G., 1988. *Low conductance gramicidin A channels are head-to-head dimers of beta 6.3-helices.* Biophysical Journal, 53(5), 689-695.

A Various behaviors of a single membrane

The same membrane can show a huge variety of behaviors. In the following graphs all traces contained stems from the same membrane. It is a 6:4 DMPG:DMPC membrane in 1M LiCl at a temperature of 22.8°C. The trace in figure 51 is recorded at a voltage of 100mV while all traces in figures 52 and 53 are recorded at 200mV. In figures 52 and 53 the traces are ordered chronological from bottom to top. The baseline is shifted for all traces.

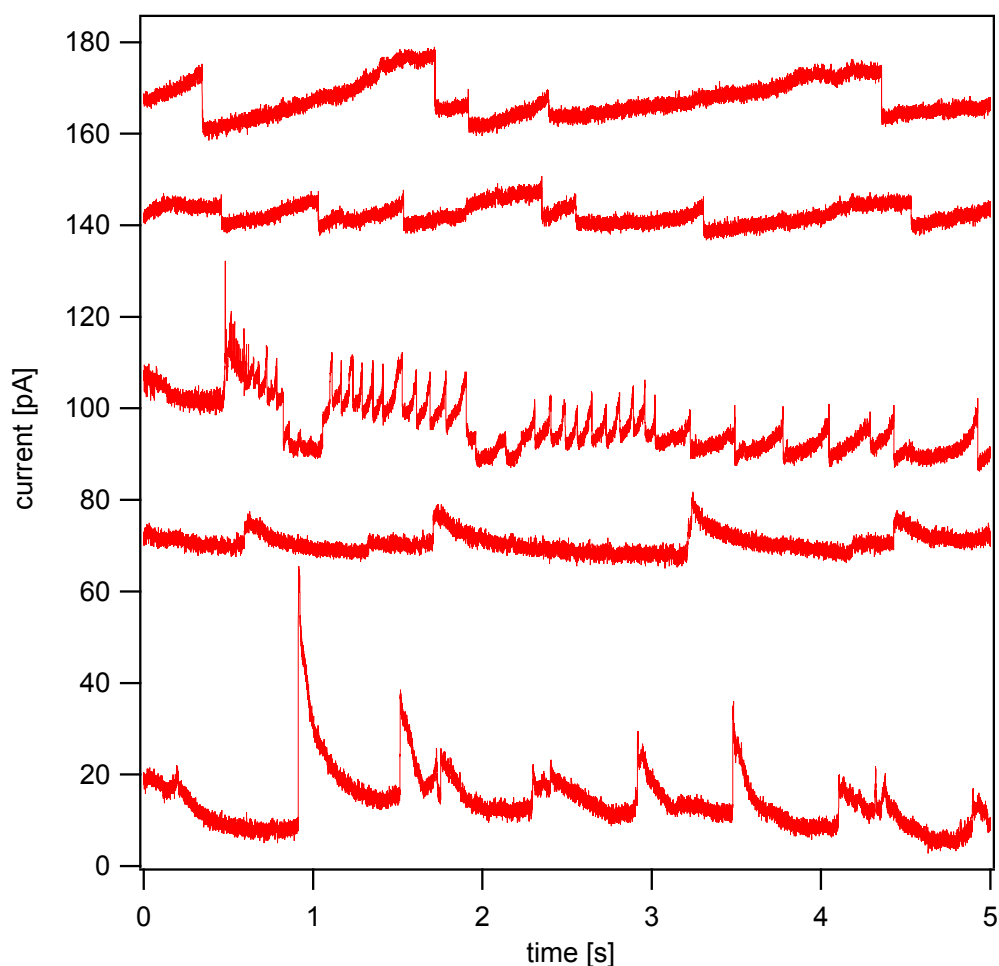


Figure 51:

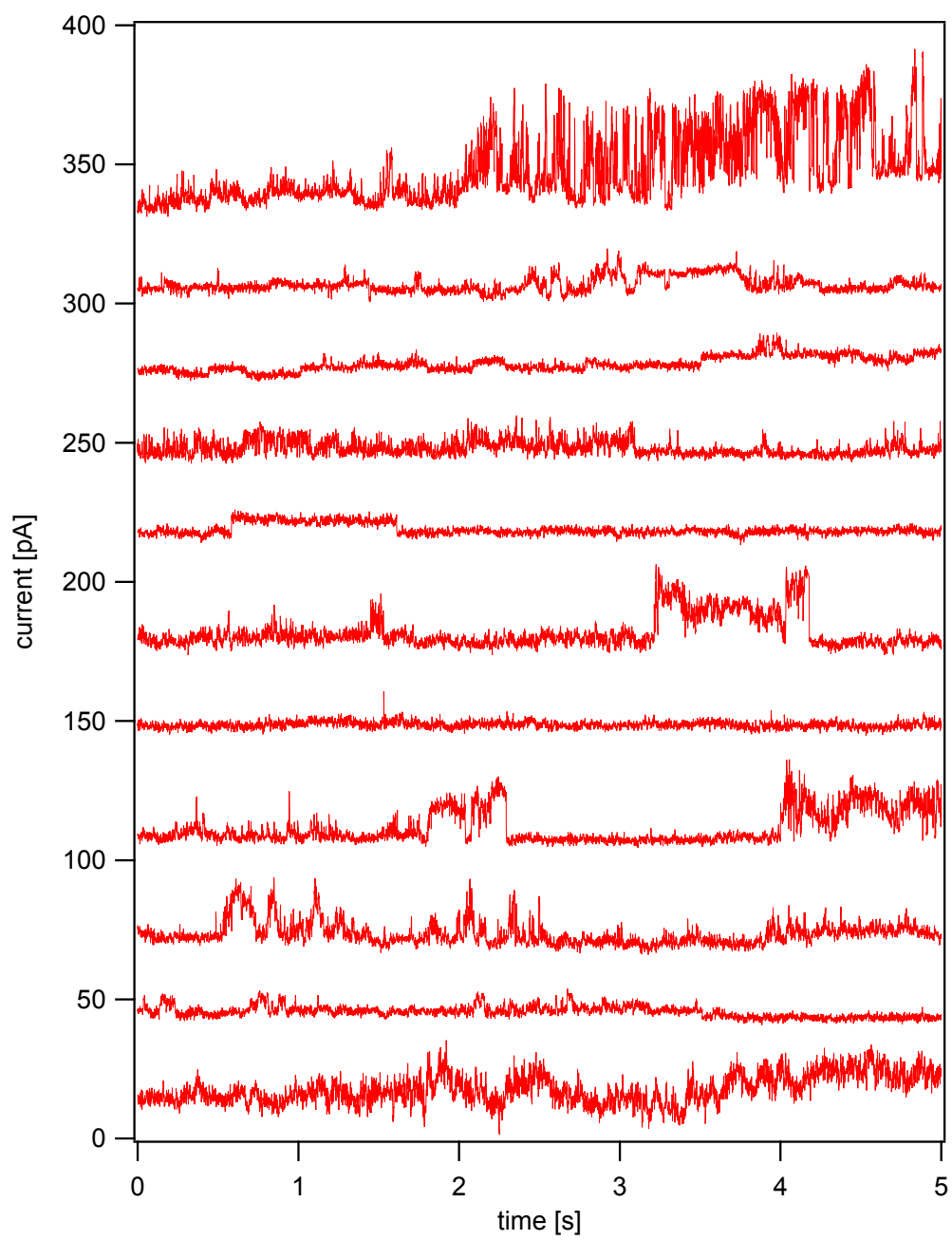


Figure 52:

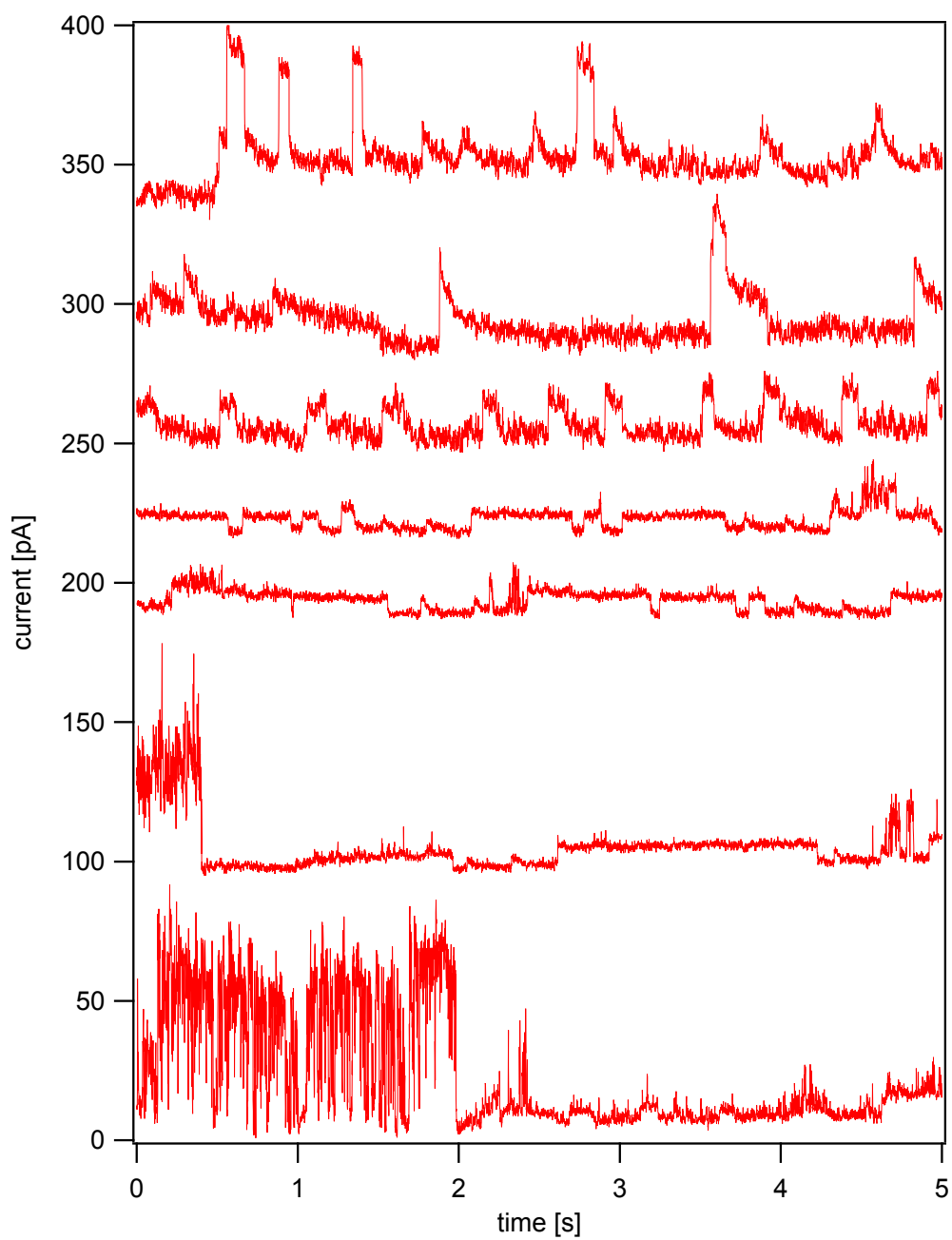
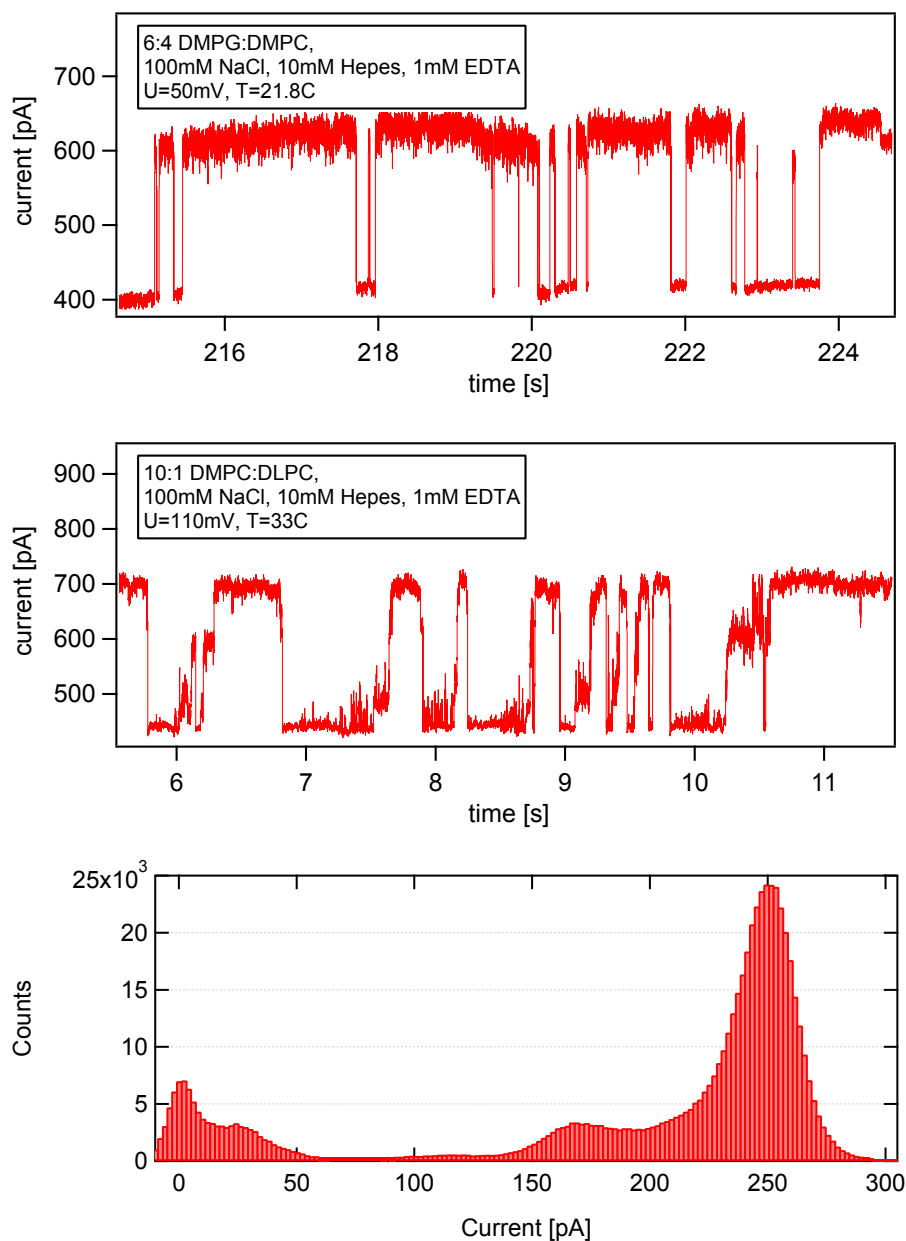


Figure 53:

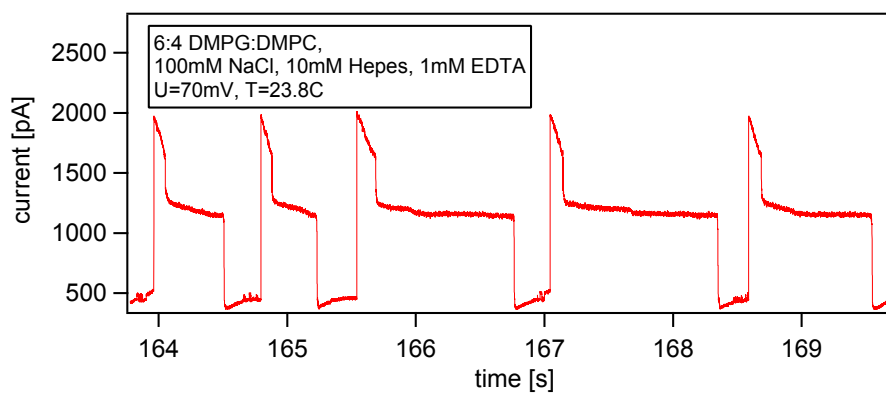
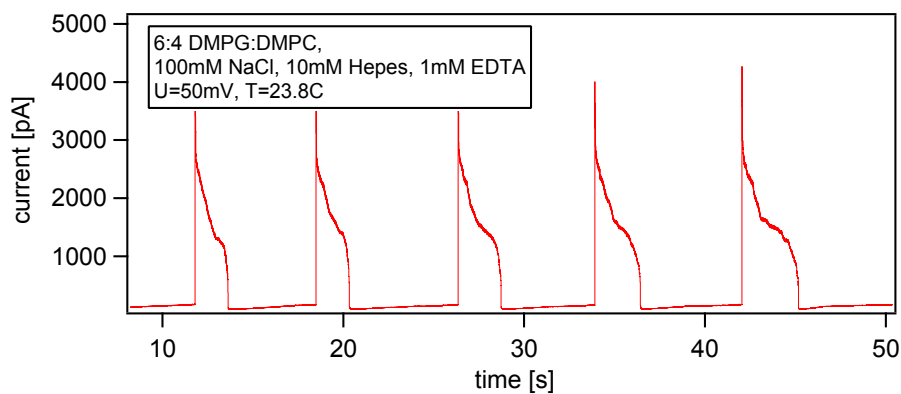
B Supplementary figures of various membrane behaviors

B.1 Stable quantized events

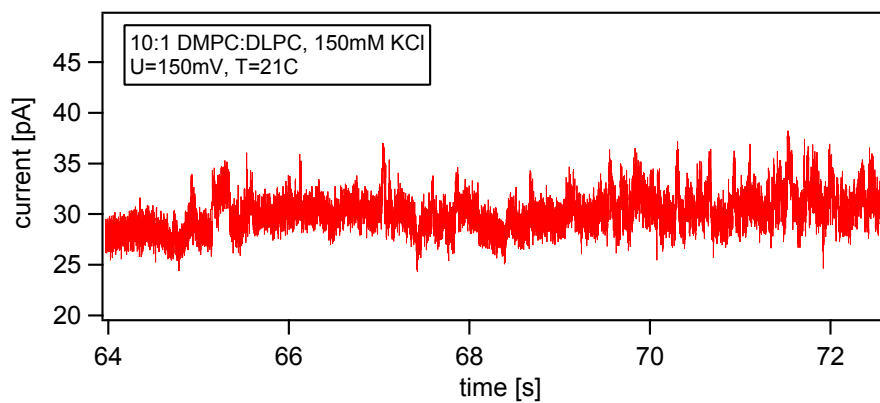


Histogram of a longer part of the trace shown above with the baseline subtracted. Between the baseline at 0pA and the dominating current amplitude of 250pA is seen several peaks from subconductance states.

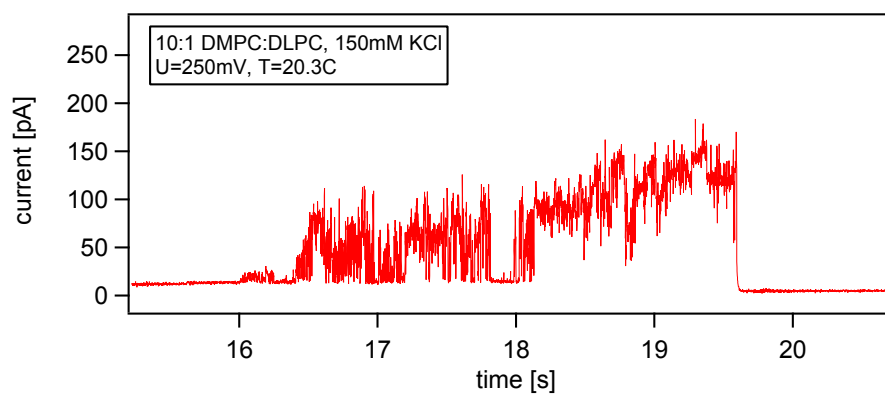
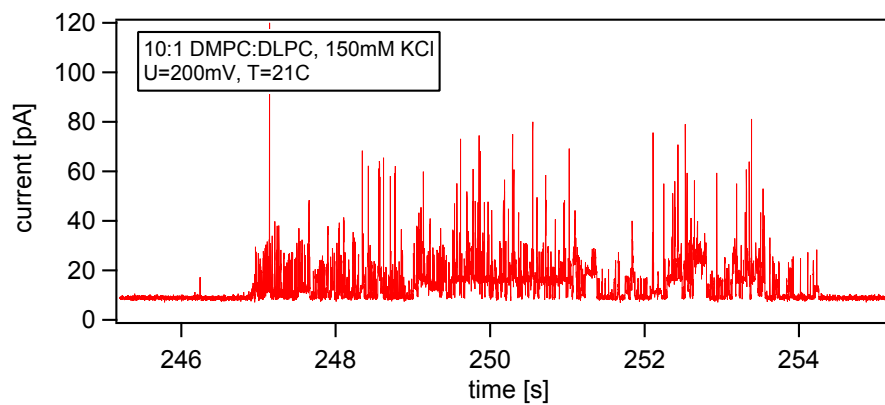
B.2 Overload events



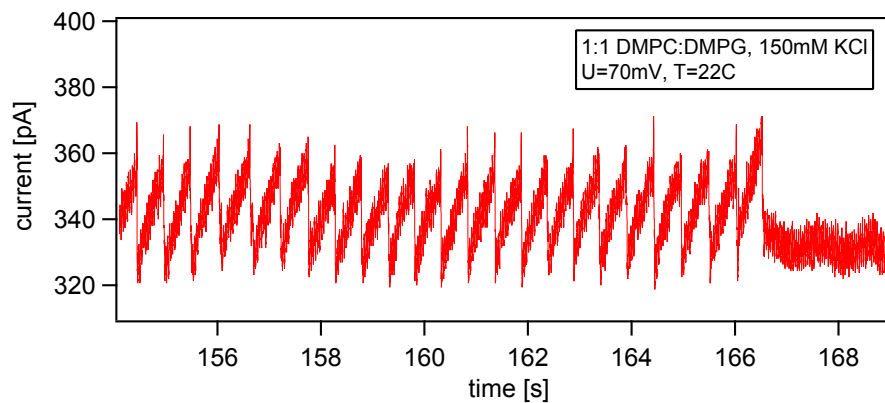
B.3 Non-quantized events

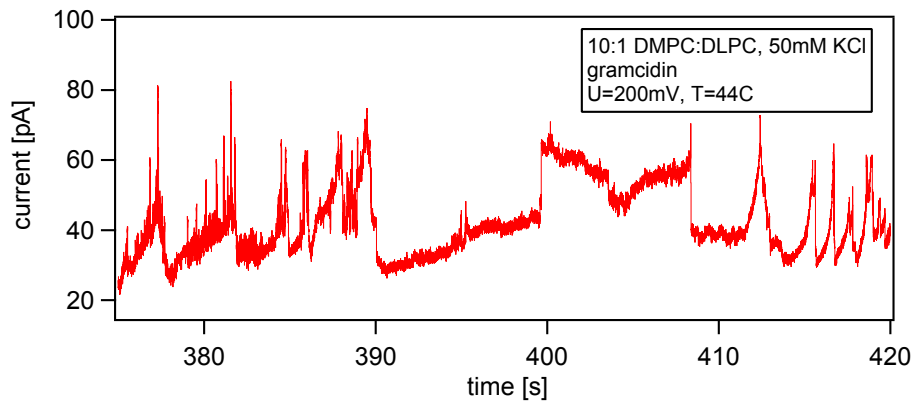
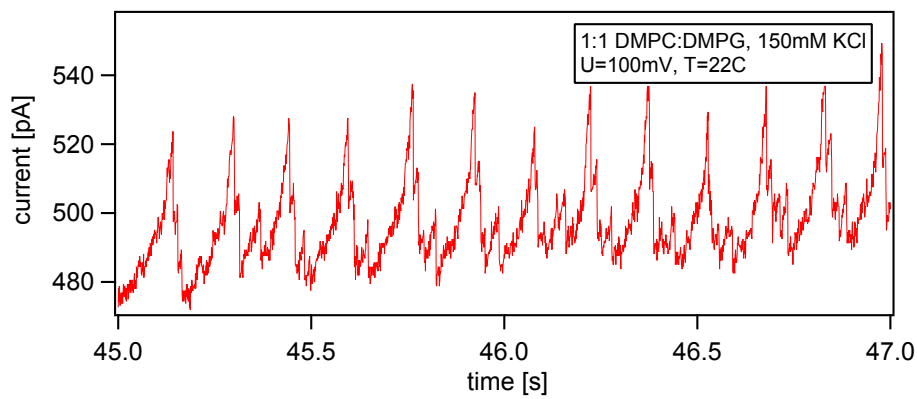
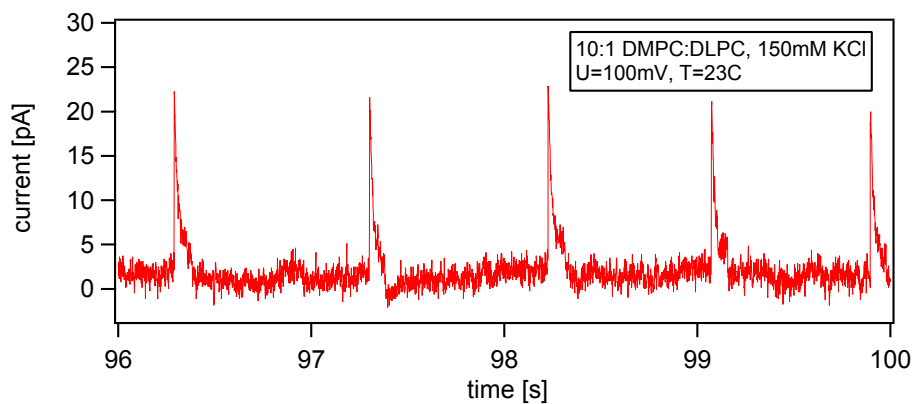


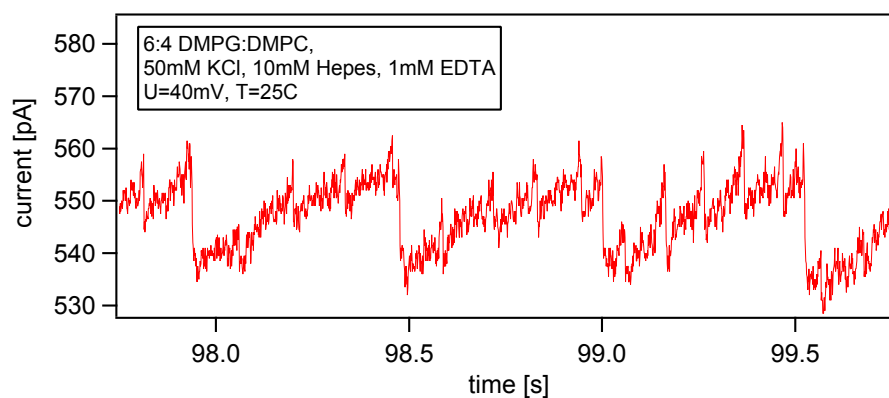
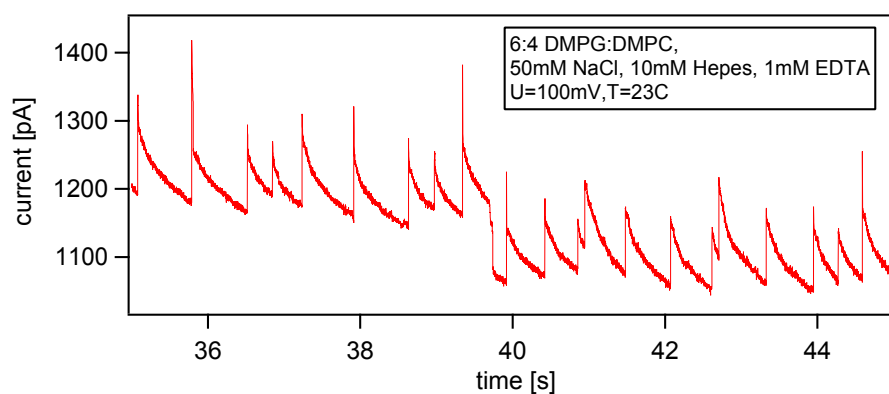
B.4 Burst



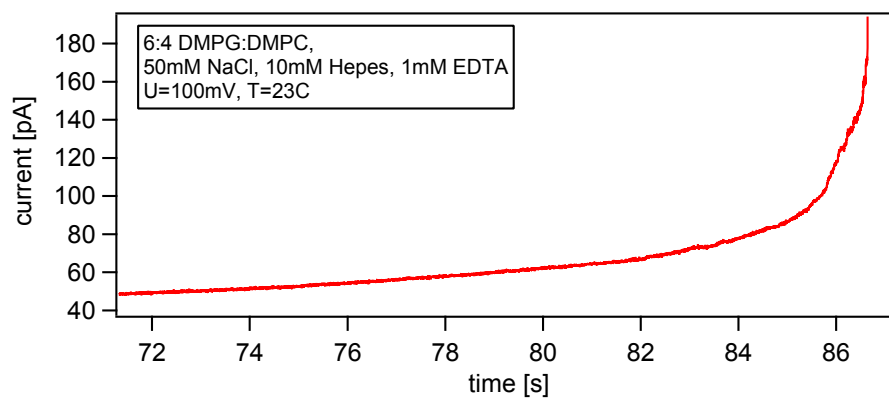
B.5 Sawteeth



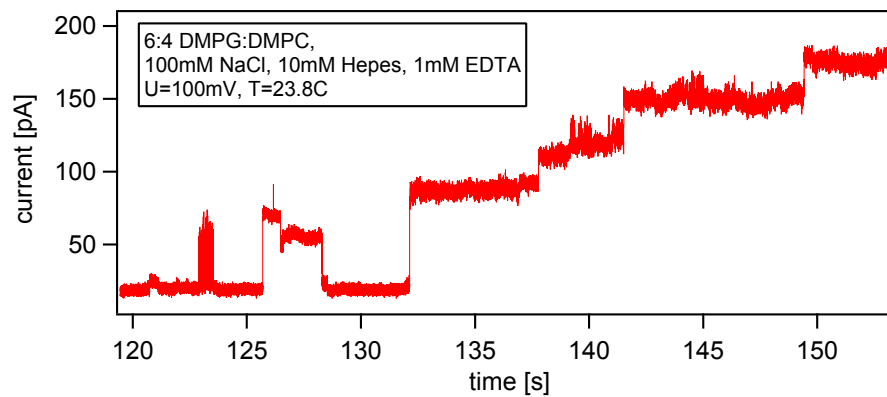
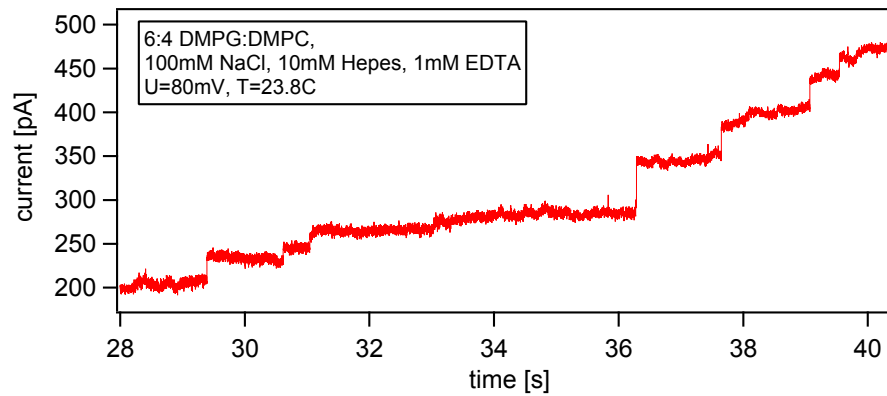
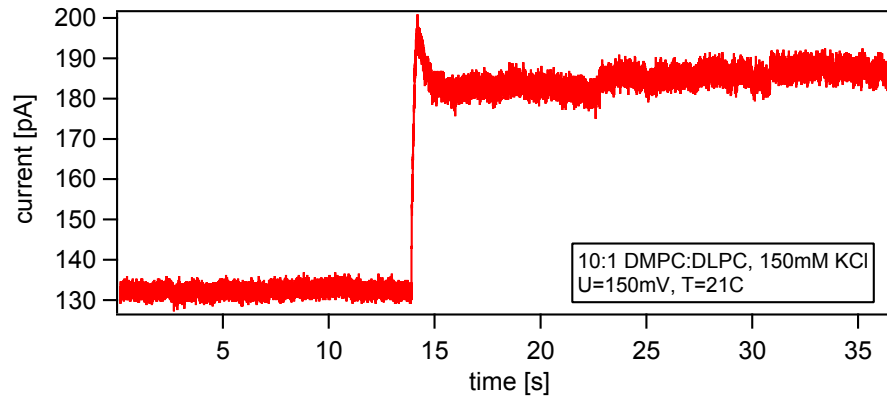




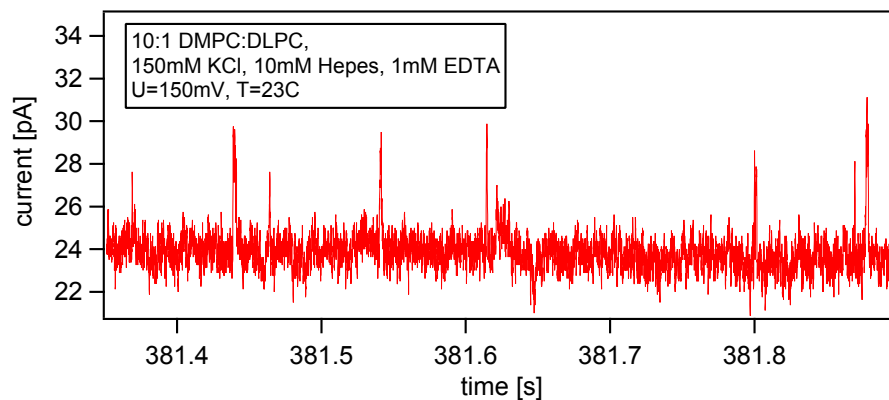
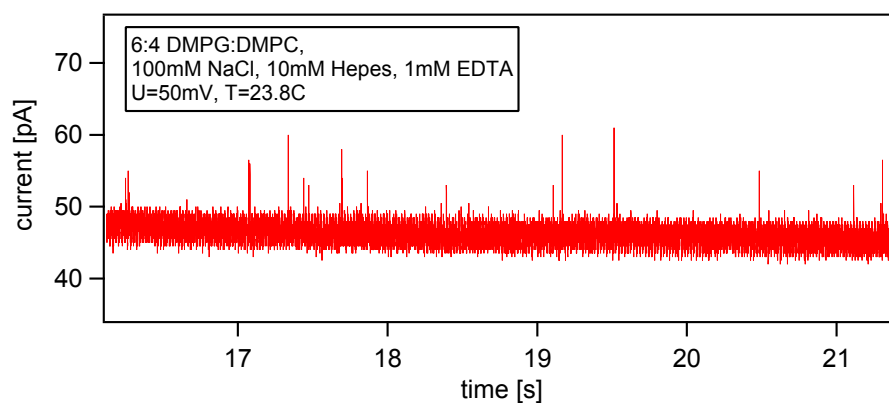
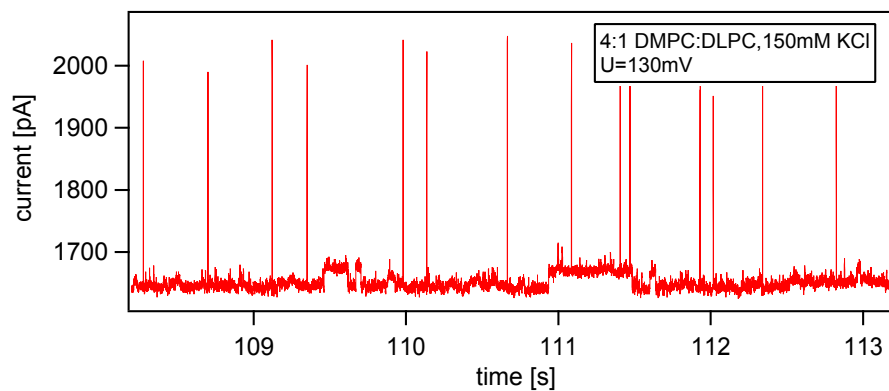
B.6 Baseline drift



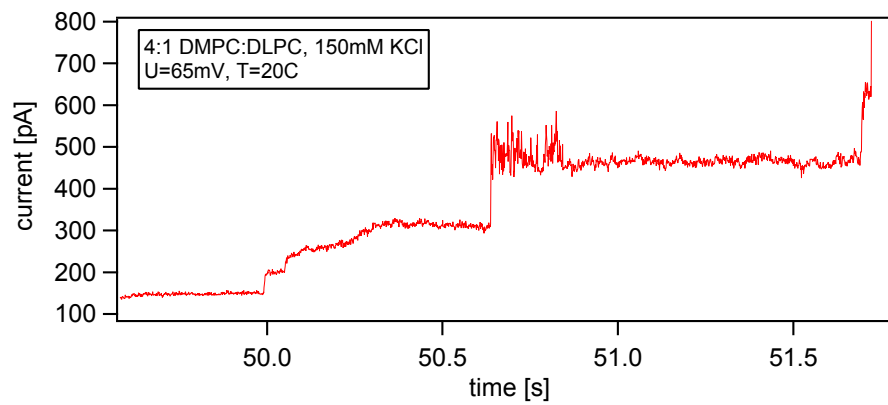
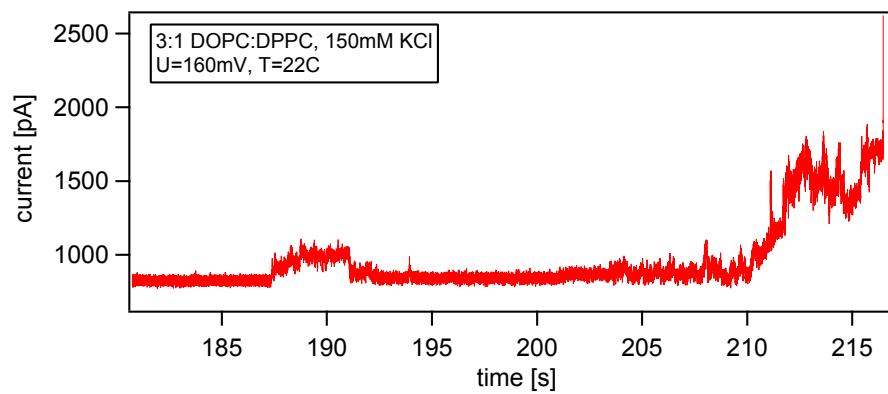
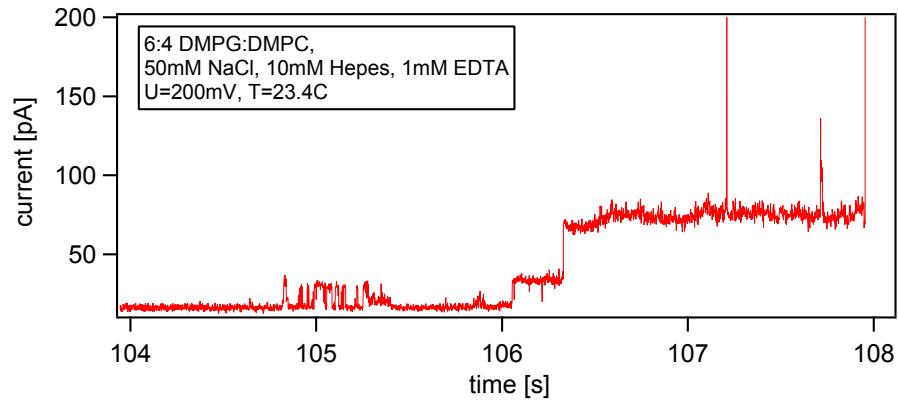
B.7 Baseline jumps and stairs

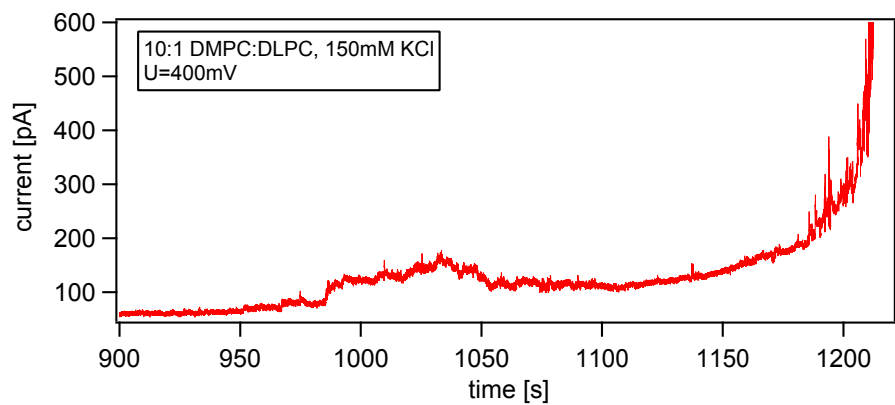
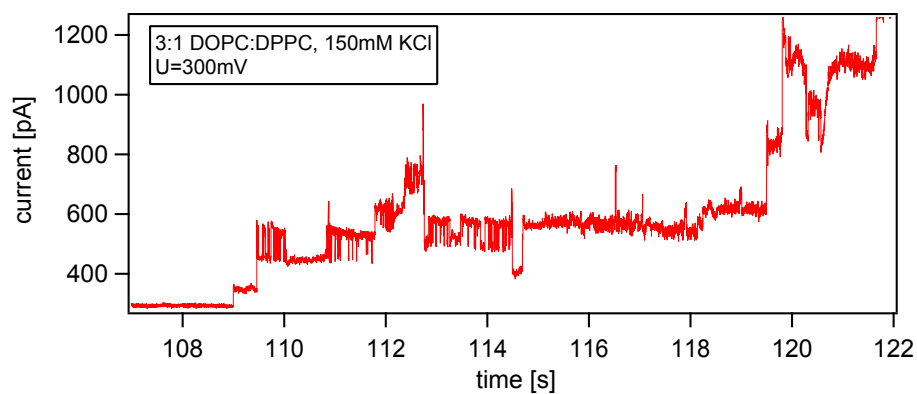
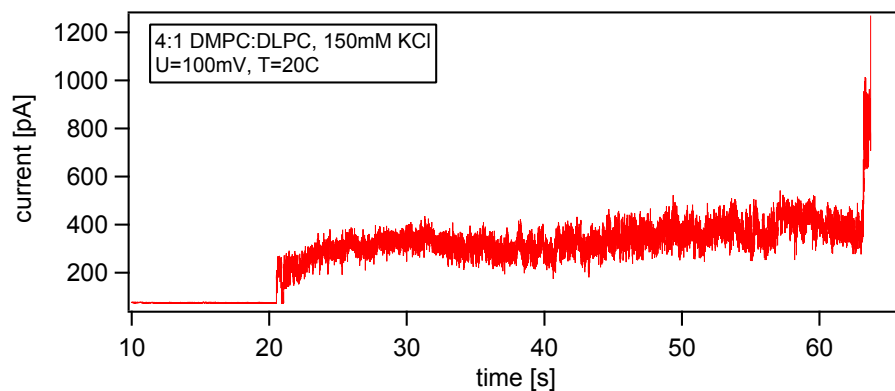


B.8 Spikes



B.9 Breakage





C Protein channel data

Unspecific events seen with a patch clamp setup.

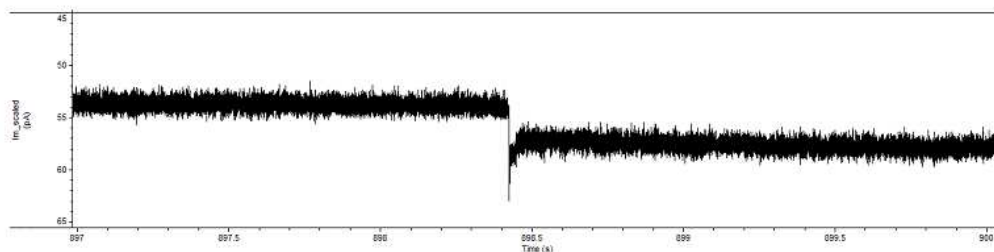


Figure 54: Baseline jump found for an inside-out configuration on a CHO cell with a M2M8P channel. $U=-60\text{mV}$. Courtesy K. Witschas.

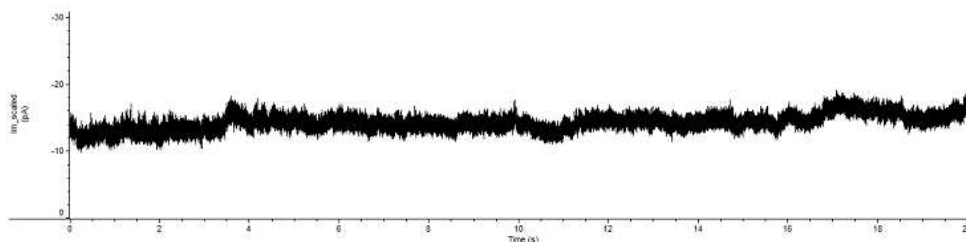


Figure 55: Uneven baseline in native HEK293 cell made in inside-out configuration. $U=60\text{mV}$. Courtesy K. Witschas.

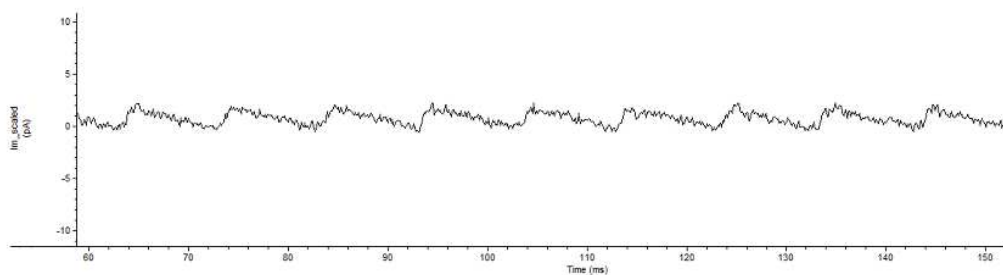


Figure 56: Sawteeth shaped current trace due to noise from cooling circuit in Axopatch 200B headstage. Courtesy K. Witschas.

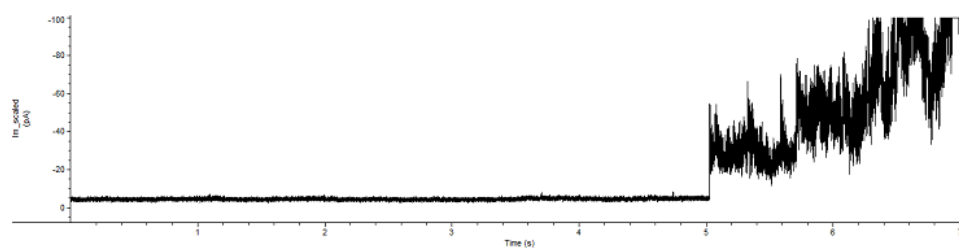


Figure 57: Break of seal to a native HEK293 cell in inside-out configuration. $U=60\text{mV}$. Courtesy K. Witschas.

D Voltage dependence

The presented data is based on 2 membranes. One that is measured on at 22.2°C and another where it is done at 32°C. The data is measured over a longer time span with temperature scans in between.

